GROUND-BASED AND AERIAL REMOTE SENSING METHODS FOR ESTIMATING COTTON GROWTH, WATER STRESS, AND DEFOLIATION

by

GLEN L. RITCHIE

(Under the Direction of James E. Hook and Craig W. Bednarz)

ABSTRACT

Remote sensing of visible and near-infrared crop reflectance has been closely tied to crop growth and health. The purpose of this research was to extend the application of remote sensing for irrigation and defoliation management of cotton (*Gossypium hirsutum* L.). Leaf area index of cotton subjected to defoliation treatments was regressed against normalized indices of visible and near-infrared reflectance. It was determined that combinations of red edge and near-infrared reflectance most accurately estimate leaf area index. A camera system comprising off-the-shelf digital cameras was tested as a means of collecting visible and near-infrared reflectance data throughout the growing season and a correction factor for exposure value was derived to allow estimates of relative reflectance. Vegetation indices based on camera and spectrometer reflectance measurements were compared with crop ground cover over three seasons and found to be sensitive to changes in ground cover within a limited ground cover range. Irrigation treatments based on changes in ground cover and vegetation index values were found to use less water and have yields comparable to treatments irrigated based on soil tension measurements.

INDEX WORDS: Remote sensing, Cotton, Defoliation, Irrigation, Exposure, Vegetation Index, Soil moisture

GROUND-BASED AND AERIAL REMOTE SENSING METHODS FOR ESTIMATING COTTON GROWTH, WATER STRESS, AND DEFOLIATION

by

GLEN L. RITCHIE

B.S., Utah State University, 2000

M.S., Utah State University, 2003

A Dissertation Submitted to the Graduate Faculty of The University of Georgia in Partial Fulfillment of the Requirements for the Degree

DOCTOR OF PHILOSOPHY

ATHENS, GEORGIA

2007

GROUND-BASED AND AERIAL REMOTE SENSING METHODS FOR ESTIMATING COTTON GROWTH, WATER STRESS, AND DEFOLIATION

by

GLEN L. RITCHIE

Major Professor:	Craig W. Bednarz
Co-Major Professor:	James E. Hook
Committee:	Craig K. Kvien
	William E. Vencill
	Dana G. Sullivan
	Calvin D. Perry

Electronic Version Approved:

Maureen Grasso
Dean of the Graduate School
The University of Georgia
August 2007

ACKNOWLEDGEMENTS

Several people have invested time, money, and resources in my education, for which I am grateful. The greatest sacrifice has come from Kristina, my lovely wife who has gracefully managed an ever-growing household while I have studied, researched, and attended classes and meetings throughout Georgia and the United States. I would be remiss in not mentioning my children, two of whom have attended school the same time I have.

I would like to thank my parents, Brent and Janis Ritchie, as well as my siblings, for their examples and encouragement. The in-laws have been great, too.

Craig Bednarz invited me to complete my research under his guidance in Tifton, and Jim Hook took me on as a graduate student in 2006. They have both been great mentors. In addition, I would like to thank those whom I worked with at Utah State University, most notably Bruce Bugbee, my advisor at USU.

I've enjoyed working under Steve M. Brown, who has helped direct my research during the past year. William Vencill, Craig Kvien, Dana Sullivan, and Calvin Perry have contributed valuable advice and helped me out immensely as members of my committee.

Several professors outside my committee have made significant contributions to my growth as a scientist, most notably Peter Hartel, Miguel Cabrera, and Wayne Parrott. Several people have helped me with clerical and organizational tasks, including Vivienne Sturgill, Evelyn Folds, and Pat Boatner.

I have been privileged to work with several outstanding people, including Cory Mills, Jared Whitaker, Rob Millings, Sidney Cromer, Rad Yager, Ivey Griner, Bo Faircloth, Ashley Sealy, Lola Sexton, Trey Davis, and Dudley Cook.

The research for this dissertation was funded by the Georgia Cotton Commission and Cotton Incorporated.

TABLE OF CONTENTS

Page

LIST OF TABLES

Page

LIST OF FIGURES

Page

CHAPTER 1

INTRODUCTION AND LITERATURE REVIEW

This literature review summarizes the effects of water stress on cotton growth. It also examines the relationship of cotton reflectance with growth, leaf area index (LAI), and water stress, as well as the application of remote sensing technology to the identification of these factors. Current remote sensing methods are examined as methods for determining water stress in cotton, and the chapter concludes with a problem statement and justification for this research.

Cotton Growth and Water Stress

The wild ancestors of domestic cotton (*Gossypium hirsutum* L.) were perennial vines, and despite selective breeding for determinate-type growth habits, cotton produces abundant vegetative growth if adequate water and nutrients are available. Excessive vegetative growth diverts the plant's energy away from lint and seed production. Plant growth regulators such as mepiquat chloride are often applied to irrigated cotton to decrease growth, prevent boll rot, and facilitate machine harvest (Jost *et al.*, 2006). However, decreasing irrigation application to a level that allows adequate, but not excessive growth might allow high-yielding cotton with less water usage and lower plant growth regulator requirements.

All plants are affected by soil moisture deficit. Water is the primary component of actively growing crop plants, with water content ranging from 70-90% of the crop plant fresh mass. Water is essential to nutrient transport, chemical reactions, cell enlargement, transpiration, and several other plant processes. Moisture deficit limits crop growth and development by inhibiting cellular growth, changing enzyme concentrations, and eventually affecting respiration, photosynthesis, and assimilate translocation (Gardner *et al.*, 1984).

Bednarz *et al.* (2002) stated that cotton grown in South Georgia requires about 460 mm of water for maximum yields. Although South Georgia receives about 600 mm of water during the growing season on average (Anonymous, 2006), periodic dry periods often cause crop water stress, which can be resolved by irrigation (Bednarz *et al.*, 2002). In Georgia, an estimated 640,000 acres of cotton are irrigated, mostly with overhead irrigation such as center pivots (Harrison, 2005).

In cotton, moisture deficit at varying levels reduces plant height, leaf area index (LAI), fruit production and retention, and ultimately impacts yield (Pettigrew, 2004). Ball *et al.* (1994) observed that cotton leaf expansion was highly sensitive to water stress, which supports the statement by Gardner *et al.* (1984) that tissue expansion is particularly sensitive to plant water status. The authors observed that root elongation was less sensitive to stress, and that root growth increased upon recovery from water stress. Dumka *et al.* (2004) attributed the enhanced root growth in plants recovering from water stress to delayed fruiting, and observed a shift in fruiting patterns on the plants that were water stressed. Another significant effect of water stress is the abscission of cotton fruiting structures in water stressed plants. Guinn and Mauney (1984) observed that severe water deficit during flowering causes an immediate loss of bolls and decreases future flowering. This can result in delayed maturity or decreased yield, depending on the plant's ability to compensate. The authors noted that suboptimal irrigation, on the other hand, had little effect on overall flowering and boll retention rates in their study, although it substantially decreased yield. This was attributed to poor maturation of bolls under water-stressed conditions.

Because tissue expansion and vegetative growth are affected prior to severe water stress, measurements of vegetative growth, such as remote sensing vegetative indices, may be capable

of detecting changes in water status in time to correct deficiencies. However, for these measurements to be effective, they must be sensitive to a wide range of vegetative cover and be as consistent as possible over time.

Remote Sensing and Crop Growth

Remote sensing has been used for decades as a large scale production tool for estimating and modeling crop growth (Ko *et al.*, 2006; Plant *et al.*, 2000; Roerink *et al.*, 1996; Yang *et al.*, 2001b). Full-season crop monitoring techniques can help cotton growers produce a quality crop and make management decisions for following years. However, for remote sensing to be effective for in-season irrigation management decisions, it must provide a quick, accurate method for identifying crop growth characteristics and detecting stress events (Roerink *et al.*, 1996).

Two types of remote sensing imagery are commonly used for monitoring crop growth and stress. Thermal imagery has been used to detect changes in crop temperature due to water or other stress (Cohen *et al.*, 2005; Pinter *et al.*, 2003), while combinations of visible and shortwave infrared imagery have primarily been used to detect changes in crop growth (Ahlrichs and Bauer, 1982; Boissard *et al.*, 1992; Bouman, 1992; Hinzman *et al.*, 1984; Huete, 1988; Ko *et al.*, 2006; Yang *et al.*, 2004).

Of these, reflectance imagery is less expensive. Shortwave reflectance has also been shown to be sensitive to leaf water content (Aldakheel and Danson, 1997; Danson *et al.*, 1992; Peñuelas *et al.*, 1997; Ripple, 1986), particularly , but field-scale measurements using reflectance regions sensitive to water are hampered by atmospheric moisture (ASD, 1999).

Cameras and spectrometers estimate plant health and growth by measuring reflected radiation at visible and near-infrared wavelengths. Plant reflectance is well-characterized. Chlorophyll

absorbance dominates plant reflectance, with anthocyanin and xanthophyll absorbance also contributing to reflectance (Sims and Gamon, 2002). Green leaves reflect little visible radiation, mostly in the green, but they reflect large portions of near-infrared radiation. The red edge forms a boundary between the visible and near-infrared, and is a region of rapidly increasing reflectance with wavelength. In contrast, soil reflectance tends to slope gently upward from the visible to the near-infrared. Whole plant reflectance is influenced by both leaf chlorophyll density and ground cover fraction. Therefore, soil reflectance, leaf chlorophyll density, and leaf area index (LAI; m^2 leaf area / m^2 ground area) all heavily influence crop reflectance.

Spectral indices maximize the spectral contribution from vegetation and minimize the effects of soil reflectance, usually through ratios or normalized ratios of visible and near-infrared reflectance (Huete *et al.*, 1985; Major *et al.*, 1990). These indices accurately estimate percent plant ground cover (the fraction of soil covered by plants) or leaf area index in many crops, because reflectance is highly correlated with leaf area even when plants are nitrogen- or water-stressed (Ritchie, 2003).

Although several reflectance regions throughout the shortwave infrared spectrum have been compared to crop health (for example, Osborne *et al.,* 2002), combinations of green, red, red edge, and near-infrared (NIR) reflectance have consistently produced many of the closest relationships with crop growth and health, due to chlorophyll absorbance and leaf mesophyll structure (Carter and Spiering, 2002; Gitelson and Merzlyak, 1998; Horler *et al.*, 1983). Additionally, indices based on these wavelengths allow the use of imaging devices with silicon photodetectors, which are less expensive than those made with materials that detect radiation above 1000 nm (ASD, 1999).

The most commonly used vegetation index to estimate LAI is the normalized difference vegetation index (NDVI), although there are several indices derived from the NDVI that are used to correct for soil or atmospheric effects (Gao, 1996; Huete, 1988; Huete *et al.*, 1985; Plant *et al.*, 2000) The NDVI consists of a normalized ratio of reflectance at a wavelength of interest and a reference wavelength in the form $(\lambda_{reference} - \lambda_{interest})/(\lambda_{reference} + \lambda_{interest})$, where λ is the wavelength. The reference wavelength is usually (but not always) in the near-infrared portion of the spectrum, since the near-infrared reflectance is not affected by chlorophyll (Curran, 1989). The most famous version of the NDVI uses red reflectance as the wavelength of interest (Rouse *et al.*, 1973), but ratios that include other wavelengths often estimate chlorophyll content more closely than red (Gitelson and Merzlyak, 1997).

Carter and Spiering (2002) noted that combinations of green or red edge reflectance and near-infrared reflectance had a broader range of spectral sensitivity than did indices based on red reflectance, while Gitelson and Merzlyak (1997) observed increased accuracy of ground cover estimates by using a combination of green and near-infrared reflectance. Conversely, DeTar *et al.* (2006) stated that combinations of near-infrared reflectance and red reflectance (λ = 686 nm) provided the most effective two-band estimates of growth changes in water stressed cotton. Peñuelas *et al.* (1997) suggested the use of a ratio of reflectance at 900 nm and 970 nm (a water absorption band) to estimate leaf water content.

Vegetation indices provide a robust method for identifying crop growth characteristics and detecting general stress events. Crop absorbance and reflectance are closely tied to biomass (Klassen *et al.*, 2003; Osborne *et al.*, 2002; Plant *et al.*, 2000), although Pinter *et al.* (2003) warned that most vegetation indices lack the ability to diagnose specific stresses or determine why biomass levels differ. However, the identification of stressed regions of a field allows

closer examination of the underlying causes, and remote sensing allows a closer examination of stressed locations. Therefore, timeliness and sensitivity to general plant stress are important remote sensing characteristics.

Irrigation and Remote Sensing

Remote sensing and variable application are less closely associated with water than with other plant amendments, due to the scarcity of field-scale variable rate irrigation systems. However, the increasing urban demands of water have made the water supply an important issue, and it is likely that water issues will continue to be dominant factors in future cotton production (Hutson, 2004). Efficient irrigation techniques that result in high cotton yields will allow cotton producers to maximize their yield potential for a given water supply.

The introduction of variable rate technology has been shown to increase the application efficiency of several crop amendments (Koch *et al.*, 2004; Yang *et al.*, 2001a) and is being used commercially. However, site-specific technology has only recently been introduced for irrigation (Perry *et al.*, 2002). Site-specific center pivot irrigation is unique from other site-specific application, because of the limited spatial resolution of the system. Irrigation decisions also require intensive crop moisture monitoring and quick irrigation decisions.

The cost and timeliness of sensors, imaging platforms, flyovers, and image analysis affect production-level remote sensing (Pinter *et al.*, 2003), and many of these costs are based on the system complexity. Remote sensing of plant stress for irrigation is unique in its need for rapid processing and decision making, as well as the dynamic crop growth characteristics related to water status. In-season analysis must be quick, simple, and sensitive enough to changes in vegetative growth to let the producer make irrigation decisions. Minimizing the costs and processing time is important, because producers faced with other production tasks may be

inclined to ignore the data until after the growing season if it is not delivered quickly and in a simple manner.

Remote Sensing Platforms

Remotely sensed imagery provides both spatial and temporal estimates of cotton crop growth and health (Plant *et al.*, 2000; Zarco-Tejada *et al.*, 2005). Most broad-scale remote sensing is provided via airplane or satellite imagery. Although its use in production agriculture is still somewhat limited due to factors such as cost, system complexity, timeliness, and the influence of atmospheric conditions, advances in remote sensing technology have made remote sensing a more economical and practical approach for crop management.

Current remote sensing platforms such as satellites, airplanes, and ground-based platforms are already used to obtain field-scale imagery with limited user intervention (Sui *et al.*, 2005; Vierling *et al.*, 2006; Yang *et al.*, 2001b; Yang *et al.*, 2003), helping growers produce a quality crop and make management decisions for following years.

Satellites and airplanes cover a broad spatial area (typically larger than a single irrigated field) with a single image. Aerial images measure reflected incident radiation from the sun and can be affected by atmospheric conditions (Jackson *et al.*, 1983).

Other intermediate platforms for both imagery and spectrometry, such as tethered blimps (Chen and Vierling, 2006; Vierling *et al.*, 2006) have been suggested. Advantages of these systems include price and scheduling flexibility, particularly for coverage of a few acres or less. However, the use of a spectrometer from a blimp requires extensive design to ensure an accurate field of view (Vierling *et al.*, 2006), and the tethered blimp is limited in how high it can be flown.

Ground-based reflectance on a field scale is based on individual reflectance measurements, usually collected at several points throughout the field. The measurements can be either passive (measurements of reflected sunlight) or active (measurements of reflected light from an electric light source). Passive measurements are sensitive to ambient lighting conditions, while active reflectance measurements often use a modulated light source to minimize the effects of ambient light, as described by Sui *et al.* (2005).

The Consumer Digital Camera

Consumer-level digital cameras can make remote sensing technology even more accessible by offering low cost, quick download times, and ease of use for imaging. Like spectrometers and research cameras, consumer cameras separate reflected radiation by wavelength (Adams *et al.*, 1998).

However, digital cameras have several unique characteristics that can affect the usefulness of these systems for agronomic management. Digital cameras designed for the consumer market are increasingly being used as research instruments due to their low cost and ease of use. Levin *et al.* (2005) demonstrated that a consumer-grade digital camera could be used to accurately measure visual spectral properties of soils, and consumer cameras have been used for imaging work in a variety of disciplines, including forestry (Inoue *et al.*, 2004), microscopy (Wunsam and Bowman, 2001), and even plastic reconstructive surgery (Galdino *et al.*, 2001).

However, off-the-shelf consumer grade cameras differ from research grade cameras and spectrometers, and these differences can affect the usefulness of the consumer cameras in agronomic remote sensing. Point and shoot characteristics can lead to misleading measurements by allowing imaging that does not quantify automatic adjustments that the camera makes.

Spectrometers often use filters or light dispersion to separate wavelengths of incoming radiation into discrete reflectance bands and are often equipped with wavelength-specific optics (Sui *et al.*, 2005). Though practical for research, this adds expense and complexity to the imaging system. Consumer cameras, on the other hand, are designed for ease of use. The filters are integrated within the camera sensor, as described by Adams *et al.* (1998).

Several parameters affect the camera image collection. Camera shutter speed controls the time incoming light makes contact with the sensor, while aperture (F-stop) controls the amount of light that can pass into the camera. Changes in aperture and shutter speed can compensate for each other, resulting in a standardized measure of exposure. Film speed (ISO) determines the sensitivity of the sensor to incoming radiation. White balance affects the color balance between red, green, and blue color channels. It allows the camera to correct hue and produce realistic looking pictures under cloudy conditions or electric lights.

Nearly all consumer cameras have completely automatic settings where the camera controls shutter, aperture, white balance, film speed, and contrast, allowing the user to point and shoot without adjusting settings. Mid-level consumer cameras (those with prices currently ranging from about $100 to $500) also have manual settings that allow the user to adjust some or all of these parameters. The cameras are designed to approximate a standardized measurement of human visual response (Sharma, 2003), and can have overlapping sensitivity between pixels that detect red, green, and blue (RGB) channels (Hong *et al.*, 2000; Wu *et al.*, 2000). There is currently no standardized method for adjusting camera color parameters, so RGB output differs by camera (Hong *et al.*, 2000).

Many of the features that are attractive for general use can compromise remote sensing work. For instance, the Nikon 4300 default settings include automatic corrections for exposure,

aperture, ISO number, and white balance (Nikon). In addition, these cameras use hot mirrors to minimize near-infrared (NIR) radiation transmission, limiting the camera spectral range to the visible spectrum (Chieng and Rahimzadeh, 2005). This prevents the influence of NIR radiation on the camera color channels, but also prevents the camera from sensing NIR radiation. The NIR region has long been associated with crop growth and health (Rabideau *et al.*, 1946), and is widely used for vegetation indices, such as those based on the ratio vegetation index (RVI) and the normalized difference vegetation index (NDVI) (Jordan, 1969; Rouse *et al.*, 1973).

Many of the point and shoot features in consumer grade cameras can confound spectral estimates. However, many of these features can be adjusted in the manual camera user settings. Features that should be locked include white balance, image adjustment, and ISO speed, since all of these features can affect the image exposure and channel balance. Aperture on the Nikon 4300 cannot be locked, and locking the shutter speed has a significant tradeoff. With a single shutter speed, changes in exposure can be eliminated as a source of image variation, but there is a risk of miscalculation of the correct shutter speed. A shutter speed that is set too fast will not allow sufficient image exposure, and a shutter speed that is set too slow will overexpose the image, resulting in image saturation. The use of one shutter speed limits the camera to a narrow dynamic range. A more robust solution would be the correction of images based on camera exposure, allowing images to be collected with a variety of exposure levels.

Making a camera NIR sensitive involves modification of the camera by replacing the hot mirror with a filter that transmits infrared rather than visible radiation. However, the procedure is often not too technically demanding (Chieng and Rahimzadeh, 2005), and the consumer camera might then be practical for the same remote sensing estimates as cameras designed for near-infrared imaging. This would require a separate camera for collection of visible channels, and the

cameras would require some method of exposure correction between cameras. A correction designed to compensate for changes in exposure might allow these cameras to be used as a viable remote sensing device, and because most successive camera models use similar optical systems, many of the principles applied to the specific camera will be similar to those of other camera models, particularly those in the same product line.

Research Objectives

The research for this dissertation was based on the following research objectives:

1. Determine the combinations of visible and near-infrared reflectance wavelengths most sensitive to cotton growth and leaf area index changes;
2. Develop a method for calibrating consumer-grade digital cameras to provide a consistent vegetation index (NDVI) measurements from visible and near-infrared brightness values;
3. Compare the sensitivity of ground-based and aerial vegetation indices for estimating crop ground cover; and
4. Evaluate an irrigation scheduling program based on detection of growth changes using vegetation indices.

These objectives are highly interrelated. Determining the combinations of visible and near-infrared reflectance wavelengths sensitive to the broadest range of cotton growth and leaf area index changes identifies an index that can be used at the maximum range of crop growth. This improves the sensitivity of the ground-based indices to estimate crop ground cover and detect changes in growth due to stress.

Developing a calibration method for combining digital cameras to ascertain NDVI allows the use of this index with a limited amount of user intervention, while allowing consistent measurements

throughout the growing season. It also allows a more appropriate comparison between an index based only on visible channels with an index based on visible and near-infrared channels. Finally, comparing the sensitivity of ground-based and aerial vegetation indices to crop growth allows the identification of limiting factors in each system for detecting growth changes based on these indices.

References

Adams, J., K. Parulski, and K. Spaulding. 1998. Color processing in digital cameras. Micro IEEE 18:20-30.

Ahlrichs, J.S., and M.E. Bauer. 1982. Relation of agronomic and multispectral reflectance characteristics of spring wheat canopies. LARS Technical Report 121082:26p. Purdue University, Lafayette, IN.

Aldakheel, Y.Y., and F.M. Danson. 1997. Spectral reflectance of dehydrating leaves: measurements and modelling. Int. J. Remote Sens. 18:3683-3690.

Anonymous. 2006. Camilla 3 SE, Georgia (091500): Period of record monthly climate summary. Southeast Regional Climate Center.

ASD. 1999. Analytical Spectral Devices, Inc. technical guide. 3rd ed., Boulder, Colorado.

Ball, R.A., D.M. Oosterhuis, and A. Mauromoustakos. 1994. Growth dynamics of the cotton plant during water-deficit stress. Agron. J. 86:788-795.

Bednarz, C.W., J.E. Hook, R. Yager, S. Cromer, D. Cook, and I. Griner. 2002. Cotton crop water use and irrigation scheduling, p. 61-64, *In* A. S. Culpepper, ed. 2002 Georgia Cotton Research-Extension Report.

Boissard, P., J.-G. Pointel, and J. Tranchefort. 1992. Estimation of the ground cover ratio of a wheat canopy using radiometry. Int. J. Remote Sens. 13:1681-1692.

Bouman, B.A.M. 1992. Accuracy of estimating the leaf area index from vegetation indices derived from crop reflectance characteristics, a simulation study. Int. J. Remote Sens. 13:3069-84.

Carter, G.A., and B.A. Spiering. 2002. Optical properties of intact leave for estimating chlorophyll concentration. J. Environ. Qual. 31:1424-1432.

Chen, X., and L. Vierling. 2006. Spectral mixture analyses of hyperspectral data acquired using a tethered balloon. Remote Sens. Environ. 103:338-350.

Chieng, C., and A. Rahimzadeh. 2005. Hacking Digital Cameras. Wiley Publishing, Inc., Indianapolis.

Cohen, Y., V. Alchanatis, M. Meron, Y. Saranga, and J. Tsipris. 2005. Estimation of leaf water potential by thermal imagery and spatial analysis. J. Exp. Bot. 56:1843-1852.

Curran, P.J. 1989. Remote sensing of foliar chemistry. Remote Sens. Environ. 30:271-278.

Danson, F.M., M.D. Steven, T.J. Malthus, and J.A. Clark. 1992. High-spectral resolution data for determining leaf water content. Int. J. Remote Sens. 13:461-470.

DeTar, W.R., J.V. Penner, and H.A. Funk. 2006. Airborne remote sensing to detect plant water streess in full canopy cotton. Transactions - American Society of Agricultural and Biological Engineers 49:655-665.

Dumka, D., C.W. Bednarz, and B.W. Maw. 2004. Delayed Initiation of Fruiting as a Mechanism of Improved Drought Avoidance in Cotton. Crop Sci 44:528-534.

Galdino, G.M., J.E. Vogel, and C.A.V. Kolk. 2001. Standardizing digital photography: It's not all in the eye of the beholder. Plastic & Reconstructive Surgery 108:1334-1344.

Gao, B.-C. 1996. NDWI -- a normalized difference water index for remote sensing of vegetation liquid water from space. Remote Sens. Environ. 58:257-266.

Gardner, F.P., R.B. Pearce, and R.L. Mitchell. 1984. Physiology of crop plants. 1st ed. Iowa State Press.

Gitelson, A.A., and M.N. Merzlyak. 1997. Remote estimation of chlorophyll content in higher plant leaves. Int. J. Remote Sens. 18:2691-2697.

Gitelson, A.A., and M.N. Merzlyak. 1998. Remote sensing of chlorophyll concentration in higher plant leaves. Adv. Space Res. 22:689-692.

Guinn, G., and J.R. Mauney. 1984. Fruiting of cotton. II. Effects of plant moisture status and active boll load on boll retention. Agron. J. 76:94-98.

Harrison, K. 2005. Irrigation Survey, 2005. The University of Georgia College of Agricultural and Environmental Sciences Cooperative Extension Service.

Hinzman, L.D., M.E. Bauer, and C.S.T. Daughtry. 1984. Growth and Reflectance Characteristics of Winter Wheat Canopies 111484. Laboratory for Applications of Remote Sensing, Purdue University, West Layfayette, IN.

Hong, G., M.R. Luo, and P.A. Rhodes. 2000. A study of digital camera colorimetric characterization based on polynomial modeling. Color Research and Application 26:76-84.

Horler, D.N.H., M. Dockray, J. Barber, and A.R. Barringer. 1983. Red edge measurements for remotely sensing plant chlorophyll content. Adv. Space Res. 3:273-277.

Huete, A.R. 1988. A soil-adjusted vegetation index (SAVI). Remote Sens. Environ. 25:295-309.

Huete, A.R., R.D. Jackson, and D.F. Post. 1985. Spectral response of a plant canopy with different soil backgrounds. Remote Sens. Environ. 17:37-53.

Hutson, S.S., N.L. Barber, J.F. Kenny, K.S. Linsey, D.S. Lumia, and M.A. Maupin. 2004. Estimated use of water in the United States in 2000. U.S. Dept. of the Interior, U.S. Geological Survey ; Denver, CO : For sale by U.S. Geological Survey, Branch of Information Services, Reston, Va.

Inoue, A., K. Yamamoto, N. Mizoue, and Y. Kawahara. 2004. Effects of image quality, size and camera type on forest light environment estimates using digital hemispherical photography 126:89-97.

Jackson, R.D., P.N. Slater, and P.J. Pinter. 1983. Discrimination of growth and water stress in wheat by various vegetation indices through clear and turbid atmospheres. Remote Sens. Environ. 13:187-208.

Jordan, C.F. 1969. Derivation of leaf area index from quality of light on the forest floor. Ecology 50:663-666.

Jost, P.H., J.R. Whitaker, S.M. Brown, and C.W. Bednarz. 2006. Use of plant growth regulators as a management tool in cotton, *In* U. o. G. C. Extension, (ed.).

Klassen, S.P., G. Ritchie, J. Frantz, D. Pinnock, and B. Bugbee. 2003. Real-time imaging of ground cover: Relationships with radiation capture, canopy photosynthesis, and daily growth rate. In: Digital Imaging and Spectral Techniques: Applications to Precision Agriculture and Crop Physiology. ASA Special Publication no. 66.

Ko, J., S.J. Maas, S. Mauget, G. Piccinni, and D. Wanjura. 2006. Modeling water-stressed cotton growth using within-season remote sensing data. Agron. J. 98:1600-1609.

Koch, B., R. Khosla, W.M. Frasier, D.G. Westfall, and D. Inman. 2004. Economic Feasibility of Variable-Rate Nitrogen Application Utilizing Site-Specific Management Zones. Agron. J. 96:1572-1580.

Levin, N., E. Ben-Dor, and A. Singer. 2005. A digital camera as a tool to measure colour indices and related properties of sandy soils in semi-arid environments. Int. J. Remote Sens. 26:5475-5492.

Major, D.J., F. Baret, and G. Guyot. 1990. A ratio vegetation index adjusted for soil brightness. Int. J. Remote Sens. 11:727-740.

Nikon, U.S.A. 2004. Nikon Coolpix 4300 [Online] http://www.nikonusa.com/specs/25507.pdf (posted January 15, 2007).

Osborne, S.L., J.S. Schepers, D.D. Francis, and M.R. Schlemmer. 2002. Use of spectral radiance to estimate in-season biomass and grain yield in nitrogen- and water-stressed corn. Crop Sci. 42:165-171.

Peñuelas, J., J. Piñol, R. Ogaya, and I. Filella. 1997. Estimation of plant water concentration by the reflectance water index WI (R900/R970). Int. J. Remote Sens. 18:2869-2875.

Perry, C.D., S. Pocknee, O. Hansen, C. Kvien, G. Vellidis, and E. Hart. 2002. 2002 ASAE Annual International Meeting / CIGR 15th World Congress, Chicago, IL.

Pettigrew, W.T. 2004. Physiological consequences of moisture deficit stress in cotton. Crop Sci. 44:1265-1272.

Pinter, P.J., J.L. Hatfield, J.S. Schepers, E.M. Barnes, M.S. Moran, C.S.T. Daughtry, and D.R. Upchurch. 2003. Remote sensing for crop management. Photogrammetric Engineering & Remote Sensing 69:647-664.

Plant, R.E., D.S. Munk, B.R. Roberts, R.L. Vargas, D.W. Rains, R.L. Travis, and R.B. Hutmacher. 2000. Relationships between remotely sensed reflectance data and cotton growth and yield. Trans. ASAE 43:535-546.

Rabideau, G.S., C.S. French, and A.S. Holt. 1946. The absorption and reflection spectra of leaves, chloroplast suspensions, and chloroplast fragments as measured in an Ulbricht Sphere. Am. J. Bot. 33:769-777.

Ripple, W.J. 1986. Spectral reflectance relationships to leaf water stress. Photogramm. Eng. Remote Sens. 52:1669-1675.

Ritchie, G.L. 2003. Use of ground-based canopy reflectance to determine radiation capture, nitrogen and water status, and final yield in wheat, Utah State University, Logan, Utah.

Roerink, G.J., W.G.M. Bastiaanssen, J. Chambouleyron, and M. Menenti. 1996. Relating Crop Water Consumption to Irrigation Water Supply by Remote Sensing. Water Resources Management 11:445-465.

Rouse, J.W., R.H. Haas, J.A. Schell, and D.W. Deering. 1973. Monitoring vegetation systems in the great plains with ERTS, p. 309-317. Third ERTS Symposium, NASA SP-351, Vol. 1. NASA, Washington, DC.

Sharma, G. 2003. Digital Color Imaging Handbook. CRC Press.

Sims, D.A., and J.A. Gamon. 2002. Relationships between leaf pigment content and spectral reflectance across a wide range of species, leaf structures and developmental stages. Remote Sens. Environ. 81:337-354.

Sui, R., J.B. Wilkerson, W.E. Hart, L.R. Wilhelm, and D.D. Howard. 2005. Multi-spectral sensor for detection of nitrogen status in cotton. Applied Engineering in Agriculture 21:167-172.

Vierling, L., M. Fersdahl, X. Chen, Z. Li, and P. Zimmerman. 2006. The short-wave aerostat-mounted imager (SWAMI): A novel platform for acquiring remotely sensed data from a tethered balloon. Remote Sens. Environ. 103:255-264.

Wu, W., J.P. Allebach, and M. Analoul. 2000. Imaging colorimetry using a digital camera. J. Imaging Sci. Technol. 44:267-279.

Wunsam, S., and J.C. Bowman. 2001. Economical digital photomicroscopy. Journal of Paleolimnology 25:399-403.

Yang, C., J.H. Everitt, and J.M. Bradford. 2001a. Comparisons of uniform and variable rate nitrogen and phosphorus fertilizer applications for grain sorghum. Trans. ASAE 44:193-200.

Yang, C., J.M. Bradford, and C.L. Wiegand. 2001b. Airborne multispectral imagery for mapping variable growing conditions and yields of cotton, grain sorghum, and corn. Trans. ASAE 44(6):1983-1994.

Yang, C., J.H. Everitt, and J.M. Bradford. 2004. Airborne hyperspectral imagery and yield monitor data for estimating grain sorghum yield variability. Trans. ASAE 47:915-924.

Yang, C., S.M. Greenberg, J.H. Everitt, T.W. Sappington, and J. J.W. Norman. 2003. Evaluation of cotton defoliation strategies using airborne multispectral imagery. Trans. ASAE 46:869-876.

Zarco-Tejada, P.J., S.L. Ustin, and M.L. Whiting. 2005. Temporal and spatial relationships between within-field yield variability in cotton and high-spatial hyperspectral remote sensing imagery. Agron. J. 97:641-653.

CHAPTER 2

ESTIMATING DEFOLIATION OF TWO DISTINCT COTTON TYPES WITH REFLECTANCE DATA[1]

[1] Ritchie, G.L., and C.W. Bednarz. 2005. Estimating defoliation of two distinct cotton types using reflectance data. Journal of Cotton Science 9:182-188. Reprinted here with permission of publisher.

Abstract

Cotton defoliation is an important part of cotton harvest preparation. Estimates of cotton defoliation allow producers to monitor harvest readiness and make further defoliation decisions as necessary. However, visual estimates are subjective and may differ from one reviewer to the next. Here, we propose a spectrometric method for quantifying cotton defoliation. In 2003 and 2004, leaf area index (LAI) was monitored on 0.91 m sections of row of multiple environments to quantify percent defoliation. Reflectance over each plot was measured using a narrow-band spectrometer, and normalized difference vegetation index (NDVI) models composed of reflectance at all wavelengths were regressed against LAI to determine which wavelengths most accurately estimated changes in LAI. Both linear and quadratic models were tested for their usefulness in estimating LAI. Quadratic models more accurately estimated LAI in the red spectral region than did linear models, but reached maximum values at an LAI of about 1.5. Therefore, the quadratic models were of limited usefulness. At the red edge (about 705 nm to 720 nm), the quadratic and linear models had similar coefficients of determination, which were higher than those derived from linear models in other wavelengths. These results suggest that reflectance indices based on red edge measurements can offer accurate, consistent defoliation estimates, and could potentially increase defoliation efficiency and decrease costs.

KEYWORDS

Remote sensing; leaf area index; wavelength; red edge

Introduction

Cotton producers chemically defoliate their crop to terminate its growth and prepare it for machine harvest. Defoliation gives the producer some control over harvest timing and increases harvest efficiency. However, cotton variety and growing conditions influence the effectiveness of these chemicals. Some conditions require two applications for proper defoliation, especially on irrigated cotton. The timing of the second application is generally based on the effectiveness of the first application, and most defoliation estimates are based on visual observations. Although estimates allow cotton producers to determine the success of their strategy and decide on further management strategies, visual estimates are subjective and therefore can vary. Remote sensing can automate and standardize these estimates (Yang *et al.*, 2003).

Cameras and spectrometers estimate plant health and growth by measuring reflected radiation at visible and near-infrared wavelengths. Plant reflectance is well-characterized, with most of the reflectance characteristics based on the spectral properties of chlorophylls and carotenoids (Sims and Gamon, 2002). Chlorophylls exhibit strong absorption of blue and red light, while carotenoids primarily absorb blue light (Gitelson *et al.*, 2002). In green plants, chlorophyll absorbance dominates leaf reflectance. Green leaves reflect little visible radiation because of the heavy absorbance of red and blue radiation by chlorophyll, but they reflect large portions of near-infrared radiation (Fig. 2.1). The red edge forms a boundary between the visible and near-infrared, and is a region of rapidly increasing reflectance with wavelength. In contrast, soil reflectance tends to slope gently upward from the visible to the near-infrared.

Assuming atmospheric effects are minimized, three factors affect the reflectance of a cotton crop at each place in a field: soil reflectance, the chlorophyll density in each leaf, and the leaf area. Spectral indices maximize the spectral contribution from vegetation and minimize the

effects of soil reflectance, usually through visible and near-infrared reflectance ratios (Huete *et al.*, 1985; Major *et al.*, 1990). These indices accurately estimate percent plant ground cover (the fraction of soil covered by plants) or leaf area index (LAI; m^2 leaf area / m^2 ground area) in many crops, because reflectance is highly correlated with leaf area even if plants are nitrogen- or water-stressed (Ritchie, 2003).

The normalized difference vegetation index (NDVI) is widely used to estimate LAI. The NDVI consists of a normalized ratio of reflectance at a wavelength of interest and a reference wavelength in the form $(\lambda_{reference} - \lambda_{interest})/ (\lambda_{reference} + \lambda_{interest})$, where λ is the wavelength. The reference wavelength is often (but not always) in the near-infrared portion of the spectrum, since the near-infrared reflectance is not affected by chlorophyll (Curran, 1989). One commonly used version of the NDVI uses red reflectance as the wavelength of interest, but ratios that include other wavelengths often estimate chlorophyll content more closely than red (Gitelson and Merzlyak, 1997).

Although defoliation estimates should be similar to general ground cover estimates, there are few reports in the literature about using this technology for estimating defoliation. Yang *et al.* (2003) tested airborne color-infrared digital images obtained from an airplane as one method for estimating the success of several defoliation regimes. However, the study focused on differentiating treatments rather than estimating LAI, and leaf area data were collected only near the conclusion of their study. The study showed that differences in defoliation level can be identified by remote sensing, but they did not quantify these differences.

The objective of this study was two-fold. The first goal was to quantify defoliation level based on reflectance data and identify the spectral regions that most appropriately estimate LAI

before and during the defoliation process. The second was to compare LAI estimates using NDVI with human defoliation estimates.

Materials and Methods

Studies were conducted in four cotton fields at three locations (Coastal Plain Experiment Station Ponder Farm, Gibbs Farm, and a locally rented field called the Water Tower Field) in 2003. All three locations are in Tift County, Georgia. The Water Tower Field was planted with Delta&Pineland 555 BG/RR cotton with rows running east to west. One field at the Ponder Farm was planted with Delta&Pineland 555 BG/RR cotton with rows running north and south, and another one was planted with Stoneville 4892 BG/RR cotton with rows running north to south. The Gibbs Farm field was planted with Stoneville 4892 BG/RR cotton with rows running east to west. The soil series for all three fields is a Tifton loamy sand (fine-loamy, kaolinitic, thermic Plinthic Kandiudults). A comprehensive defoliation treatment of 110 g ha^{-1} thidiazuron (DROPP), 1.5 L ha^{-1} ethephon, and 0.44 L ha^{-1} tribufos (DEF 6) was applied when 75% of the cotton bolls were open using a Spider sprayer (West Texas Lee, Inc., Idalou, TX) with TeeJet 8002 spray nozzles (Spraying Systems Co., Wheaton, IL). In this study, the cotton LAI before defoliant was applied ranged from 1.0 (sparse cotton) to slightly over 2.0 (rank cotton). Reflectance was measured at each field prior to defoliant application, then at 1 to 3 day intervals until the plants were completely defoliated. The cotton was sampled on four dates in the Water Tower Field, and on three dates in the other fields.

Four plots were chosen at random on each sampling date at each site. Plots were marked using bicycle flags prior to sampling. Reflectance was measured at 1 m above the row center at each plot using a PAR/NIR spectrometer (Apogee Instruments, Logan, UT) with a fiber optic cable with a 30E full angle field of view. Two sample readings were recorded from 0.91 m (3 ft)

of row and averaged to give an estimate of LAI. Leaves were then removed from the plants in the 0.91 m of row, and leaf area was measured with a leaf area meter (Model LI-3100C, LI-COR Environmental, Lincoln, NE).

Reflectance characteristics of each plot were compared with leaf area using regression analysis of NDVI vs. LAI at all wavelengths to determine which wavelengths were most suitable for defoliation estimates. Linear and quadratic best-fit equations were calculated in Microsoft Excel. After data sets were analyzed for each field and determined to not have significantly different slopes or intercepts, then pooled to determine an overall model that would be most appropriate for estimating LAI.

In 2004, four human volunteers estimated defoliation rate at the Gibbs farm in a field of Delta&Pineland 555 BG/RR at sixteen randomly chosen places in the field with varying defoliation on three dates, and these estimates were regressed against LAI. The volunteers each had at least two years of cotton defoliation estimation experience and five years or more of leaf area estimating experience. Prior to the volunteers making their estimates, one of the volunteers was invited to give estimates of percent defoliation at both low and high LAI to allow all of the volunteers to base defoliation estimates off the same general scale. The NDVI was also regressed against LAI to verify the accuracy of the model determined in 2003, as well as compare NDVI with human observation for determining percent defoliation.

Results and Discussion

The correlation or goodness of fit was based on the coefficient of determination (r^2) of NDVI vs. LAI. The coefficient of determination is a measure of the fraction of variance of the dependent variable that is explained by the independent variable. LAI was chosen as the independent

variable, although for linear equations with one x and one y variable, the coefficient of determination does not change based on which is the independent variable.

A comparison between NDVI and LAI for all wavelengths for the pooled data from 2003 suggested the strongest correlations existed when one of the wavelengths is between 750 and 850 nm and other wavelength is between 705 and 720 nm (Fig. 2.2). The correlations showed the same trend regardless of which wavelength was designated λ_1 and which was designated λ_2, because reversing λ_1 and λ_2 merely gives positive and negative values of the same number. It was also observed that the highest correlations were obtained in relationships to visible wavelengths when part of the NDVI included a wavelength between 750 and 850 nm. Tarpley *et al.* (2000) and Read *et al.* (2002) observed similar trends in nitrogen estimation at both the cotton leaf and canopy levels. Leaf nitrogen content and LAI are both closely related to chlorophyll content, so it is reasonable that the same trends are observed for studies of both LAI and nitrogen content. It is useful to note that even with the potentially confounding influence of leaf chlorophyll content in plants approaching the end of their life cycle, high correlations were observed between LAI and NDVI.

This high correlation was observed at each test site, with the highest r^2 between reflectance indices and LAI for each field ranging from 0.82 to 0.96 for individual fields and 0.83 for the pooled data (Fig. 2.3). All fields except the Gibbs field had maximum r^2 values above 0.90.

As observed in Fig. 2.2, correlations between NDVI and LAI were wavelength dependent: In Fig. 2.3, LAI had a higher linear correlation with NDVI values calculated from the red edge (highest $r^2 = 0.83$) than with NDVI values calculated from the green (highest $r^2 = 0.73$) and red spectral regions (highest $r^2 = 0.79$).

Quadratic LAI estimates had higher r^2 values in the green and red spectral regions than linear estimates, and were similar to quadratic estimates at the red edge (Fig. 2.4). However, a notable difference between quadratic LAI estimates derived from the red region and those at the red edge was the range of the quadratic model. The high coefficients of determination (r^2) for the quadratic models based on the red wavelengths were misleading, because the curves became asymptotic at the highest LAI (Fig. 2.5). The result for each of these wavelengths was a curve with a high r^2, but little usefulness above a certain LAI. As shown in Fig. 2.6, the quadratic model derived from red edge data gave a higher leaf area estimate at high ground cover levels and a lower leaf area estimate at low levels of ground cover than did the quadratic model derived from the red region. This difference suggests that red edge model is superior to the red model over the full range of LAI encountered in this study.

Carter and Spiering (2002) noted that vegetation indices and chlorophyll content in single intact leaves had maximum r^2 values at the red edge, similar to results from our field study. However, they observed that r^2 values in green were comparable with values at the red edge, while those in the red were very low. In contrast, we observed that r^2 values based on ratios of green reflectance were lower than those based on the red and the red edge portions. Part of this apparent contradiction can be explained by the difference in single leaf and plant canopy reflectance measurements. In a single leaf, chlorophyll absorbance saturates at low leaf chlorophyll contents, because the sensor views only the leaf. Conversely, cotton canopy LAI estimates are relatively unaffected by leaf chlorophyll content. Instead, the dominant factor is the suppression of ground reflectance and the emergence of leaf reflectance in a scene with increasing LAI. This increases the dynamic range of ratios that use red reflectance, so they can cover a moderate range of LAI. However, this study suggests that the ratios that include the red

edge cover a wider dynamic range than those based on red reflectance, even when viewing an entire cotton canopy. It is unclear why green reflectance does not indicate LAI as well as red reflectance.

The 2004 spectral estimates of LAI were consistent with the 2003 findings. The highest linear r^2 between NDVI and LAI was 0.90 and occurred at about 710 nm. The pooled data for 2003 and 2004 also showed the same trend, with the highest r^2 value of 0.83 occurring at about 710 nm. This high correlation value using data from two cropping seasons and two cotton varieties suggests that NDVI using a reference wavelength of 710 nm can provide a stable, consistent method for estimating LAI during the process of defoliation.

Estimates of percent defoliation by human reviewers yielded r^2 values with LAI for each person, but estimates of percent defoliation between people varied widely, especially at higher LAI (Fig. 2.7).

General estimates of percent defoliation showed good correlation with LAI when compared to all LAI values, with r^2 values ranging from 0.73 to 0.96 (Table 1). Table 1 shows that coefficients of determination at low LAI (below 0.5) also tended to be high, ranging from 0.55 to 0.87. However, estimates of defoliation at LAI greater than 0.5 revealed some of the inherent weaknesses in human defoliation ratings. One of the reviewers reported defoliation values that did not show a significant correlation with LAI (reviewer 2; $r^2 = 0.03$), and one reported defoliation values that trended up rather than down with LAI (reviewer 1; slope = 18.2). Two of the reviewers estimated defoliation with r^2 values similar to those of the NDVI method at both high and low LAI. Both of these reviewers reported defoliation values that had r^2 values above 0.48 (reviewer 3 $r^2 = 0.81$; reviewer 4 $r^2 = 0.48$) and similar slopes at both low and high LAI.

Another issue in visual determination of percent defoliation was evident in the wide range of defoliation estimates at higher LAI. For instance, reviewer estimates of percent defoliation at LAI = 0.89 ranged from 15% defoliation to 65% defoliation. This wide range of estimates suggests that it would be difficult to compare defoliation estimates directly between reviewers. Part of this problem can be attributed to differing opinions as to what amount of leaf area constitutes a 0 level of defoliation. A leafy cotton canopy will require some level of defoliation to reach a similar LAI to that of a less leafy cotton canopy that has not been defoliated. Therefore, it is difficult to define what even constitutes percent defoliation. Furthermore, it is more complex to rate plants with more leaf area, and there is a greater chance for error. It makes sense, therefore, to tie defoliation estimates to a standardized estimate of LAI, such as spectral measurements.

Overhead leaf area estimates can be based on several scales of view, from ground-level measurements to satellite imagery. Each scale offers unique challenges. Ground-based measurements do not require an aerial platform, and the sensors can be mounted on tractors or other field equipment. However, near-remote measurements only cover a small ground area, and are sensitive to sensor height and plant height. Other issues, such as platform cost and atmospheric interference can also significantly affect management strategies with aerial and satellite imagery. Aerial and satellite platforms are often at the mercy of weather conditions, and the turnaround time from data acquisition to data release can be prohibitive for use in defoliation scheduling.

Another pertinent concern is the influence of senesced or dehisced leaves on leaf area and harvestability estimates. Because these leaves have lost the majority of their chlorophyll, they do not have the characteristic chlorophyll reflectance seen in healthy leaves. Most of these leaves

fall to the ground, but many, particularly when the producer uses a dehiscent, remain on the plant until harvest. We did not encounter significant numbers of dehisced leaves in our studies, but this issue might need to be addressed on a case-by-case basis.

Conversely, green leaves that fall from the plant could potentially cause an overestimation of LAI when using NDVI. This can often be attributed to using a "green leaf defoliant" (e.g. a mixture of cyclanilide and ethephon), or simply due to wind or other mechanical removal of leaves. In our study, green leaves on the ground were not removed prior to spectral measurements, and this may have been a source of some of the variability in NDVI measurements. However, this effect may be minimized by at least two factors. The first is the rapid loss of water and breakdown of chlorophyll in senesced leaves (Daughtry and Biehl, 1985). The second is the decreased influence of each leaf in the spectral scene based on its distance from the sensor, a principle that is discussed by Klassen *et al.* (2003). The change in spectral influence would be greater if the sensor is close to the cotton plant.

The use of a spectral system for estimating defoliation would advance defoliation work in several areas. First, standardized estimates based on spectral changes would allow consistent estimates of defoliation both spatially and temporally. This might help quantify the effects of different conditions on defoliation rates. Defoliation estimates could also be performed on a larger scale, and defoliation might be performed as a variable rate application based on georeferenced LAI estimates. This could potentially improve efficiency of defoliant applications, as well as decrease application rates.

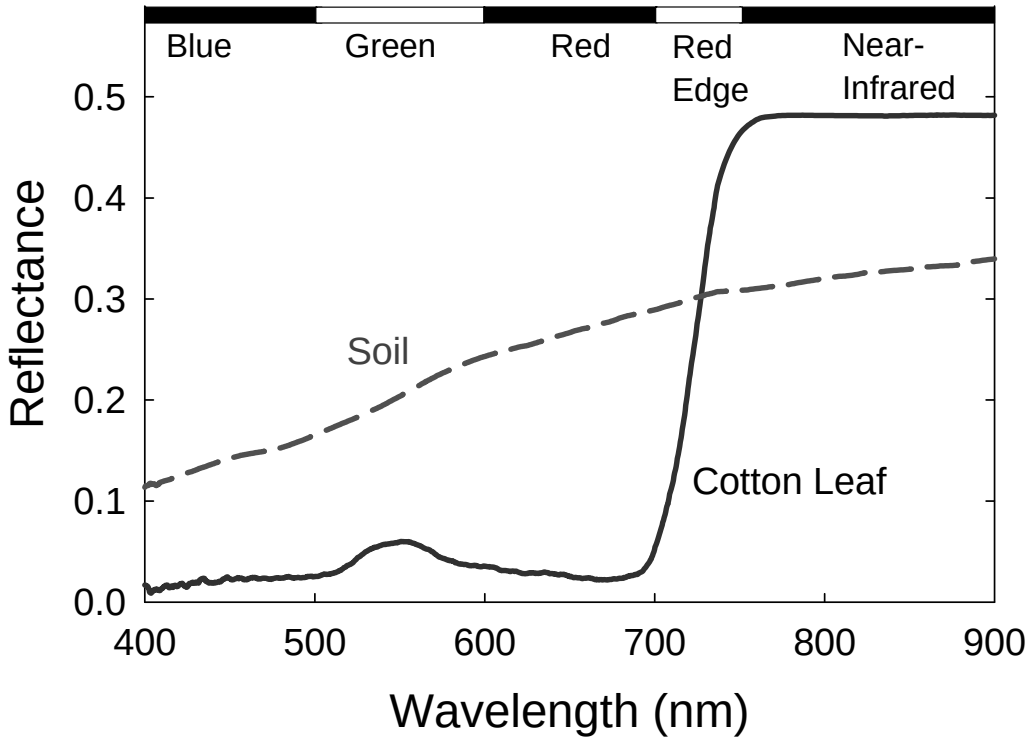

Fig. 2.1. Characteristic leaf and soil reflectance at different wavelengths from 400-900 nm.

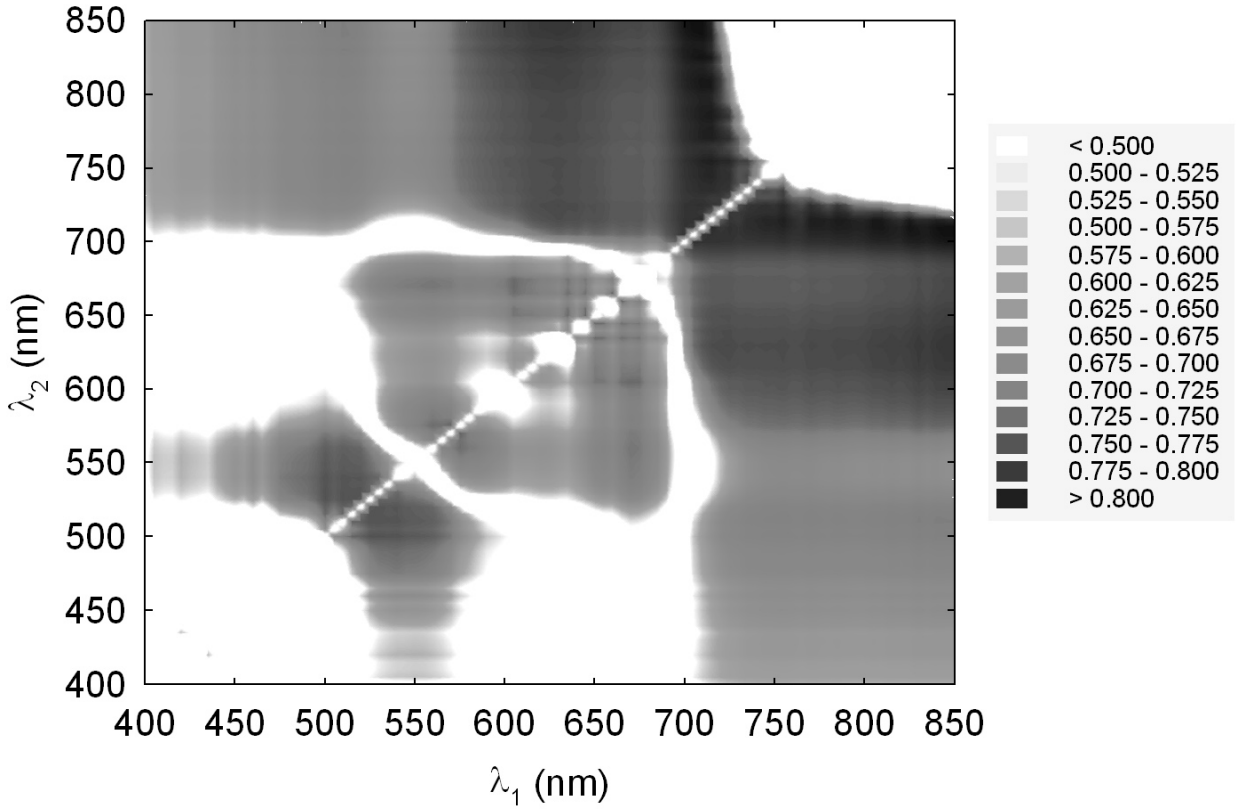

Fig. 2.2. Coefficient of determination (r^2) for the relationships between LAI and two-band combinations in the NDVI equation $(\lambda_2 - \lambda_1)/(\lambda_2 + \lambda_1)$ during the 2003 season. The regions with the highest r^2 values consisted of combinations of wavelengths at the red edge (700-715 nm) and near-infrared (750-850 nm) regions of the spectrum.

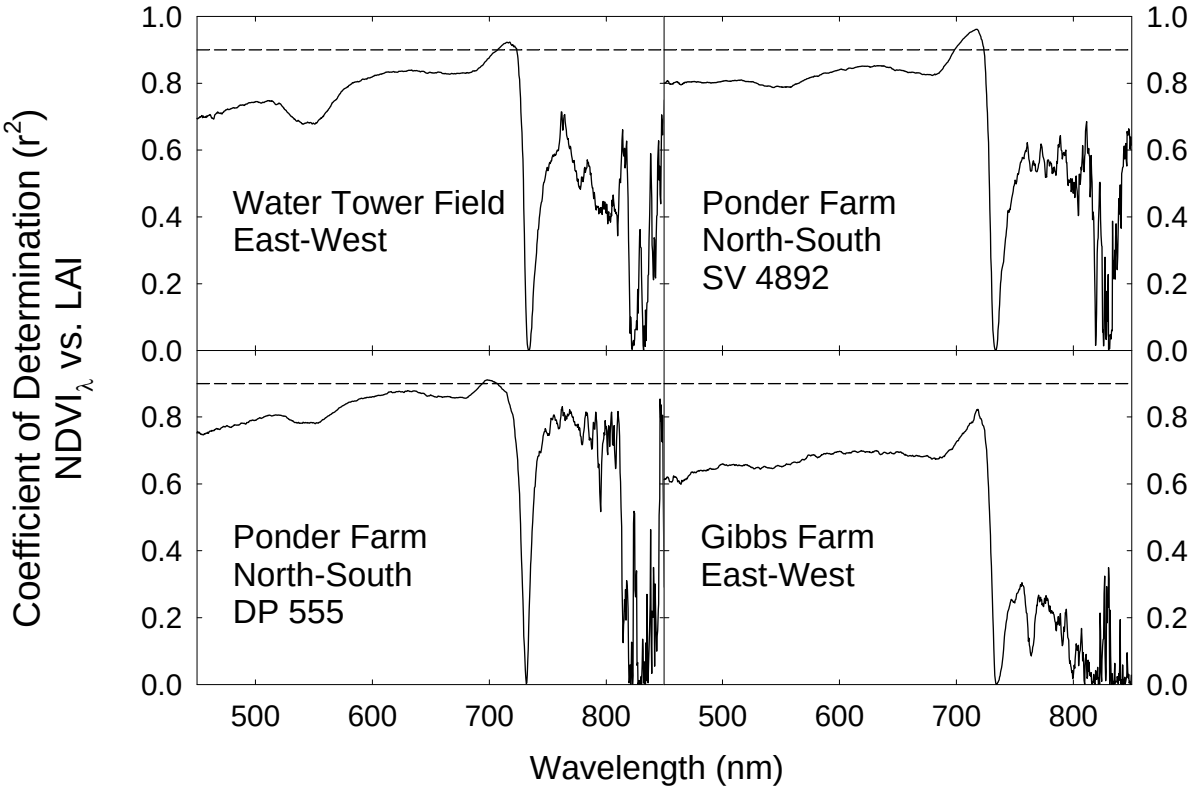

Fig. 2.3. Coefficient of determination (r^2) of NDVI by wavelength of interest (8) for each field in the 2003 defoliation trial. The reference wavelength (λ_1) was an average of reflectance between 800-850 nm, and the wavelength of interest (λ_2) appears on the horizontal axis. The dashed line represents an r^2 of 0.90.

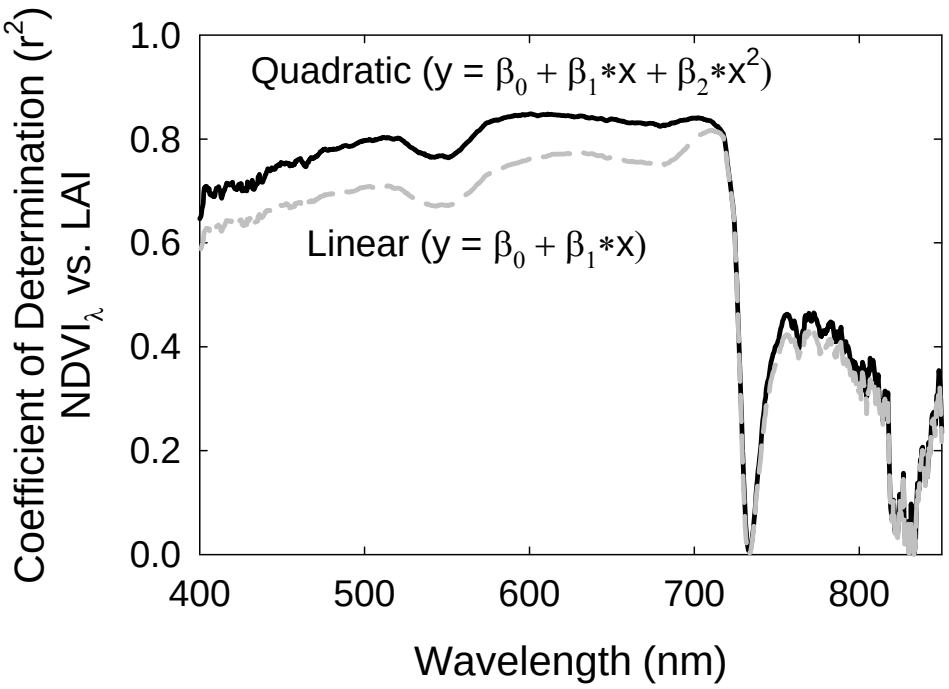

Fig. 2.4. Coefficient of determination (r^2) vs. wavelength for linear (gray line) and quadratic (black line) relationships of cotton canopy reflectance with leaf area index from the 2003 study. Coefficients were derived at each wavelength for 51 leaf area samples.

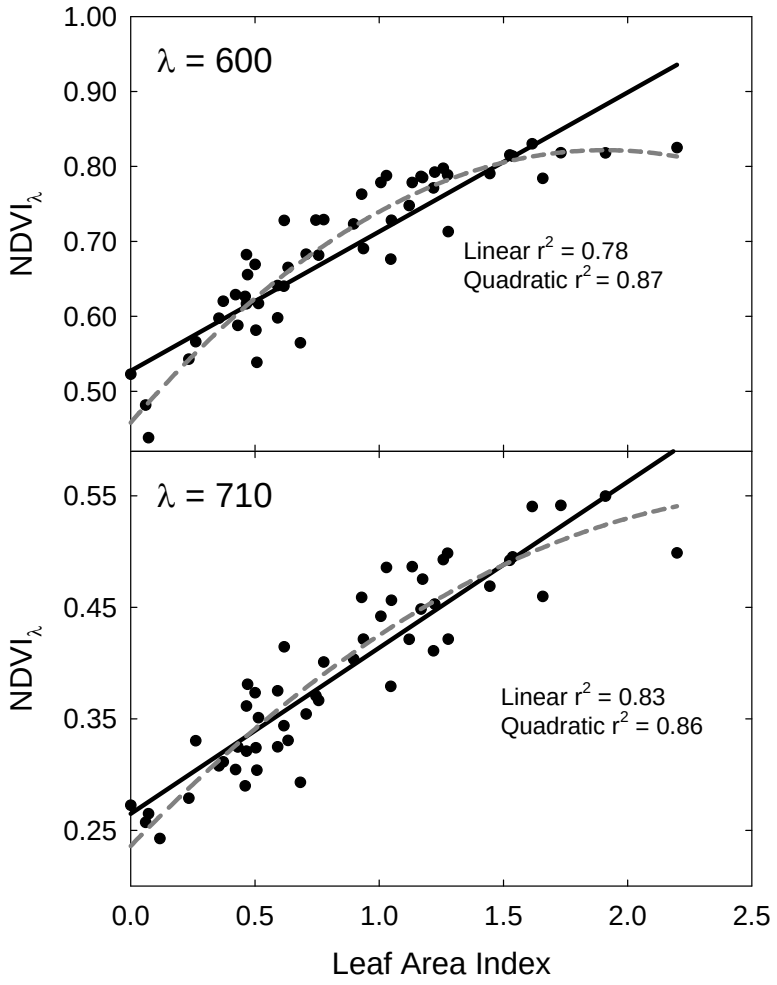

Fig. 2.5. Comparing the fit of linear (solid line) and quadratic (dashed line) equations for NDVI vs. leaf area index at 600 nm and 710 nm. NDVI based on a wavelength in the red region reached a maximum at a LAI of about 1.5, while NDVI based on a wavelength at the red edge continued to slope upward at higher LAI levels.

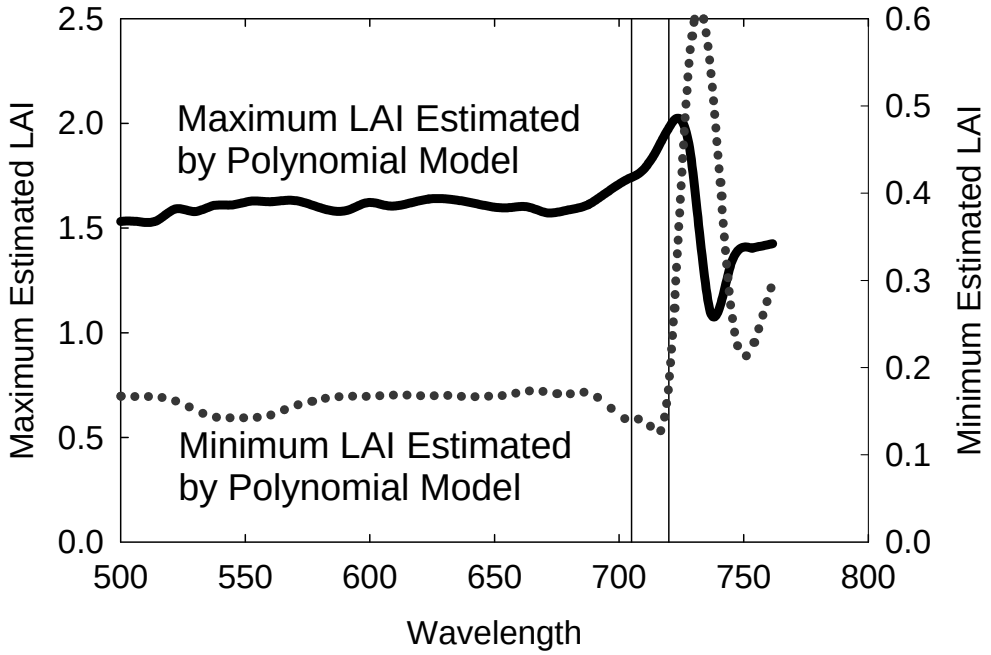

Fig. 2.6. Comparison of NDVI by wavelength as an estimate of LAI. The best spectral indicator of LAI should give a low minimum estimated LAI and a high maximum LAI. Based on this principle, the spectral region between 705 nm and 720 nm (vertical lines) yielded the best estimates of high and low NDVI.

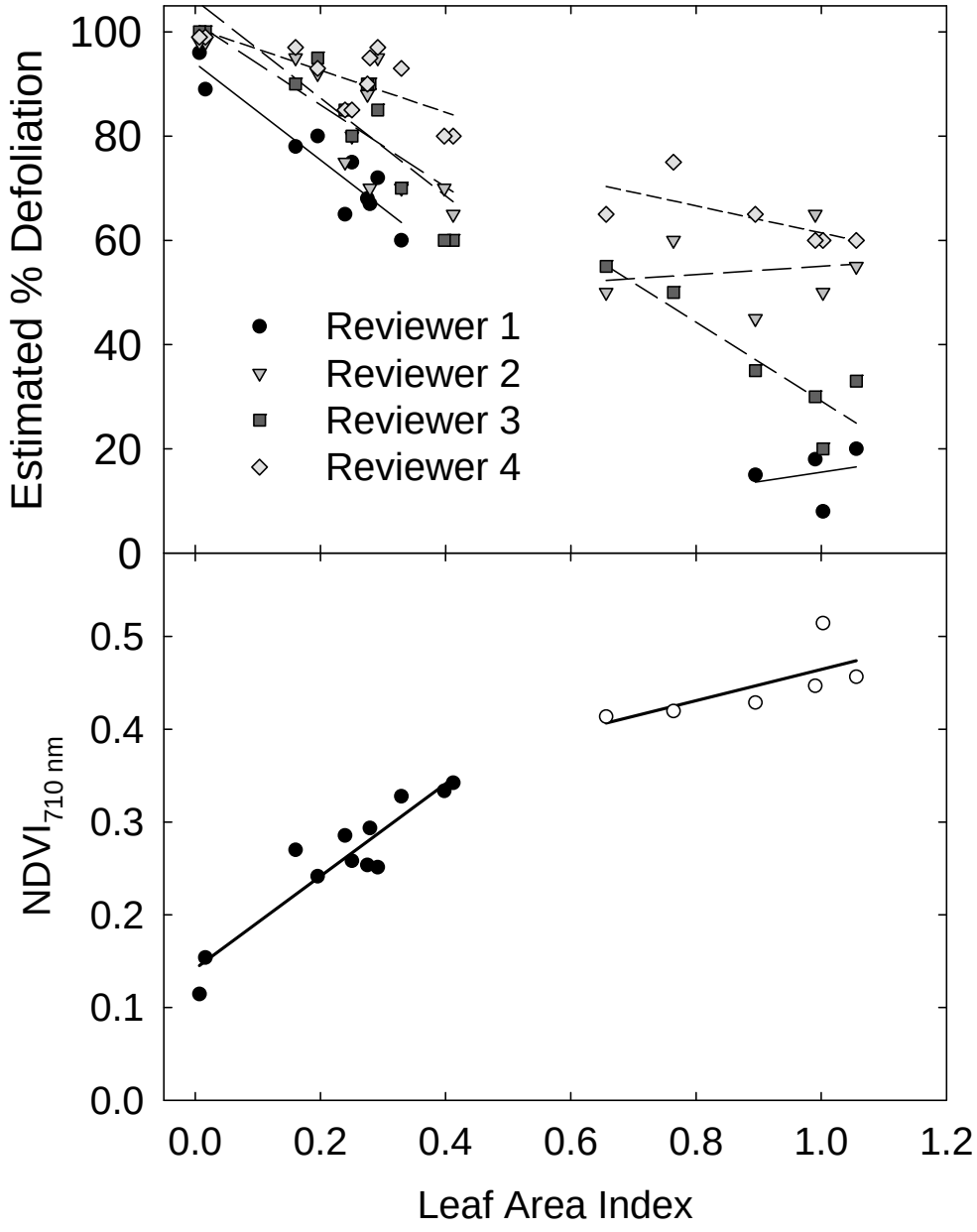

Fig. 2.7. Comparison of NDVI710 nm with reviewer estimates of defoliation. Comparison of NDVI with a reference wavelength of 710 nm ($NDVI_{710\ nm}$) and estimates of defoliation by four reviewers with LAI at low (LAI < 0.5) and high (LAI > 0.5) LAI levels.

Table 2.1. Comparison of LAI estimates at low (LAI < 0.5) and high (LAI > 0.5) LAI levels based on coefficient of determination (r^2) and slope for NDVI based on a reference wavelength of 710 nm ($NDVI_{710\ nm}$) and four reviewers.

Reviewer	r^2 (all LAI)	r^2 (LAI<0.5)	Slope (LAI<0.5)	r^2 (LAI>0.5)	Slope (LAI>0.5)
$NDVI_{710\ nm}$	0.90	0.87	0.50	0.50	0.17
1	0.96	0.87	-92.8	0.54	18.2
2	0.73	0.64	-78.9	0.03	7.86
3	0.94	0.76	-94.1	0.81	-75.7
4	0.90	0.55	-40.4	0.48	-26.0

References

Carter, G.A., and B.A. Spiering. 2002. Optical properties of intact leave for estimating chlorophyll concentration. J. Environ. Qual. 31:1424-1432.

Curran, P.J. 1989. Remote sensing of foliar chemistry. Remote Sens. Environ. 30:271-278.

Daughtry, C.S.T., and L.L. Biehl. 1985. Changes in spectral properties of detached birch leaves. Remote Sens. Environ. 17:281-289.

Gitelson, A.A., and M.N. Merzlyak. 1997. Remote estimation of chlorophyll content in higher plant leaves. Int. J. Remote Sens. 18:2691-2697.

Gitelson, A.A., Y. Zur, O.B. Chivkunova, and M.N. Merzlyak. 2002. Assessing carotenoid content in plant leaves with reflectance spectroscopy. Photochem. Photobiol. 75:272-281.

Huete, A.R., R.D. Jackson, and D.F. Post. 1985. Spectral response of a plant canopy with different soil backgrounds. Remote Sens. Environ. 17:37-53.

Klassen, S.P., G. Ritchie, J. Frantz, D. Pinnock, and B. Bugbee. 2003. Real-time imaging of ground cover: Relationships with radiation capture, canopy photosynthesis, and daily growth rate. In: Digital Imaging and Spectral Techniques: Applications to Precision Agriculture and Crop Physiology. ASA Special Publication no. 66.

Major, D.J., F. Baret, and G. Guyot. 1990. A ratio vegetation index adjusted for soil brightness. Int. J. Remote Sens. 11:727-740.

Read, J.J., L. Tarpley, J.M. McKinion, and K.R. Reddy. 2002. Narrow-waveband reflectance ratios for remote estimation of nitrogen status in cotton. J. Environ. Qual. 31:1442-1452.

Ritchie, G.L. 2003. Use of ground-based canopy reflectance to determine radiation capture, nitrogen and water status, and final yield in wheat, Utah State University, Logan, Utah.

Sims, D.A., and J.A. Gamon. 2002. Relationships between leaf pigment content and spectral reflectance across a wide range of species, leaf structures and developmental stages. Remote Sens. Environ. 81:337-354.

Tarpley, L., and K.R. Reddy. 2000. Reflectance indices with precision and accuracy in predicting cotton leaf nitrogen concentration, pp. 1814 Crop Sci., Vol. 40.

Yang, C., S.M. Greenberg, J.H. Everitt, T.W. Sappington, and J. J.W. Norman. 2003. Evaluation of cotton defoliation strategies using airborne multispectral imagery. Trans. ASAE 46:869-876.

CHAPTER 3

PREPARATION OF A LOW-COST DIGITAL CAMERA SYSTEM FOR REMOTE SENSING[1]

[1] Ritchie, G.L., D.G. Sullivan, C.D. Perry, J.E. Hook, and C.W. Bednarz. To be submitted to *Transactions ASAE*.

Abstract

Off-the-shelf consumer digital cameras offer a convenient and user-friendly remote sensing method, if they can provide consistent remote sensing data. Two Nikon COOLPIX 4300 digital cameras were evaluated in tandem to determine the effectiveness of a cross-camera calibration procedure that would allow concurrent use of these cameras to obtain visible and near-infrared images without preset shutter speeds or aperture settings. One camera was not modified, and the other was modified to be near-infrared sensitive using a Hoya R720 filter. Each camera was calibrated at 5 exposure levels using a reflectance target consisting of 26 diffuse reflective color samples, and equations were developed that would allow exposure compensation and the conversion of brightness values to relative reflectance values. The procedure was tested on 36 cotton plots (*Gossypium hirsutum*) in an irrigation study during the 2006 growing season. Images obtained on 8 dates during the season using the two cameras were corrected for exposure and converted to relative reflectance values. The normalized difference vegetation index (NDVI) values from the plots were then compared with ground-based spectrometer measurements of NDVI. The corrected camera-based NDVI values were closely correlated (r^2 = 0.72) with the spectrometer NDVI values, suggesting that the camera system can provide a consistent estimate of crop reflectance characteristics if exposure compensation is provided.

Introduction

Remotely sensed imagery provides both spatial and temporal estimates of cotton crop growth and health (Plant *et al.*, 2000; Zarco-Tejada *et al.*, 2005). Most broad-scale remote sensing is provided via airplane or satellite imagery. Although its use in production agriculture is still somewhat limited due to factors such as cost, system complexity, timeliness, and the influence of

atmospheric conditions, advances in remote sensing technology have made remote sensing a more economical and practical approach for crop management.

Consumer-level digital cameras may make this technology even more accessible through improved optics, quick download time, and the separability of images into component colors (Adams *et al.*, 1998). However, digital cameras have several unique characteristics that can affect the usefulness of these systems for agronomic management.

The Consumer Digital Camera

Digital cameras designed for the consumer market are increasingly being used as research instruments due to their low cost and ease of use. Levin *et al.* (2005) demonstrated that a consumer-grade digital camera could be used to accurately measure visual spectral properties of soils, and the Nikon COOLPIX camera line has been used for imaging work in a variety of disciplines, including forestry (Inoue *et al.*, 2004), microscopy (Wunsam and Bowman, 2001), and even plastic reconstructive surgery (Galdino *et al.*, 2001). Although the Nikon COOLPIX 4300 was used for this study, it is likely that any camera with the right features and image quality could be useful for imaging. However, off-the-shelf consumer grade cameras differ from research grade cameras and spectrometers, and these differences can affect the usefulness of the consumer cameras for agronomic management. One valid concern is that the point and shoot characteristics might lead to misleading measurements by allowing imaging that does not quantify automatic adjustments that the camera makes.

Spectrometers often use filters or light dispersion to separate wavelengths of incoming radiation into discrete reflectance bands and are often equipped with wavelength-specific optics (Sui *et al.*, 2005). Though practical for research, this adds expense and complexity to the imaging system.

Consumer cameras, on the other hand, are designed for ease of use. The filters are integrated within the camera sensor, as described by Adams *et al.* (1998).

Several parameters affect the camera image collection. Camera shutter speed controls the time incoming light makes contact with the sensor, while aperture (F-stop) controls the amount of light that can pass into the camera. Changes in aperture and shutter speed can compensate for each other, resulting in a standardized measure of exposure. Film speed (ISO) determines the sensitivity of the sensor to incoming radiation. White balance affects the color balance between red, green, and blue color channels. It allows the camera to correct hue and produce realistic looking pictures under cloudy conditions or electric lights.

Nearly all consumer cameras have completely automatic settings where the camera controls shutter, aperture, white balance, film speed, and contrast, allowing the user to point and shoot without adjusting settings. Mid-level consumer cameras (those with prices currently ranging from about $100 to $500) also have manual settings that allow the user to adjust some or all of these parameters. The cameras are designed to approximate a standardized measurement of human visual response (Sharma, 2003), and can have overlapping sensitivity between pixels that detect red, green, and blue (RGB) channels (Hong *et al.*, 2000; Wu *et al.*, 2000). There is currently no standardized method for adjusting camera color parameters, so RGB output differs by camera (Hong *et al.*, 2000).

Many of the features that are attractive for general use can compromise remote sensing work. For instance, the Nikon 4300 default settings include automatic corrections for exposure, aperture, ISO number, and white balance (Nikon). In addition, these cameras use hot mirrors to minimize near-infrared (NIR) radiation transmission, limiting the camera spectral range to the visible spectrum (Chieng and Rahimzadeh, 2005). This prevents the influence of NIR radiation

on the camera color channels, but also prevents the camera from sensing NIR radiation. The NIR region has long been associated with crop growth and health (Rabideau *et al.*, 1946), and is widely used for vegetation indices, such as those based on the ratio vegetation index (RVI) and the normalized difference vegetation index (NDVI) (Jordan, 1969; Rouse *et al.*, 1973).

Many of the point and shoot features in consumer grade cameras can confound spectral estimates. However, many of these features can be adjusted in the manual camera user settings. Features that should be locked include white balance, image adjustment, and ISO speed, since all of these features can affect the image exposure and channel balance. Aperture on the Nikon 4300 cannot be locked, and locking the shutter speed has a significant tradeoff. With a single shutter speed, changes in exposure can be eliminated as a source of image variation, but there is a risk of miscalculation of the correct shutter speed. A shutter speed that is set too fast will not allow sufficient image exposure, and a shutter speed that is set too slow will overexpose the image, resulting in image saturation. The use of one shutter speed limits the camera to a narrow dynamic range. A more robust solution would be the correction of images based on camera exposure, allowing images to be collected with a variety of exposure levels.

Making a camera NIR sensitive involves modification of the camera by replacing the hot mirror with a filter that transmits infrared rather than visible radiation. However, the procedure is often not too technically demanding (Chieng and Rahimzadeh, 2005), and the consumer camera might then be practical for the same remote sensing estimates as cameras designed for near-infrared imaging. This would require a separate camera for collection of visible channels, and the cameras would require some method of exposure correction between cameras. A correction designed to compensate for changes in exposure might allow these cameras to be used as a viable remote sensing device, and because most successive camera models use similar optical systems,

many of the principles applied to the specific camera will be similar to those of other camera models, particularly those in the same product line.

This paper presents a method for calibrating a system of visible and near-infrared cameras for exposure, both within camera and between cameras. The methodology was designed to evaluate a simple calibration system and to determine the accuracy and efficacy of using a consumer-level digital camera system to estimate visible and near-infrared reflectance.

Materials and Methods

Camera Setup

Two Nikon COOLPIX 4300 consumer digital cameras were used together for this experiment. The Nikon 4300 camera has a 4.0 megapixel (2272x1704 pixel) resolution, costs under $400 new, and weighs ~300 g with battery. Images were collected on manual setting with presets of sunlight white balance, no image adjustment, ISO 100 sensitivity, and normal noise reduction. The aperture cannot be preset, but the aperture was recorded in the camera metafile (info.txt) each time an image was collected.

The first camera was not modified and was used to collect visible images with red, green, and blue (RGB) channels. Each channel is 8-bit (256 color), resulting in a 24-bit (16.7 million color) RGB combination. The CCD is covered with a cyan-yellow-green-magenta (CYGM) filter array (Nikon, 2004).

The second camera was modified by removing the hot mirror (11 x 12 x 2.5 mm) from between the lens assembly and the CCD array and replacing it with a piece of Hoya R720 infrared filter cut to 11 x 12 mm, similar to the method described by Cheng and Rahimjadeh (2005). The visible and near-infrared transmission characteristics of both the hot mirror and the filter are shown in Fig. 3.1, as determined using a StellarNet spectrometer (Apogee Instruments, Logan,

UT) on a white polytetrafluoroethylene (PTFE) reflectance target under direct sunlight. Although the camera was modified to be insensitive to visible radiation, the resulting image still has RGB channels (Fig. 3.3) that are influenced by both the algorithm in the camera that corrects for color balance and the differing sensitivity of the filter array components to NIR radiation. The optical characteristics of both cameras were tested to estimate the practicality of using a tandem of visible and near-infrared cameras to estimate vegetation indices.

RGB channels and the Near-Infrared

The RGB channels were tested individually to determine which channel would yield the most consistent estimates of infrared. A reflectance panel constructed of several swatches with different reflectivity was constructed (Fig. 3.3). The swatches included a white reflectance standard made of polytetrafluoroethylene (PTFE), a photographic gray card, and several diffuse paint samples with varying visible and NIR reflectance. All of the materials in the reflectance target had unique reflectance properties, including total reflectance by wavelength and reflectance of corresponding wavelengths. Many of the dominant colors were chosen from the same color swatches, allowing the same reflectance characteristics at different brightness levels. Photographs were collected at 5 exposure levels simultaneously with each camera. The images were downloaded and opened in Adobe Photoshop CS2 (Adobe Systems, Inc., San Jose, CA), and a region in the center of each target color was selected using the rectangular marquee tool. The brightness of each channel was observed using the histogram function and recorded in a spreadsheet. Brightness value standard deviations did not exceed 2.0 for any of the targets, and typically ranged from 1 to 1.5.

Exposure and Lens Distortion Correction

Relative exposure level for each camera was calculated as shown in Equation 1:

$$E_v = \log_2(F^2 / shutter) \quad \text{Equation 1}$$

In this case, F is the camera f-stop, and shutter is the shutter speed in seconds. This equation is well-documented in photography and is based on the relationship between aperture and shutter speed in determining exposure (Jacobsen *et al.*, 2000). Corrections for exposure level were made within camera.

Lens distortion was estimated at the 8-mm focal length by photographing a reference grid with the camera normal to the grid and correcting the image in Adobe Photoshop CS2 using the lens correction filter until the lines of the grid most closely approximated vertical and horizontal parallel lines.

Calibration Panel Test of NDVI

Because this research was designed to provide a straightforward method for determining vegetation indices with a consumer grade camera system, the normalized difference vegetation index (NDVI) was used to test the calibration between cameras at multiple exposure levels. NDVI is calculated as (ΔNIR - ΔRed)/ (ΔNIR + ΔRed), where ΔNIR and ΔRed are NIR and red reflectance (Rouse *et al.*, 1973). The steps of estimating this index based on camera brightness values are outlined in Table 3.1.

NDVI for each material was determined using the Apogee spectrometer and reflectance probe. Estimated NDVI values were then calculated from the exposure-corrected brightness values of the visible and near-infrared cameras. The visible camera exposure varied by 1.4 shutter stops, and the NIR camera exposure varied by 0.95 shutter stops. The relative exposure difference between the visible and NIR cameras ranged from -2.01 to 0.39 shutter stops, based on the

calculation shown in Equation 1. Brightness values were then obtained for the visible camera red channel and the NIR camera blue channel.

Field Testing of Calibrated Cameras

The camera setup was used for monitoring the growth characteristics of cotton in an irrigation study of 36 plots conducted at the Stripling Irrigation Research Park in Camilla, Georgia in 2006 on a Lucy loamy sand (loamy, kaolonitic, thermic, Arenic, Kandiudults). Fertility, weed control, and insect scouting and control measures were in accordance with the University of Georgia Cooperative Extension Service guidelines. Images were collected at altitudes of 75 to 300 m above the plant canopy on 8 cloud free days between 10:30 AM and 12:30 PM from June 20 to July 21, 2006 (49 to 80 days after planting).

On most days, the camera field of view did not cover the entire study area, so plot image segments were collected from 37 visible images and 37 near-infrared images over the course of the study. There were 35 recorded visible exposure values that ranged from 11.2 to 14.0, with a mean exposure value of 12.9. There were 36 recorded NIR exposure values that ranged from 12.0 to 14.8, with a mean exposure of 13.9. This resulted in 37 exposure combinations between the visible and NIR cameras that ranged from -1.9 (NIR camera exposed almost 2 stops less than visible camera) to 0.4 (NIR camera exposed almost 1/2 stop greater than visible camera) and averaged -1 with a standard deviation of 0.6. The visible brightness channels were corrected to match the exposure level of the near-infrared camera. Corrected aerial NDVI measurements from the digital cameras were compared with ground-based point measurements of NDVI.

The ground based NDVI measurements were performed 1.5 m above the plant canopy using an Apogee Vis/NIR spectrometer with fiber optic cable and 30E full angle field-of-view, with reference reflectance measured using the PTFE reflectance standard used for the other tests.

Results

Near-Infrared Image Characteristics

The near-infrared images exhibited strong red channel color saturation, which resulted in images with a pink cast. As shown in Fig. 3.4, red channel brightness values saturated at incident light levels well below the saturation point of the blue and green channels. The red channel reached saturation point at a blue brightness value of 180, or about 70% of maximum. This is likely due to high transmission of near-infrared radiation by the red-transmitting filters in the color filter array. The saturation of the red channel makes it incapable of accurately measuring high levels of reflected near-infrared radiation, unless the camera white balance is adjusted to compensate for this saturation. If the red channel saturates, it must be discarded prior to image analysis to prevent misleading results. The blue and green channels did not show any appreciable color saturation, with the blue channel more sensitive to infrared light than the green channel, as shown in Fig. 3.4. The higher sensitivity of the blue channel compared to the green channel suggests that it would have a higher signal-to-noise ratio and therefore more suitability for image analysis, although comparison of brightness values between the channels shows a high linear correlation ($r^2 = 0.97$) between blue and green brightness values in most cases (Fig. 3.4).

Lens Distortion

A 3.5% barrel distortion was observed for both cameras at the 8-mm focal length, based on measurements obtained from the reference grid and correction in Photoshop. When it is necessary to georectify the images, this distortion should be taken into consideration, as well as camera angle and location. As described in the materials and methods, the lens distortion correction filter was used in this case to correct distortion when necessary. Another way to

address this issue would be to take images from a sufficient distance that the regions of interest were toward the center of the image to avoid sampling distorted pixels.

Camera Exposure and Reflectance

Changes in exposure significantly affected the relationship between camera channel brightness and target reflectance (Fig. 3.5), suggesting the importance of an exposure correction. For example from Fig. 3.5, the red channel brightness values of the gray standard (red reflectance = 18%) ranged from 92 to 193, depending on exposure level. In targets with higher reflectance, this change was not as pronounced, due to the curvilinear sensor response.

The relationship between channel brightness and reflectance was nonlinear for all channels. At a given exposure value, camera linearity is dependent upon the spectral range of the target. Targets with similar reflectance would have a nearly linear slope between reflectance and channel brightness. However, high-contrast scenes show the nonlinearity of the camera sensor. At high channel brightness levels, materials with similar brightness values will be difficult to differentiate. However, because all of the exposure levels yielded similar patterns in the relationship between channel brightness and reflectance, much of this can be corrected by changing shutter speeds and correcting to a common exposure level.

There is a strong linear relationship between channel brightness values at multiple camera exposures (r^2 = 0.986, 0.993 and 0.997 for blue, green, and red channels, respectively), as shown in Fig. 3.6. This linear relationship allows a single linear correction based on relative exposure between two exposure levels. This led to a simple correction of visible channel brightness based on change in exposure, as shown in Fig. 3.7. Coefficients of determination between reflectance and the corrected channel brightness were 0.943 for the blue channel, 0.957 for the green channel, and 0.984 for the red channel, suggesting a very tight relationship.

The near-infrared camera channels also had a curvilinear relationship between reflectance and brightness. However, the blue and green channels of the NIR camera did not respond in the same way over the entire region of the near-infrared spectrum examined. This was particularly noticeable on reflectance targets that reflected significantly less 700-800 nm than 800-900 nm light (none of the samples reflected appreciably more 700-800 nm light than 800-900 nm light). To determine the extent of the difference between channels, NIR reflectance of each target was divided into 700-800 and 800-900 nm regions, and blue and green channel brightness values were plotted against reflectance from each region (Fig. 3.8).

Reflectance targets with a 700-800: 800-900 nm reflectance ratio greater than 0.80 were termed "uniform NIR reflectance," and targets with 700-800: 800-900 nm reflectance ratio less than 0.80 were termed "varied NIR reflectance."

The NIR blue channel brightness values correlated well with 800-900 nm reflectance, regardless of whether the targets had uniform or varied NIR reflectance. However, as shown in Fig. 3.8, the blue channel brightness relationship with 700-800 nm reflectance showed large differences between targets with uniform and varied NIR reflectance. This suggests that the blue channel is relatively insensitive to 700-800 nm radiation.

The NIR green channel brightness values showed changes when compared with both the 700-800 nm and 800-900 nm reflectance of materials with varied NIR reflectance. However, when compared with an average of the 700-900 nm reflectance, all targets, including those with varied NIR reflectance had the same brightness to reflectance relationship, as shown in Fig. 3.9. It was therefore determined that the NIR green channel is sensitive to radiation from both the 700-800 nm range and the 800-900 nm range (Fig. 3.9). This might be of interest for some applications, because the 700-800 nm range corresponds with the region of rapidly increasing plant

reflectance termed the "red edge," and the 800-900 nm range corresponds with a region of nearly constant plant reflectance termed the "red shoulder." The red edge region is almost within the range of human sight, while the red shoulder region is further from the visible range, but still within the range of silicon photo detectors. However, the strong relationship between the blue and green channels on the NIR camera in the field (Fig. 3.4) suggests that it would be difficult to identify changes in plant growth by comparing the channels.

Another aspect of this concept is that the NIR camera might be used to effectively calculate two separate NIR regions, based on the difference between the reflectance characteristics of the green and blue channels.

The comparison of blue channel values with 800-900 nm reflectance and green channel values with 700-900 nm reflectance resulted in close correlations with reflectance, as shown in Fig. 3.9. Like the visible camera channels, exposure compensation with the NIR camera involved a linear correction between exposure levels. For the NIR blue channel, the compensation was simpler compared to the visible channels, because exposure could be corrected without changing the slope of the relationship (Fig. 3.10). This correction resulted in a high correlation between reflectance and the exposure-compensated channel brightness values, as shown in Fig. 3.11.

NDVI Estimates from Calibration Targets

As shown in Fig. 3.12, there was a high correlation between the spectrometer red NDVI and the camera red NDVI (r^2=0.96). The correlation was also linear, despite the nonlinear relationship between camera brightness and reflectance, suggesting that the model adequately corrected for this nonlinearity on the reflectance target.

Field Testing of Exposure Correction

This method was tested on data from a remote sensing study conducted in 2006 to verify its ability to correct for changes in exposure in remote sensing of plants. One unique aspect of the study was that relative exposure differences trended positive rather than negative, with differences ranging from -0.4 to 1.85 shutter stops. This would be expected, since plants reflect a high percentage of near-infrared radiation and a low percentage of visible light. Therefore, as the crop matures, the scene becomes brighter in the near-infrared and darker in the visible. Correction for exposure improved the relationship of camera NDVI values with those obtained with a ground-based spectrometer from an initial r^2 value of 0.37 to a final value of 0.72, as shown in Fig. 3.13.

Discussion

Characterization of the cameras revealed that consumer digital cameras can be used in tandem as a basic system to estimate visible and near-infrared reflectance, provided that several practical aspects are considered when using these cameras for remote sensing research. Assuming that the camera is set to eliminate automatic white balance correction, perhaps most dramatic is the issue of exposure measurement and correction. Calibration of the camera must take into account the calculated exposure, rather than the estimated exposure level based on the camera bracketing. Of particular concern is the incorrect aperture level recorded by the near-infrared sensitive camera in this study. It would be worthwhile to characterize the effects of aperture on brightness of any camera considered for such experiments to identify issues such as this prior to using the camera. After aperture was corrected for in the near-infrared camera, correction of cameras to exposure level was consistent within the tested range of exposure levels for each camera (at least 1.5 stops for the visible camera and at least 1 stop for the near-infrared camera). This allowed for good corrections between exposure levels, not only within camera, but between cameras.

For these tests, the selected setting was sunlight for both cameras, since nearly all of the images were collected on sunlit days. Another possibility would be to set a white correction manually, which would eliminate color saturation for the NIR camera. The disadvantage to such a white correction is that it would be difficult to duplicate between cameras, whereas an algorithm programmed into the camera firmware would have similar results between cameras of the same model.

Another issue of note is correction for lens aberrations. Lens distortion was observed with both cameras, although the percent lens distortion was nearly identical for both. Another issue to be mindful of is the effect of brightness fall-off, where brightness decreases significantly toward the corners of the image, due to the increasing obliquity in the view away from the nadir axis, as well as lens vignette effects (Dean *et al.*, 2000). However, much of this can be minimized by using images that include the regions of interest near the center of the image. If this requires the collection of multiple images for a target location, using exposure correction and a vegetation index can decrease the effects of scene brightness changes.

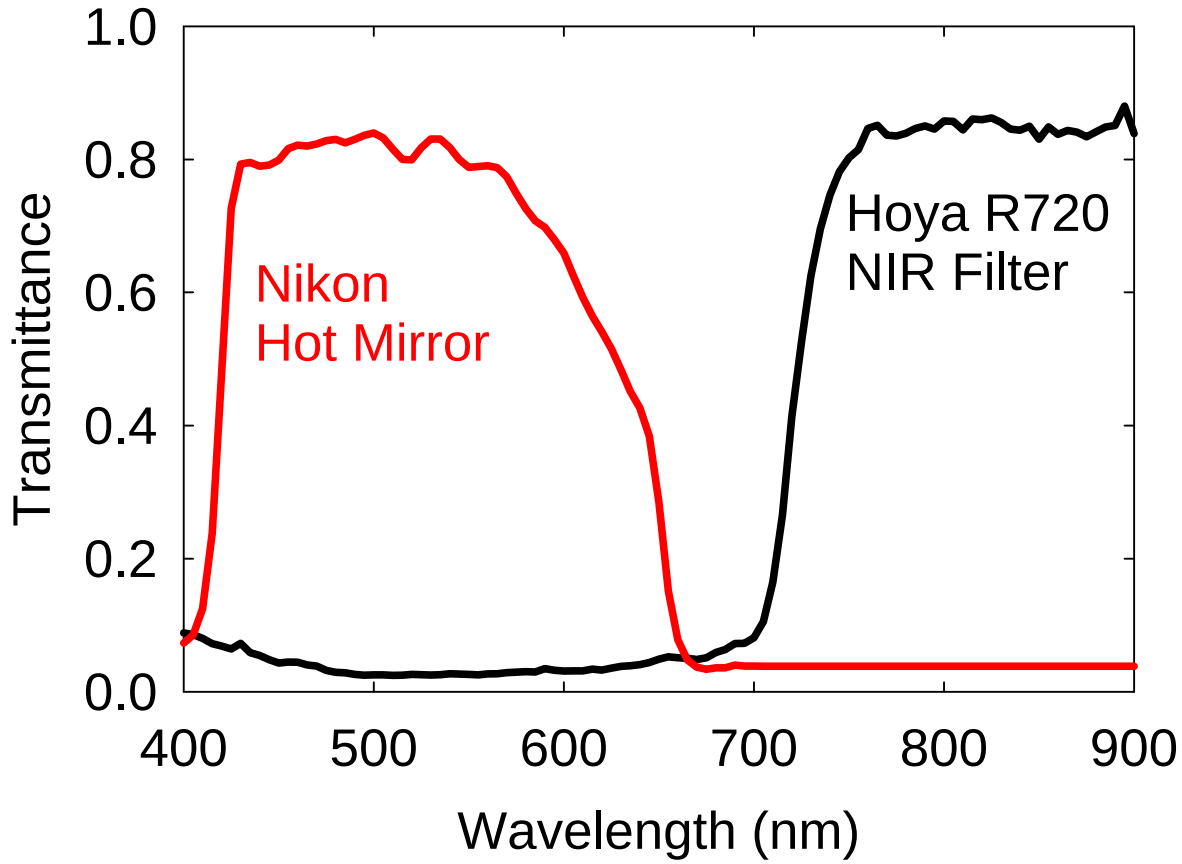

Fig. 3.8. Transmittance spectra of Nikon hot mirror and Hoya R720 infrared filter. Most hot mirror transmittance occurs at wavelengths of less than 670 nm, while most transmittance of the infrared filter occurs above 710 nm.

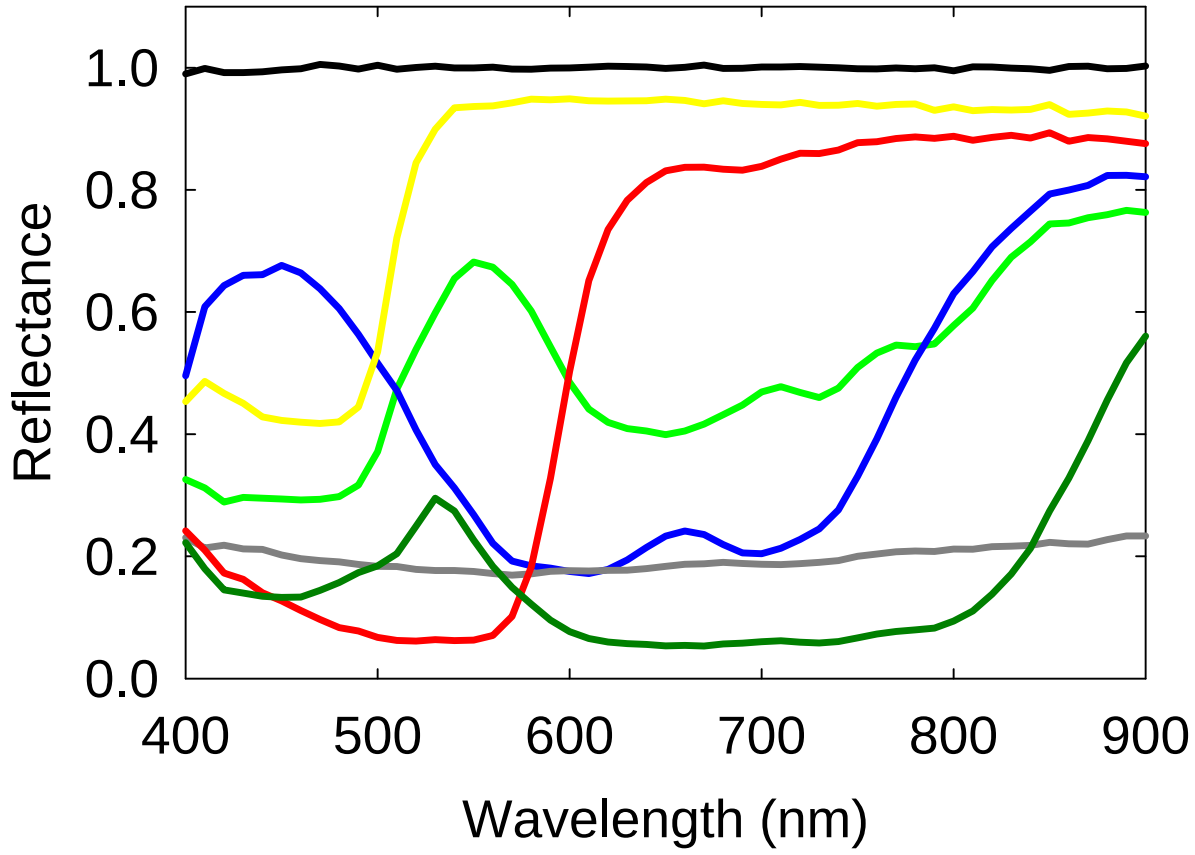

Fig. 3.9. Reflectance characteristics of selected colors from the reflectance target.

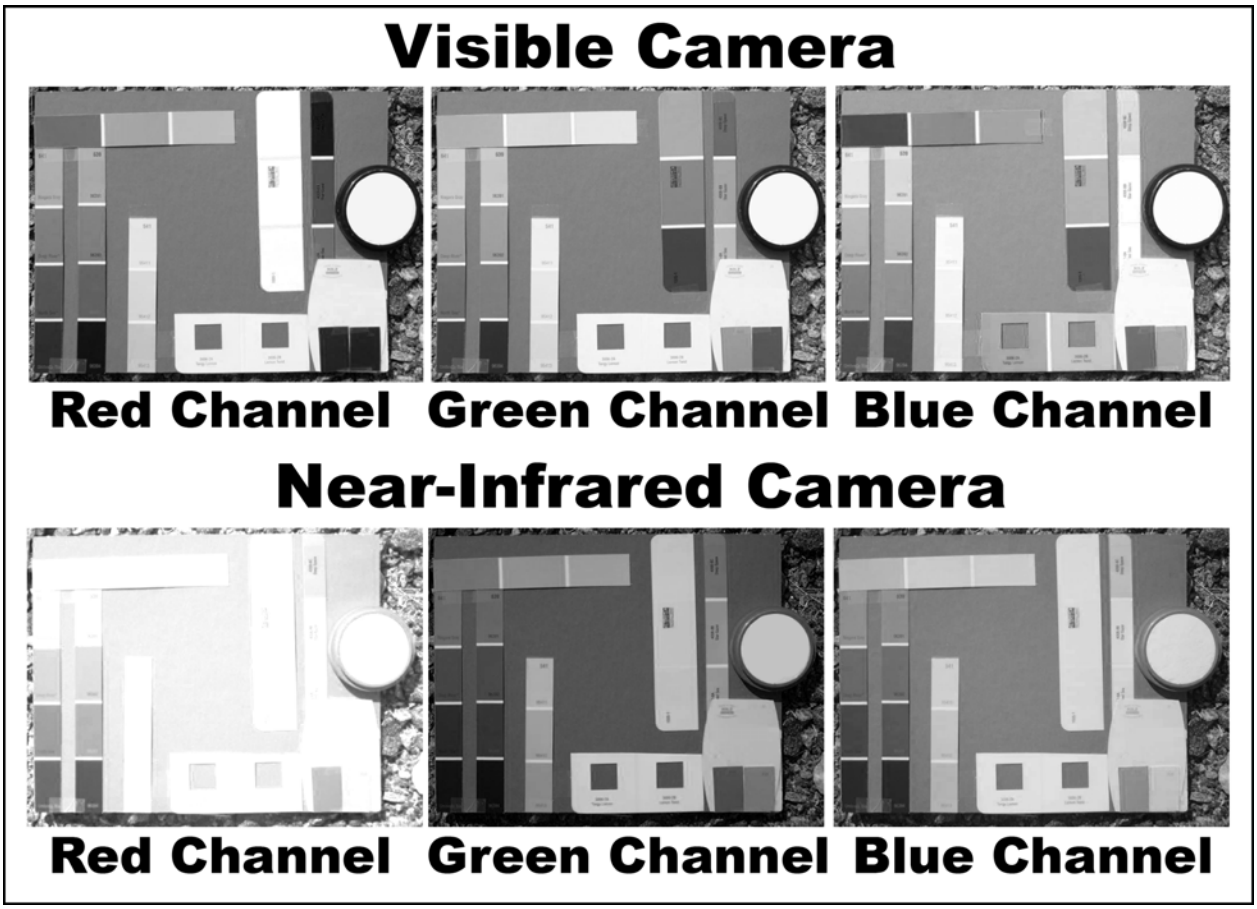

Fig. 3.10. Visible and near-infrared images of the reflectance target separated by channel.

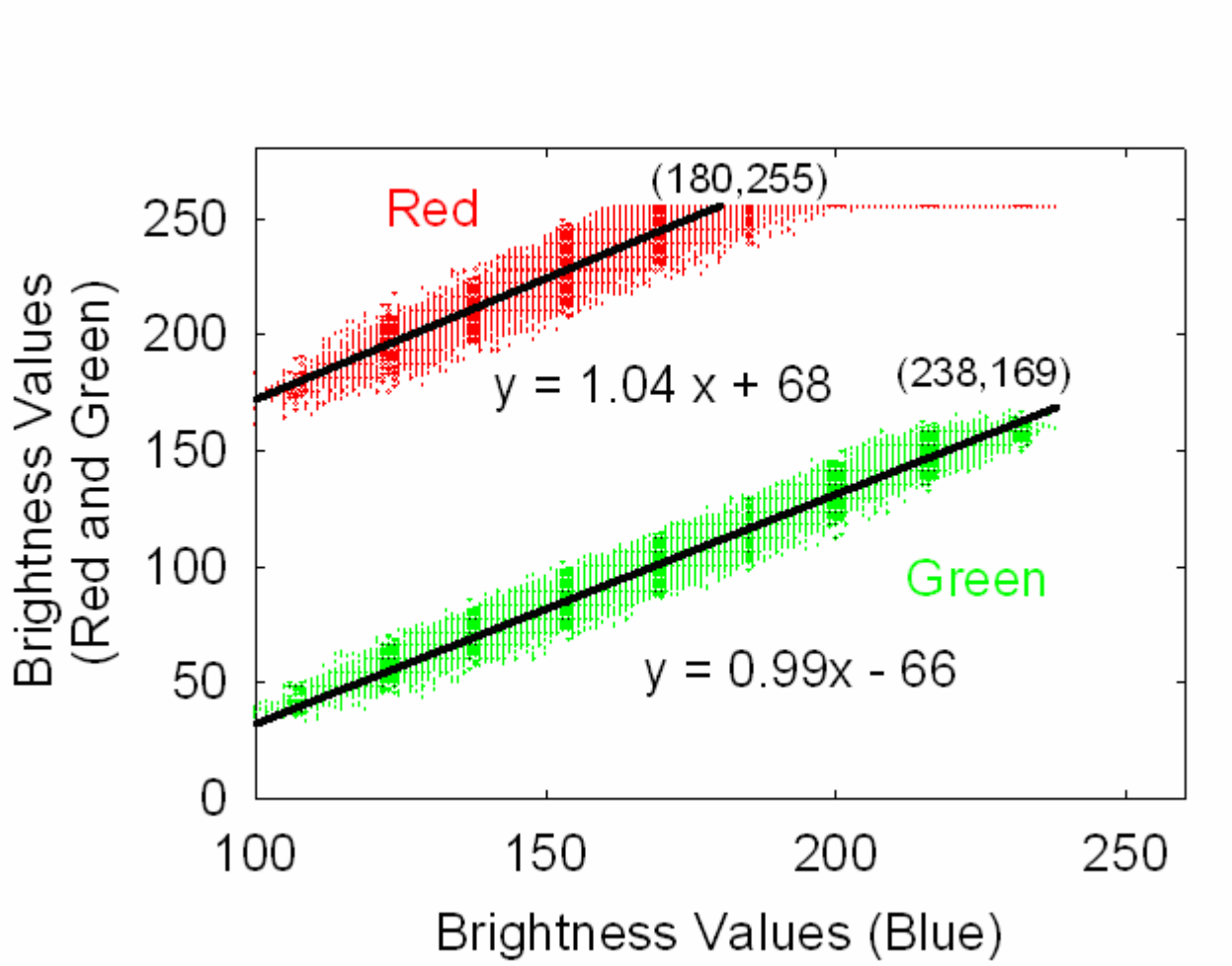

Fig. 3.11. Comparison of red, green, and blue channel brightness values from the near-infrared sensitive Nikon 4300 camera. The blue channel was chosen as the reference near-infrared channel because it had higher brightness values than the green channel and did not saturate as the red channel did.

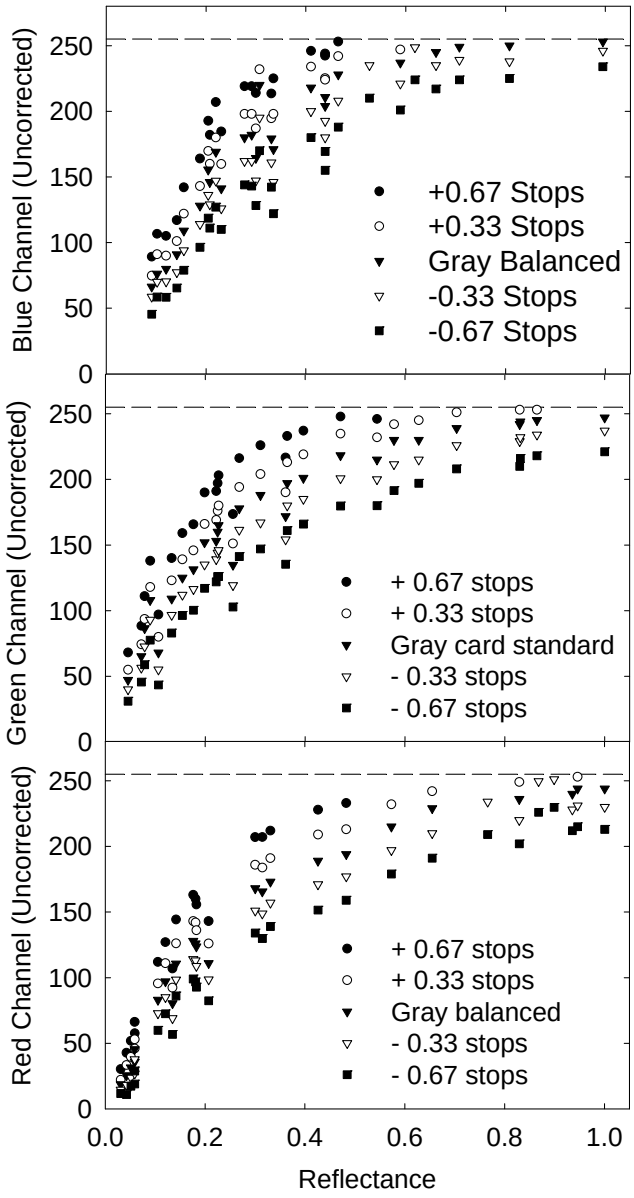

Fig. 3.12. Uncorrected brightness values of blue, green, and red channels compared with target reflectance.

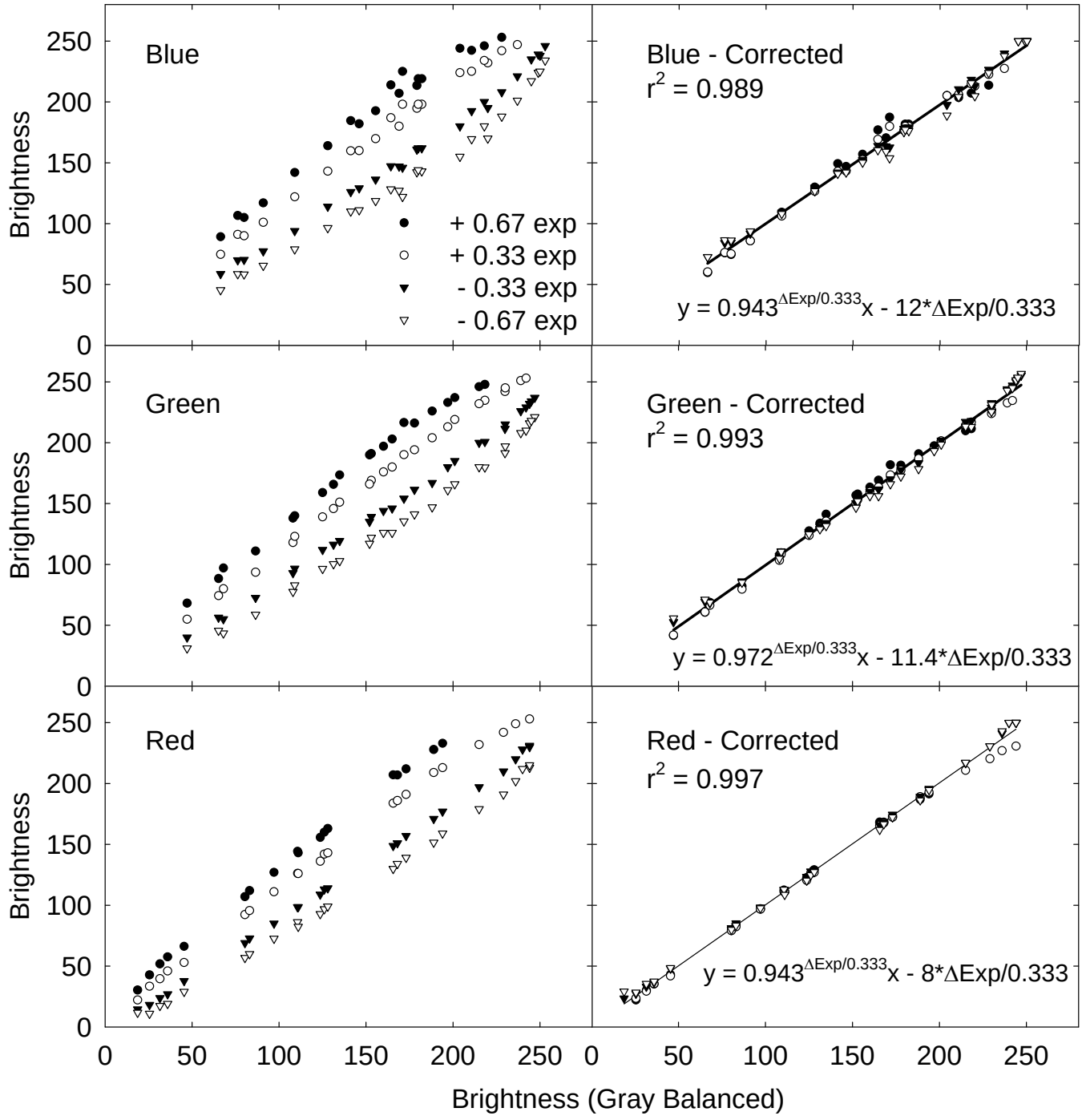

Fig. 3.13. Correction of red, green, and blue channels for camera exposure. The upper limit was 255, due to camera constraints.

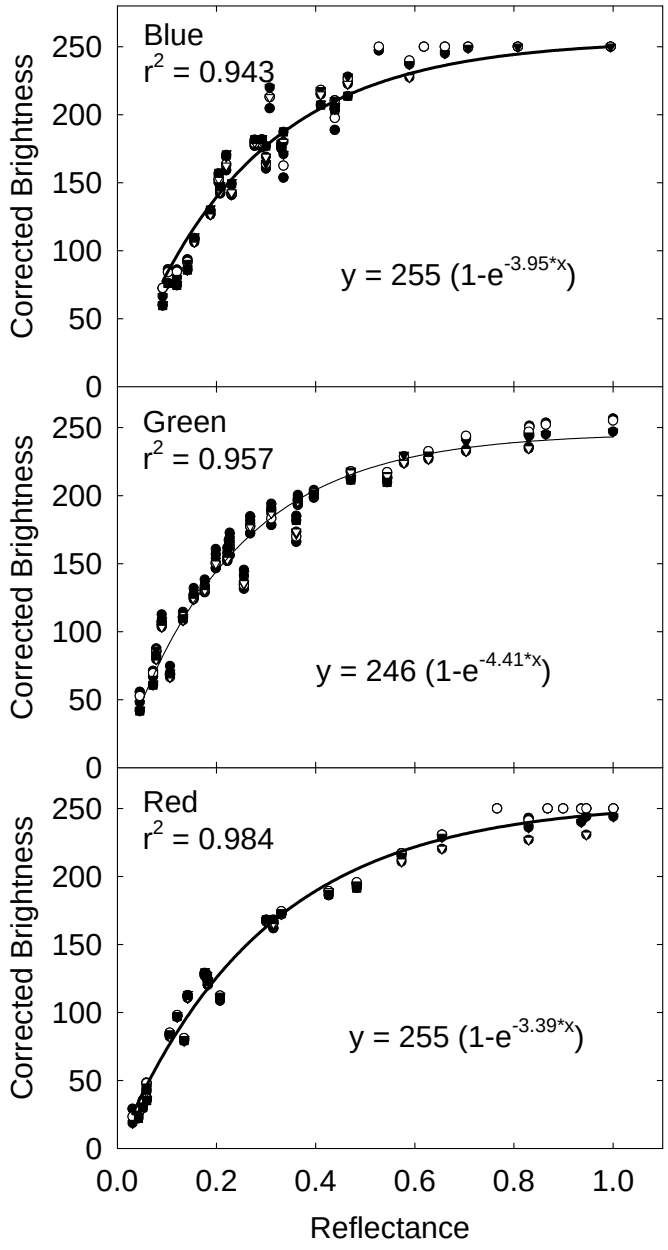

Fig. 3.14. Corrected channel brightness from visible camera at 5 exposure levels (as shown in Fig. 3.6) compared with reflectance.

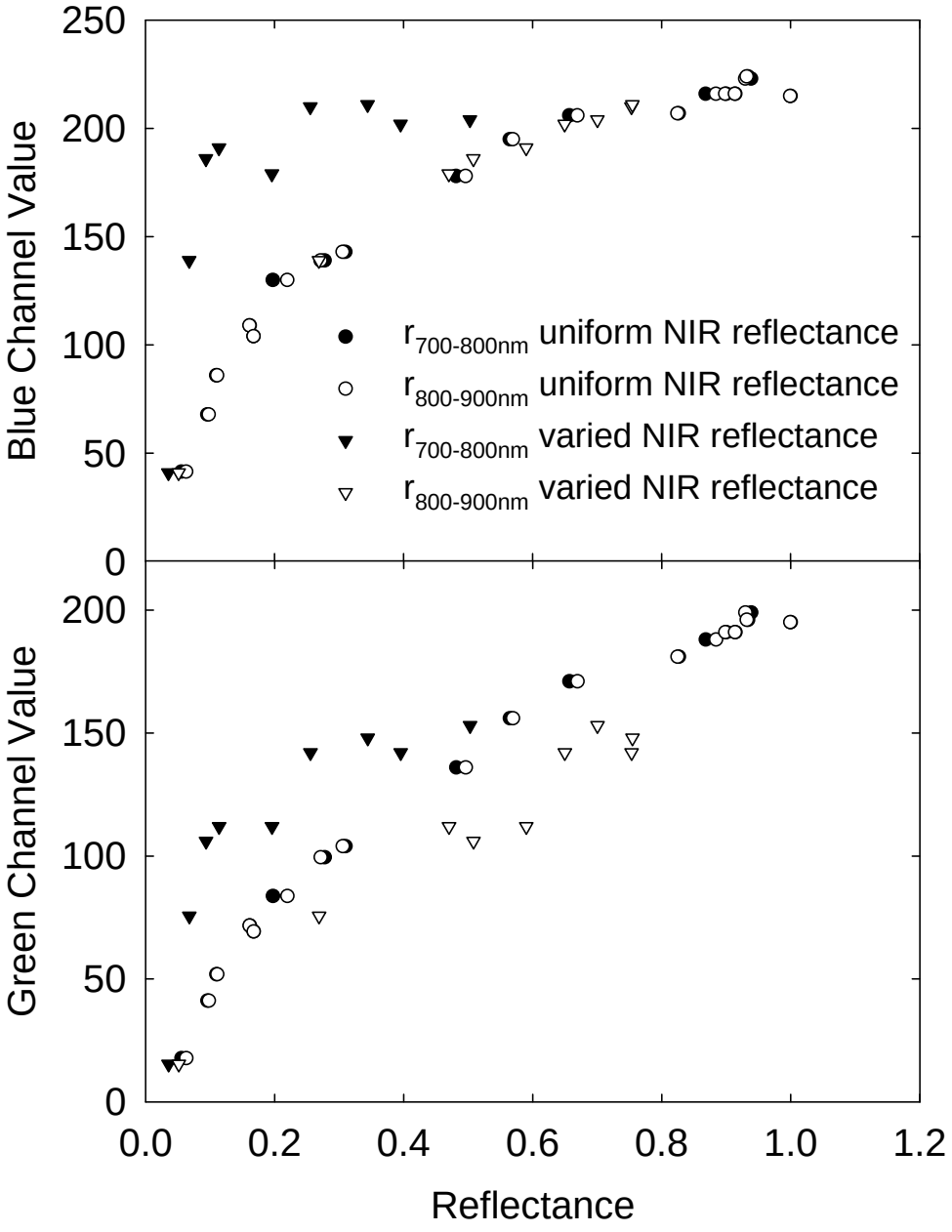

Fig. 3.15. Blue and green near-infrared camera channel values compared with NIR reflectance. Materials with a red edge: red shoulder reflectance ratio greater than 0.80 were termed "uniform NIR reflectance," while those with a ratio less than 0.80 were termed "varied NIR reflectance." None of the samples had a 700-800: 800-900 nm reflectance ratio greater than 1.03.

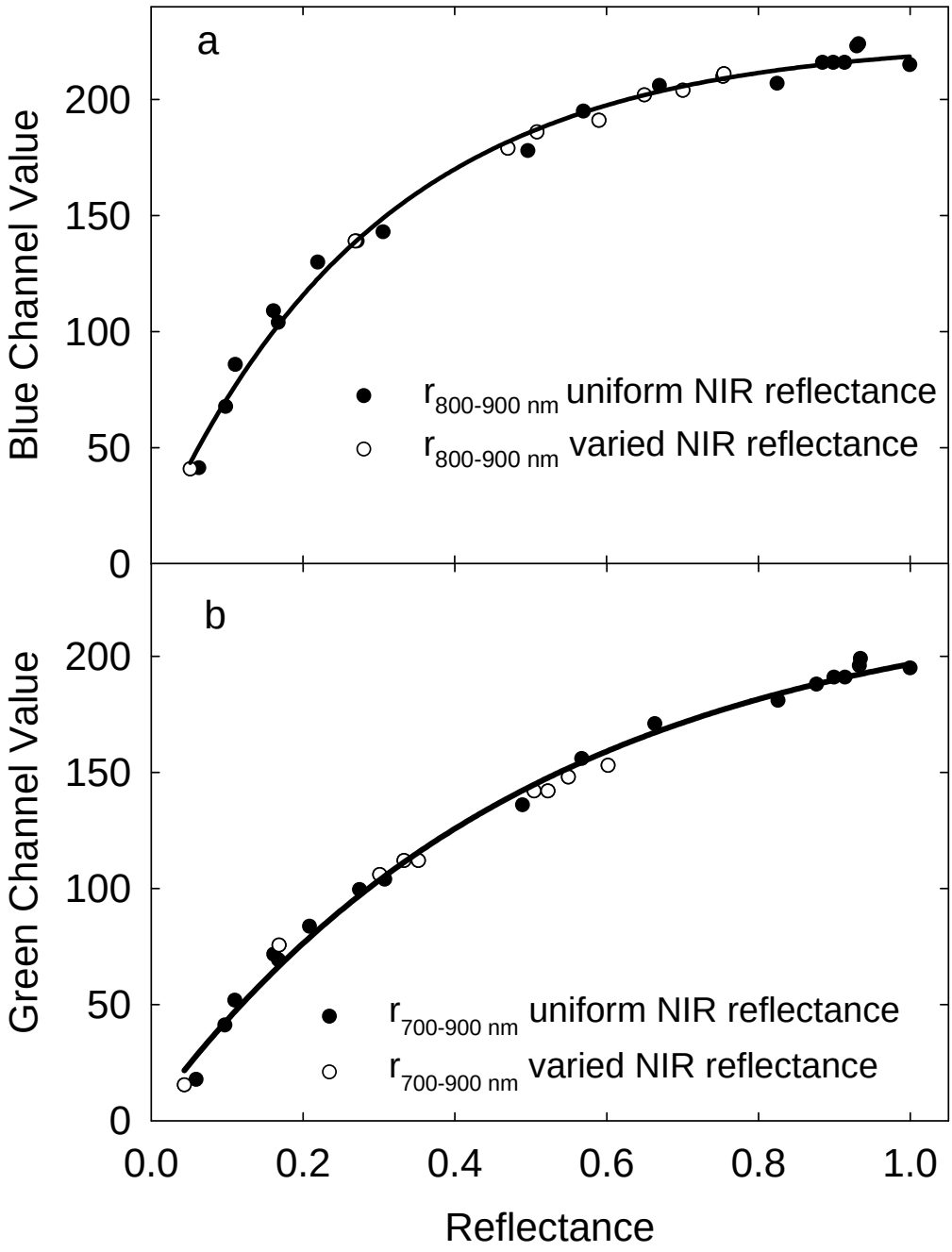

Fig. 3.16. Blue channel values compared with 800-900 nm reflectance (a) and green channel values compared with 700-900 nm reflectance (b).

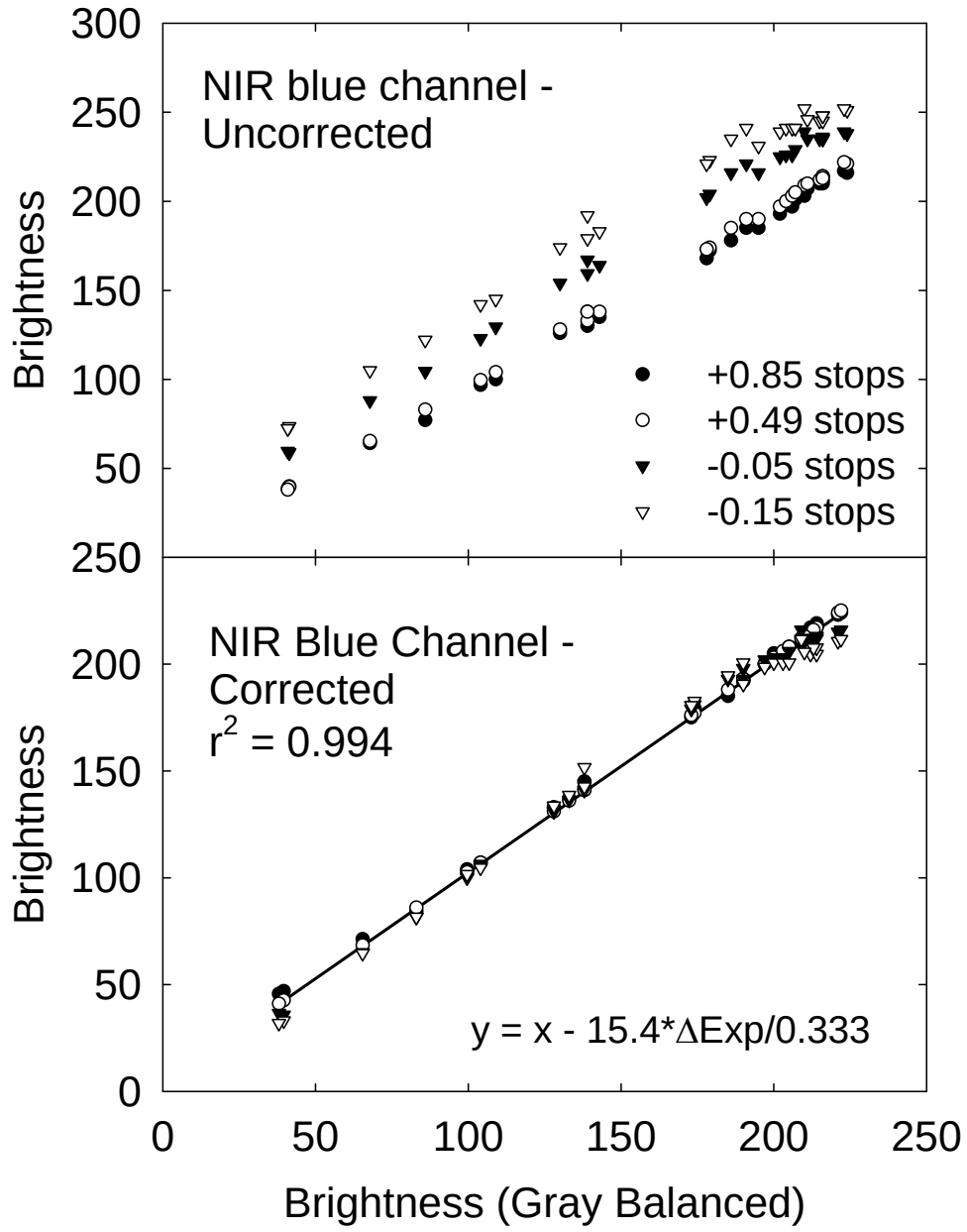

Fig. 3.17. Correction of NIR camera blue channel for camera exposure.

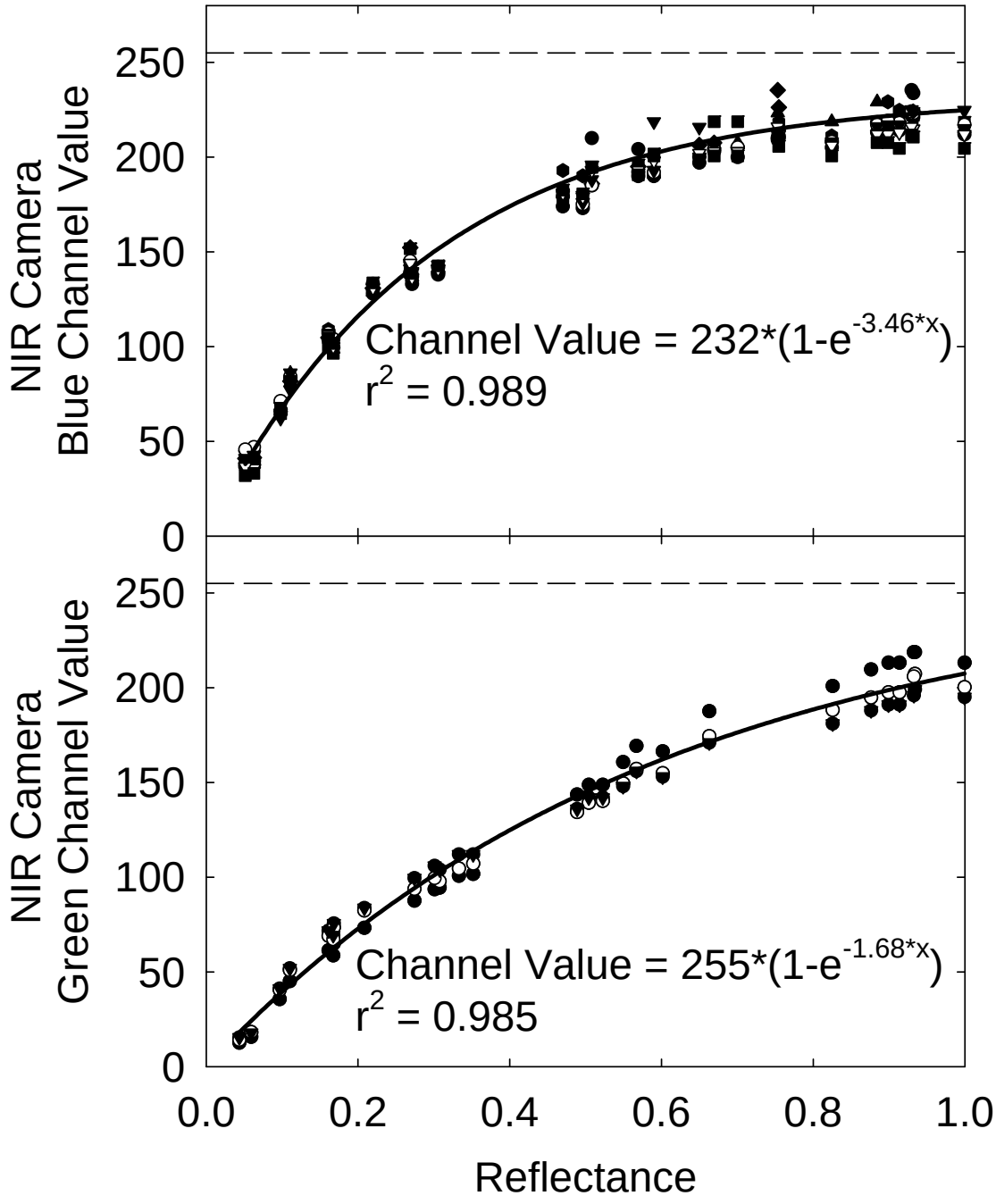

Fig. 3.18. Corrected blue and green channel values compared with 800-900 nm reflectance (blue channel) and 700-900 nm reflectance (green channel).

Table 3.2. Steps of calculating NDVI from uncorrected visible and near-infrared images. All of the steps are shown using equations for the red channel of the visible camera.

	Step	Equation
1	Collect uncorrected images	
2	Calculate exposure level of both cameras	$E_v = \log_2(F^2 / shutter)$
3	Correct brightness values of one camera to match exposure level of second camera	$y = 0.943^{\Delta E_v / 0.33} x - 8 * (\Delta E_v / 0.33)$
4	Convert brightness values to relative reflectance values	$y = -\frac{\ln(1 - \frac{x}{255})}{3.39}$
5	Calculate NDVI	$NDVI = \frac{NIR - \mathrm{Re}\, d}{NIR + \mathrm{Re}\, d}$

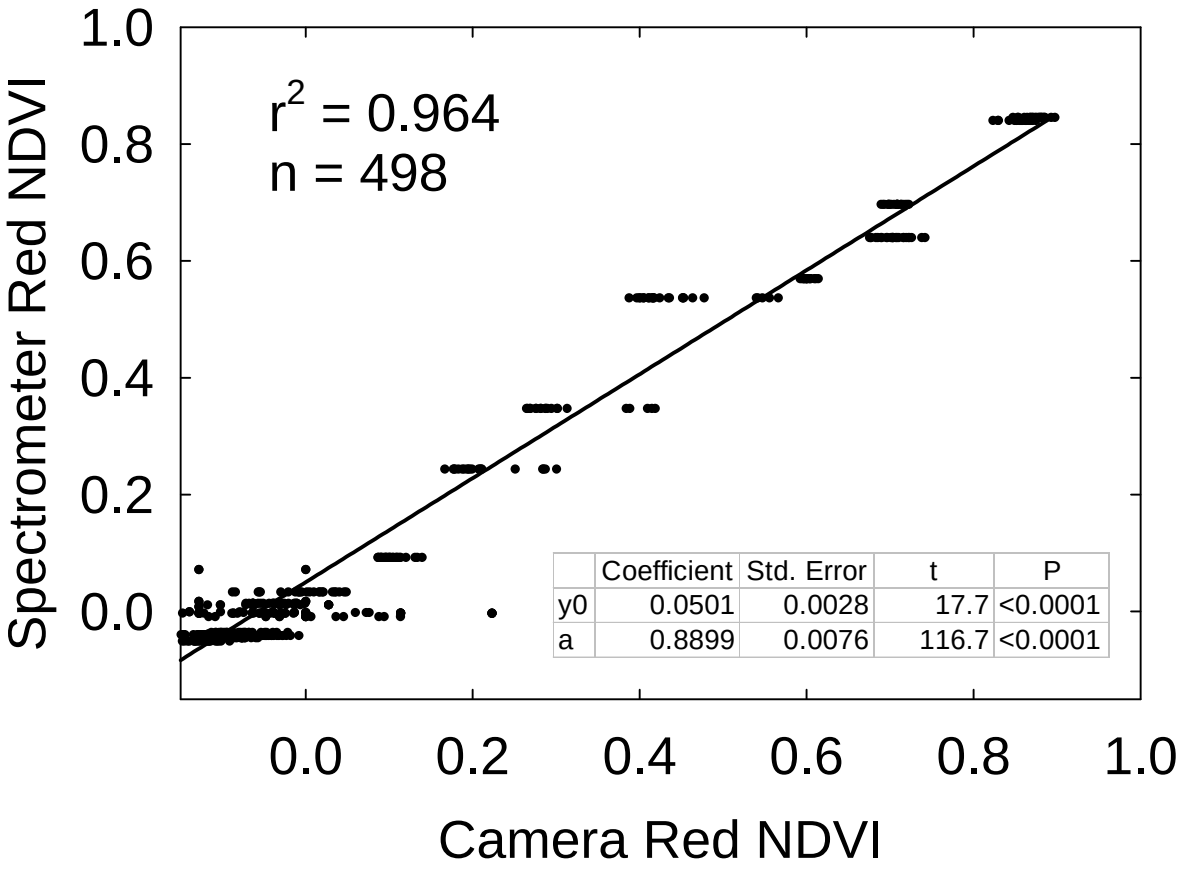

Fig. 3.19. Relationship between NDVI values of reflectance target measured using a spectrometer and reflectance probe with NDVI values calculated from corrected visible red (5 exposure levels) and NIR blue (3 exposure levels) channels. Exposure differences from the visible camera to the NIR camera based on the calculation in Equation 1 ranged from -2.0 to 0.39 shutter stops.

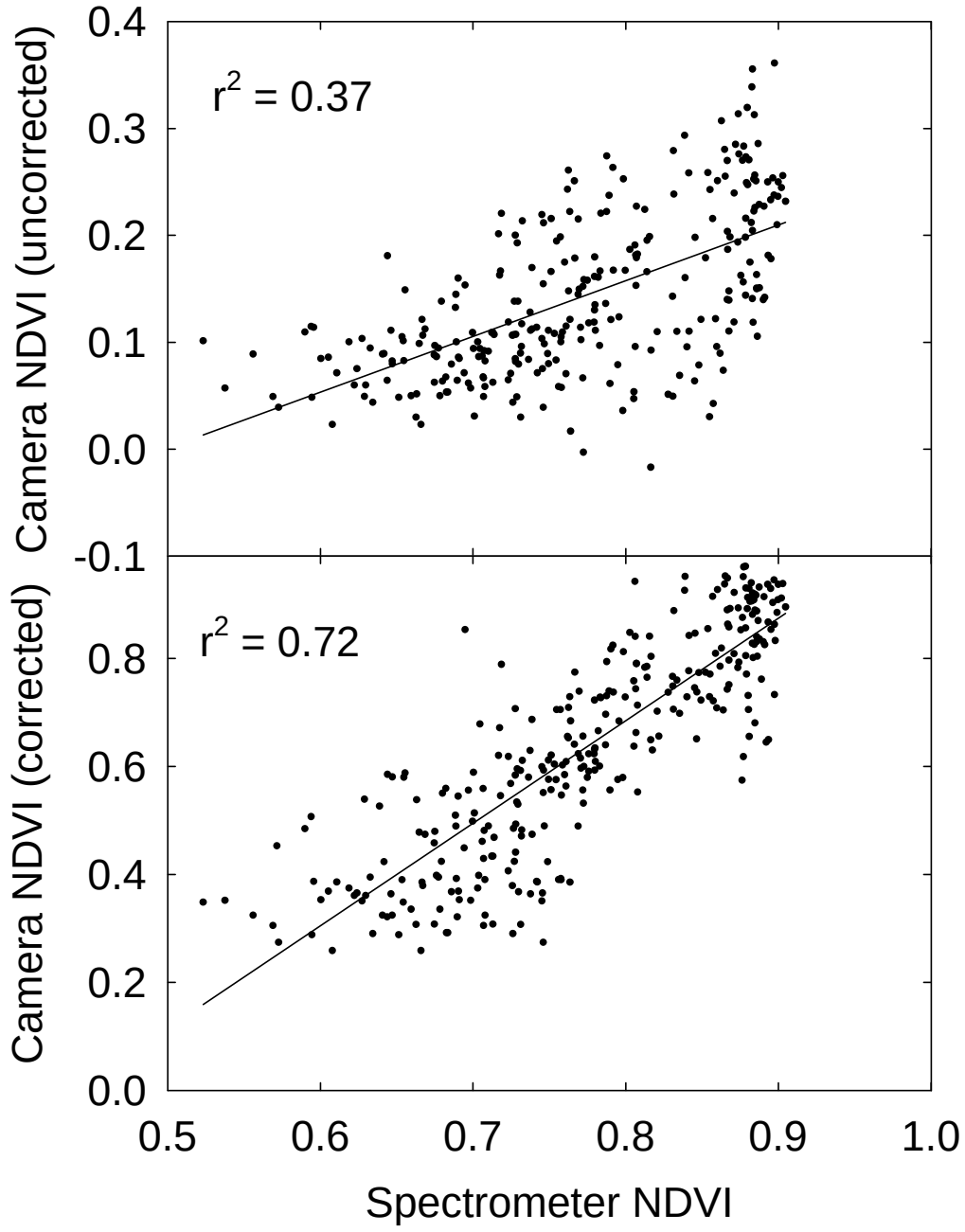

Fig. 3.20. Effect of exposure correction on relationship of camera NDVI with NDVI values obtained with a ground-based spectrometer. Comparison was made over 7 dates during the 2006 growing season on cotton. No other corrections were made.

References

Adams, J., K. Parulski, and K. Spaulding. 1998. Color processing in digital cameras. Micro IEEE 18:20-30.

Chieng, C., and A. Rahimzadeh. 2005. Hacking Digital Cameras. Wiley Publishing, Inc., Indianapolis.

Dean, C., T.A. Warner, and J.B. McGraw. 2000. Suitability of the DCS460c colour digital camera for quantitative remote sensing analysis of vegetation. ISPRS Journal of Photogrammetry and Remote Sensing 55:105-118.

Galdino, G.M., J.E. Vogel, and C.A.V. Kolk. 2001. Standardizing digital photography: It's not all in the eye of the beholder. Plastic & Reconstructive Surgery 108:1334-1344.

Hong, G., M.R. Luo, and P.A. Rhodes. 2000. A study of digital camera colorimetric characterization based on polynomial modeling. Color Research and Application 26:76-84.

Inoue, A., K. Yamamoto, N. Mizoue, and Y. Kawahara. 2004. Effects of image quality, size and camera type on forest light environment estimates using digital hemispherical photography 126:89-97.

Jacobsen, R.E., S.F. Ray, G.G. Attridge, and N.R. Axford. 2000. Camera exposure determination. The Manual of Photography, 9th ed. Focal Press, Oxford.

Jordan, C.F. 1969. Derivation of leaf area index from quality of light on the forest floor. Ecology 50:663-666.

Levin, N., E. Ben-Dor, and A. Singer. 2005. A digital camera as a tool to measure colour indices and related properties of sandy soils in semi-arid environments. Int. J. Remote Sens. 26:5475-5492.

Nikon, U.S.A. 2004. Nikon Coolpix 4300 [Online] http://www.nikonusa.com/specs/25507.pdf (posted January 15, 2007).

Plant, R.E., D.S. Munk, B.R. Roberts, R.L. Vargas, D.W. Rains, R.L. Travis, and R.B. Hutmacher. 2000. Relationships between remotely sensed reflectance data and cotton growth and yield. Trans. ASAE 43:535-546.

Rabideau, G.S., C.S. French, and A.S. Holt. 1946. The absorption and reflection spectra of leaves, chloroplast suspensions, and chloroplast fragments as measured in an Ulbricht Sphere. Am. J. Bot. 33:769-777.

Rouse, J.W., R.H. Haas, J.A. Schell, and D.W. Deering. 1973. Monitoring vegetation systems in the great plains with ERTS, p. 309-317. Third ERTS Symposium, NASA SP-351, Vol. 1. NASA, Washington, DC.

Sharma, G. 2003. Digital Color Imaging Handbook. CRC Press.

Sui, R., J.B. Wilkerson, W.E. Hart, L.R. Wilhelm, and D.D. Howard. 2005. Multi-spectral sensor for detection of nitrogen status in cotton. Applied Engineering in Agriculture 21:167-172.

Wu, W., J.P. Allebach, and M. Analoul. 2000. Imaging colorimetry using a digital camera. J. Imaging Sci. Technol. 44:267-279.

Wunsam, S., and J.C. Bowman. 2001. Economical digital photomicroscopy. Journal of Paleolimnology 25:399-403.

Zarco-Tejada, P.J., S.L. Ustin, and M.L. Whiting. 2005. Temporal and spatial relationships between within-field yield variability in cotton and high-spatial hyperspectral remote sensing imagery. Agron. J. 97:641-653.

CHAPTER 4

COMPARING THE DYNAMIC SENSITIVITY OF AERIAL AND GROUND-BASED SPECTRAL ESTIMATES OF COTTON GROUND COVER[1]

[1] Ritchie, G.L., D.G. Sullivan, C.W. Bednarz, W.E. Vencill, and J.E. Hook. To be submitted to *Crop Science*.

Abstract

Field-scale remote sensing of plant stress requires timely measurements that are sensitive to changes in crop growth and health. Aerial and ground-based remote sensing platforms can be used to identify growth characteristics through measurements of crop reflectance. Normalized difference vegetation index (NDVI) and Green:Red ratio measurements obtained from low-altitude visible and near-infrared (NIR) aerial images of cotton plots (*Gossypium hirsutum* L.) were compared with ground cover fraction measurements to determine the sensitivity of the indices to cotton growth. Ground-based spectrometer NDVI measurements were also evaluated for simplicity and sensitivity to ground cover fraction. The cotton was subjected to four irrigation regimes in a 4x4 latin square design 2004 and five regimes in a randomized block design in 2005 and 2006. Both spectrometer ($r = 0.64$ to 0.85) and camera ($r = 0.83$ to 0.88) indices were strongly correlated with ground cover fraction, particularly between ground cover fractions of 0.20 and 0.80. In addition, the indices were sensitive to changes in growth between irrigation treatments from growth stages of first square to peak bloom. Spectrometer red edge NDVI was sensitive to a wider range of ground cover than spectrometer red NDVI. Camera Green:Red ratio, the simplest index examined, had a high linear correlation ($r^2 = 0.86$) with ground cover fraction throughout the growing seasons over a three year period, suggesting that this index might allow quick, simple, and accurate crop growth estimates in a production setting.

Introduction

Remote sensing offers an attractive alternative to intensive soil or tissue sampling for broad scale crop growth and health estimates (Famiglietti *et al.*, 1999). One general class of remote sensing vegetation indices uses ratios or normalized ratios of reflected visible and near-infrared light to improve sensitivity to crop growth (Bannari, 1995; Elvidge and Chen, 1995). These indices have

been shown to be correlated with crop ground cover fraction, a sensitive indicator of changes in crop growth and radiation capture (Asrar *et al.*, 1992). Improvements in timeliness and cost of remote sensing systems will continue to expand the use of this technology, provided that simpler and less costly systems can still accurately estimate crop health.

Ground Cover Fraction and Crop Growth

Ground cover fraction is typically defined as the ratio of green vegetation to the total scene detected from the vertical direction (Purevdorj *et al.*, 1998). This measurement has been shown to be highly correlated with crop growth and radiation capture (Klassen *et al.*, 2003), and has been proposed to be a more sensitive indicator than leaf area index of crop growth and radiation capture by Asrar *et al.* (1992).

Ground cover fraction measurements are commonly made using a digital camera mounted facing down toward the crop canopy (Purevdorj *et al.*, 1998). The images are processed, and plant pixels are separated from soil pixels in software, either manually or by using software that has been designed to discriminate between plant and soil pixels. Ground cover fraction measurements have the potential to be very precise (Klassen *et al.*, 2003), but in the field, several factors may affect accuracy, including camera height, lighting conditions, and the plot separability.

Camera height affects measurements at both the ground level and at high altitudes. Ground level measurements tend to be the most precise measurements, since there are high quantities of both plant and ground pixels. However, the measurements are affected by the distance of the camera above the plant canopy, since a camera near the canopy will be influenced by the plant being closer than the soil to the camera. Increases in altitude increase the ground area sensed by each camera pixel (Fig. 4.2), so high-altitude images become impractical for ground cover estimation

when the area sensed by each pixel becomes a significant portion of row width. At this point, vegetation indices, which estimate fractional ground cover from the spectral characteristics of a scene, are more appropriate.

Remote Sensing Vegetation Indices

Current remote sensing platforms such as satellites, airplanes, and ground-based platforms are used to obtain field-scale imagery with limited user intervention (Sui *et al.*, 2005; Vierling *et al.*, 2006; Yang *et al.*, 2001; Yang *et al.*, 2003).

Satellites and airplanes cover a broad spatial area (typically larger than a single irrigated field) with a single image. Because of the high altitudes associated with these platforms crop growth estimates are made primarily with vegetation indices, such as the normalized difference vegetation index (NDVI), its variants, and other indices that minimize soil reflectance effects or atmospheric effects (Elvidge and Chen, 1995; Huete, 1988; Rouse *et al.*, 1973). Other intermediate platforms for both imagery and spectrometry, such as tethered blimps (Chen and Vierling, 2006; Vierling *et al.*, 2006) have been suggested.

Aerial images measure reflected incident radiation from the sun and can be affected by atmospheric conditions (Jackson *et al.*, 1983).

Ground-based reflectance measurements are typically collected at several points throughout the field, and reflectance measurements can be either passive (measurements of reflected sunlight) or active (measurements of reflected light from an electric light source). Active reflectance measurements often use a modulated light source to minimize the effects of ambient light, as described by Sui *et al.* (2005).

Reflectance Measurements

Although several reflectance regions throughout the shortwave infrared spectrum have been compared to crop health, combinations of green, red, red edge, and near-infrared (NIR) reflectance have consistently produced many of the closest relationships with crop growth and health, due to chlorophyll absorbance and leaf mesophyll structure (Carter and Spiering, 2002; Gitelson and Merzlyak, 1998; Horler *et al.*, 1983b).

Vegetation indices measure reflectance interactions by wavelength as ratios, differences, ratioing differences and sums, and by forming linear combinations of wavelengths in order to increase vegetation signal and minimize other effects from soil or the atmosphere (Jackson and Huete, 1991). However, most vegetation indices are also sensitive to soil properties, plant canopy geometry, solar angle, cloudiness, and other atmospheric effects (Baret and Guyot, 1991). Provided soil, plant, and atmospheric effects are accounted for, vegetation indices provide a robust method for identifying crop growth characteristics and detecting general stress events. Crop absorbance and reflectance are closely tied to biomass (Klassen *et al.*, 2003; Osborne *et al.*, 2002; Plant *et al.*, 2000), although Pinter *et al.* (2003) stated that most vegetation indices offer general estimates of crop growth and health rather than diagnosing specific stresses that contribute to differences in biomass.

Remote sensing of plant stress for irrigation is unique because of the need for rapid processing and decision making, as well as the dynamic crop growth characteristics related to water status. Much of the geoprocessing of the target site, such as defining a geometric model, choosing appropriate control points, and loading a digital elevation model, can be completed prior to the growing season. However, in-season analysis must be quick, simple, and sensitive enough to changes in vegetative growth to let the producer make irrigation decisions. Minimizing the costs

and processing time is important, because producers faced with other production tasks may be inclined to ignore the data until after the growing season if it is not delivered quickly and in a simple manner.

The objectives of this research were to compare measurements of fractional ground cover, vegetation indices based on visible and near-infrared (NIR) aerial imagery, and ground-based vegetation indices from a spectrometer for sensitivity to crop growth. The vegetation indices chosen for this study included the Green:Red ratio, as described by Adams *et al.* (1999), and the red and red-edge variants of the normalized difference vegetation index (NDVI), as described by Ritchie and Bednarz (2005).

Materials and Methods

The research was conducted at the Stripling Irrigation Research Park in Camilla, Georgia during 2004-2006. Delta & Pineland 555 BG/RR was seeded in 0.91 m rows at a rate of 126,000 plants ha^{-1}. Planting dates were 5 May 2004, 20 Apr. 2005, and 2 May 2006. In 2004, the study was conducted under a variable-rate center pivot based on the design described by Perry *et al.* (2002). Buffer regions were designated between treatment nozzle packages to avoid irrigation overlap, and all ground-level measurements were done in the center of each treatment to avoid the buffer regions. Plot lengths ranged from approximately 21 m on the inner row of the smallest treatment to 37 m on the outer row of the largest treatment. The design was a 4 x 4 Latin square with four irrigation treatments ranging from well-watered to non-irrigated. Plots were strip-tilled. Watermark™ sensors (Irrometer, Riverside, CA) were placed in each plot at depths of 20, 40, and 60 cm. Watermark sensors estimate soil tension based on electrical resistance through a granular matrix between two electrodes. The sensor has a 0-200 kPa range. Fertility, weed control, insect monitoring and control were done in accordance with the University of Georgia

Cooperative Extension Service Guidelines. To ensure a uniform stand, all plots were irrigated 13 mm prior to emergence with the overhead system.

In 2005 and 2006, the study was continued on lateral irrigation systems designed to allow watering of plots in a randomized design. There were five irrigation treatments, which ranged from well-watered to non-irrigated, with four replicates of each treatment. In 2005, all 20 plots were conventional tillage, while in 2006, 20 plots were strip-tilled, with an additional 16 plots that were conventional tillage with four of the irrigation levels.

As with the 2004 study, buffer regions were designated between treatment nozzle packages to avoid irrigation overlap, and all measurements were performed in the center of each treatment to avoid the buffer regions. Plot lengths were 21 m. Early irrigation was applied to all plots after planting at a rate of 13 mm in 2005 and 20 mm in 2006 to ensure uniform emergence. Crop height was managed using mepiquat chloride at 550 mL ha^{-1} at squaring, then 550-1400 mL ha^{-1} uniformly applied over all treatments at 1-2 week intervals based on management guidelines for a total of 3500-4200 mL per year for the studies. Prior to harvest, plots were defoliated with 2.3 L ha^{-1} ethephon plus cyclanilide and 0.7 kg ai ha^{-1} thidiazuron when the crop reached 90% open boll.

Aerial Imagery

Aerial imagery was collected using a 5 m * 2.5 m tethered blimp (Southern Balloon Works, Deland, FL) and a two-camera remote system. The blimp has a 40 N lift rating by the manufacturer. The camera system included two Nikon 4300 digital cameras, one of which was modified to be near-infrared sensitive, a Digisnap 2100 electronic shutter release device (Harbotronics, Gig Harbor, WA), and a radio control system that allowed simultaneous remote firing of the cameras from the ground. The camera settings were based on the methods described

in Chapter 3 (sunlight white balance, ISO100, image adjustment off, exposure correction applied between cameras). The blimp was flown over the plots at heights that ranged from about 45 m for ground cover measurements to about 180 m for vegetation index measurements. Images were collected 2-3 times per week on average through late bloom, with collection dates determined by environmental factors such as cloud cover and wind (>20 mph), and measurements were collected between 10 AM and 1 PM. In 2004, 6-8 rows from each plot were selected for ground cover and vegetation index measurement, due to the spatial constraints of the variable rate center pivot. In 2005 and 2006, four rows of each plot were selected from each plot. Spatial resolution varied with plant height based on the relationship shown in Fig. 4.2.

Ground Cover

Plot markers were placed adjacent to each plot for identification purposes after emergence, and images were collected 45-75 m above the cotton plots for ground cover measurements. Ground cover was estimated from the four center rows spanning the length of the plot. Images were opened in Adobe Photoshop CS2, and image angle was corrected using the measure tool and the autorotate function. The rectangular marquee tool was used to select each plot of interest, and the selection included four plant rows and four soil rows (Fig. 4.1). Each plot was extracted into its own work space. Image pixels containing plants were separated from pixels containing soil using the magic wand tool, and the number of plant pixels and total pixels were recorded from the Photoshop histogram values. Ground cover fraction was calculated as the ratio of plant pixels to total pixels. Images were collected 2-3 times per week, as weather permitted.

Normalized difference vegetation index (NDVI) values were calculated from the visible and near-infrared images based on camera brightness values and the relationship between camera brightness, camera exposure, and scene reflectance of the two cameras, as determined in Table

2.1. The center four rows of each plot were selected, and the NDVI for each plot was calculated from the mean image brightness for each plot measured from the visible and near-infrared channels.

Ratios of the mean green to mean red brightness values from the visible camera were calculated for each plot, as described by (Adamsen *et al.*, 1999). The purpose of these measurements was to determine whether an index based solely on visible brightness characteristics might be practical for estimation of crop growth.

Spectrometer Measurements

Ground-level reflectance of each plot was measured using an Apogee Vis-NIR spectrometer (Apogee Instruments, Inc., Logan, UT) with an effective spectral range of 400-900 nm and a spectral resolution of 1.4 nm (full width, half maximum height). Each reading consisted of an average of three spectral scans, and two were collected in each plot on each sampling date. A white polytetrafluoroethylene (PTFE) reflectance standard was used as a reference, and reflectance by wavelength was calculated as the ratio of scene reflectance to the reflectance of the standard. References were collected at 10-15 minute intervals, or whenever clouds were passing over. Reflectance measurements were collected only when direct sunlight was available, on average twice a week.

Spectrometer measurements from all treatments were compared with ground cover, with the exception of the most water-stressed treatment on day 76 after planting in 2004, when the crop was wilted to such an extent that the spectrometer measured very little vegetation.

Analysis

Ground cover measurements using the visible and NIR cameras were compared to determine whether one method estimated higher ground cover levels than another, as well as to determine

the error associated with the ground cover estimates. The error was calculated as the standard error of the estimate.

The camera and spectrometer-based vegetation indices were compared with ground cover and with each other to determine sensitivity to changes in crop growth from low to high levels of ground cover.

In addition, the sensitivity of each index to within-date growth variability was tested by an ANOVA comparison of treatment mean separation at three crop growth stages: between first square and first bloom, after first flower, and near peak bloom.

Results

Ground Cover

Image-based estimates of ground cover with visible and near-infrared cameras were highly correlated, as shown in Fig. 4.3 ($r^2 = 0.93$; standard error of estimate 0.04). However, the sensitivity of this method is limited by the distance of the cameras above the crop canopy. Klassen *et al.* (2003) noted that images too close to the crop canopy can overestimate ground cover, based on the distance formula. At larger distances from the crop canopy, this method is limited by the relationship between the pixel size and the crop row width (Fig. 4.2). The decreased pixel resolution limits the accuracy of this method, particularly at distances greater than 50 m, where the ratio is greater than 0.05 (5%). A second difficulty with ground cover estimation is the effect of shadows and different reflectivity of soil, both of which can complicate ground cover estimates. Cloudy conditions decrease shadows and provide the simplest ground cover estimates.

Ground Cover and Spectral Indices

Ground cover estimates and spectral estimates correlated closely throughout the growing season during each year, with correlation coefficients ranging from 0.64 to 0.95, as shown in Table 4.1. Of particular interest was the high correlation between the camera Green:Red ratio and the other indices, since this index would allow the use of a single camera, decreasing the cost and complexity of the system. A comparison of Green:Red ratio with NDVI (Fig. 4.4) showed a linear relationship with a high correlation ($r^2 = 0.90$) between the two indices. The linear correlation suggests that these indices have a similar dynamic range. A comparison of the two indices over the entire study area (Fig. 4.5 and Fig. 4.6) showed similar trends within the field, and both indices correlated closely with each other. However, the two indices were not linearly correlated, as shown in Fig. 4.6. At low index values, NDVI continued to trend downward, while the Green:Red ratio did not. The lack of change in Green:Red ratio as NDVI values decrease suggests that there is a range of low NDVI values that the Green:Red ratio does not account for. This is less noticeable in situations where soil and plant reflectance are integrated in the image, because the green plants affect both indices.

As shown in Table 4.1, the Green:Red ratio correlated more closely with ground cover and spectrometer-based indices than the camera NDVI, although the differences in correlation were small. Part of this may be due to the need for exposure correction between the visible and near-infrared cameras, as well as small alignment errors between visible and near-infrared images. Exposure correction adds a small error to estimates of NDVI, as discussed in Chapter 3.

Neither of the camera-based vegetation indices tested had a linear relationship with the entire range of ground cover. For example, Fig. 4.7 shows that Green:Red ratio values saturated at both low and high levels of ground cover. This suggests that a shortcoming of these indices is

their spectral dynamic range, an issue that has been reported by several authors (Carter and Spiering, 2002; Gitelson and Merzlyak, 1997; Horler *et al.*, 1983a).

Spectrometer-based spectral indices were closely related with each other. However, $NDVI_{710}$ showed a greater dynamic range than NDVI, as shown in Fig. 4.9. This concept was emphasized in a study on the sensitivity of indices to leaf area index (Ritchie and Bednarz, 2005), where red edge-based NDVI estimates were sensitive to a broader range of leaf area index values than NDVI estimates based on red and near-infrared reflectance.

The $NDVI_{710}$ index reached a maximum at a ground cover fraction of less than 0.80, as shown in Fig. 4.10. This index also reached a maximum at camera Green:Red ratio values greater than 1.3 (Fig. 4.8), suggesting that this index is less sensitive to high levels of ground cover than is the Green:Red ratio. However, Fig. 4.8 also indicates that $NDVI_{710}$ is more sensitive to low levels of ground cover than the camera Green:Red ratio.

Some of the scatter in the relationship between camera and spectrometer estimates of NDVI is attributable to differences in scale. As shown in Table 4.2, spectrometer and camera NDVI values of individual plots tended to be highly correlated, particularly in the well-watered treatments (irrigation treatments 1-3), with r^2 values ranging from 0.66 to 0.96 in the strip tillage plots, and from 0.78 to 0.95 in the conventional tillage plots. The slope of the relationship was also similar between plots for both tillage treatments. This suggests that some of the variance between the two methods is plot-specific, and can be described the unique relationship between the sampling points for the spectrometer and the plot at large, which was measured by the spectrometer.

Treatment Comparisons

Treatment comparisons using ground cover fraction, camera Green:Red index, and spectrometer measurements throughout the growing seasons from 2004-2006 are shown and discussed in Chapter 5. A comparison of indices during 2006 at squaring, early bloom, and near peak bloom is shown in Fig. 4.11. All of the indices showed significant differences at the P=0.05 level between irrigation treatments at all three dates, with the exception of the camera NDVI index (P=0.075). In addition, camera NDVI had larger variance, as indicated by higher treatment variances and lower significance levels at all dates.

Discussion

Ground cover fraction measurements had the broadest dynamic range of any remote sensing method tested. However, these measurements require imagery with a high pixel resolution, and separation can be complicated by shadows, soil texture and brightness, and the difficulty in analyzing pixels that include both soil and plant. Ground cover fraction is also time consuming to calculate if done by hand, and computer-based measurements require careful oversight to avoid the effects of changes in lighting, soil background, shadows, and changes in plant reflectance (Hayes and Han, 1993). However, this method is appropriate for plot-level measurements of crop growth, since it can measure entire plots at altitudes that still allow high-resolution separation of plant and soil pixels. Another advantage is the ability to conduct ground cover measurements on cloudy days, which interfere with most conventional aerial imagery. None of the spectral indices detected a full range of crop cover, although the indices were sensitive to different ranges of ground cover levels. The $NDVI_{710}$ was more sensitive to low levels of vegetation than the camera indices (Fig. 4.8), but was less sensitive to high ground cover. One probable reason for this is the increased plant influence due to its closer proximity to

the sensor. Klassen *et al.* (2003) emphasized the effect of apparent size in measurements of plant growth, suggesting that the increased influence of the plant material causes an overestimation of green cover. This over-estimated green cover, in turn, would result in saturation of the vegetation index at a lower level than if the spectrometer was further from the plants.

The camera Green:Red ratio was linearly related with camera NDVI throughout the growing season (Fig. 4.4), even though the Green:Red index is a ratio, and the NDVI is a normalized ratio with bounding levels of -1 to 1. Ratios of red and near-infrared reflectance are not linearly related with NDVI. Comparisons of these indices over a broad range of pixel values on a single date suggest that both indices detect similar treatment differences, as shown in Fig. 4.5. The relationship is approximately linear at NDVI values above 0.20, but Green:Red ratio values are linearly correlated with low values of NDVI, as shown in Fig. 4.6.

The spectrometer $NDVI_{710}$ had better dynamic range than NDVI, as well as a higher correlation with ground cover and camera vegetation indexes. This agrees with other studies (Carter and Spiering, 2002; Horler *et al.*, 1983b; Ritchie and Bednarz, 2005) that suggest that red edge measurements can improve the dynamic range of indices used to estimate chlorophyll density at both the leaf and plant canopy levels.

The results from this study suggest that the camera NDVI, camera Green:Red ratio, and spectrometer $NDVI_{710\ nm}$ indices all have useful attributes for specific remote sensing needs. The higher sensitivity of $NDVI_{710\ nm}$ suggests that it would be more appropriate for ground-based measurement systems; however, aerial systems based on this index would require more extensive consumer camera modification than indices based on visible channels. The consistency of the aerial NDVI measurements over the growing season despite the wide range of camera exposure differences suggests that this index can provide a robust NDVI estimate. The Green:Red ratio,

which has already been shown to be effective for estimating leaf senescence (Adamsen *et al.*, 1999), also provides a very simple method for ground cover estimates, although it appears to be less sensitive to low levels of ground cover than the NDVI. The Green:Red ratio allows a simple, low-cost, single camera system for remote sensing of crop growth.

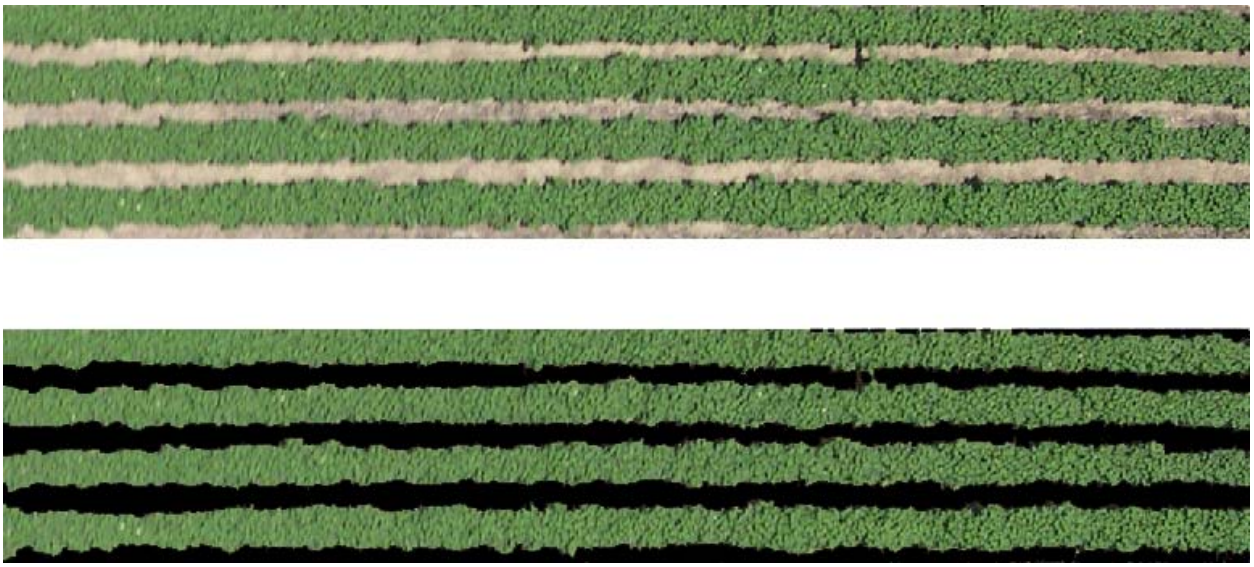

Fig. 4.21. Ground cover measurements included four plant rows and four soil rows. Plant pixels were separated from soil pixels using the magic wand selection tool, as shown by the selection mask in the bottom frame.

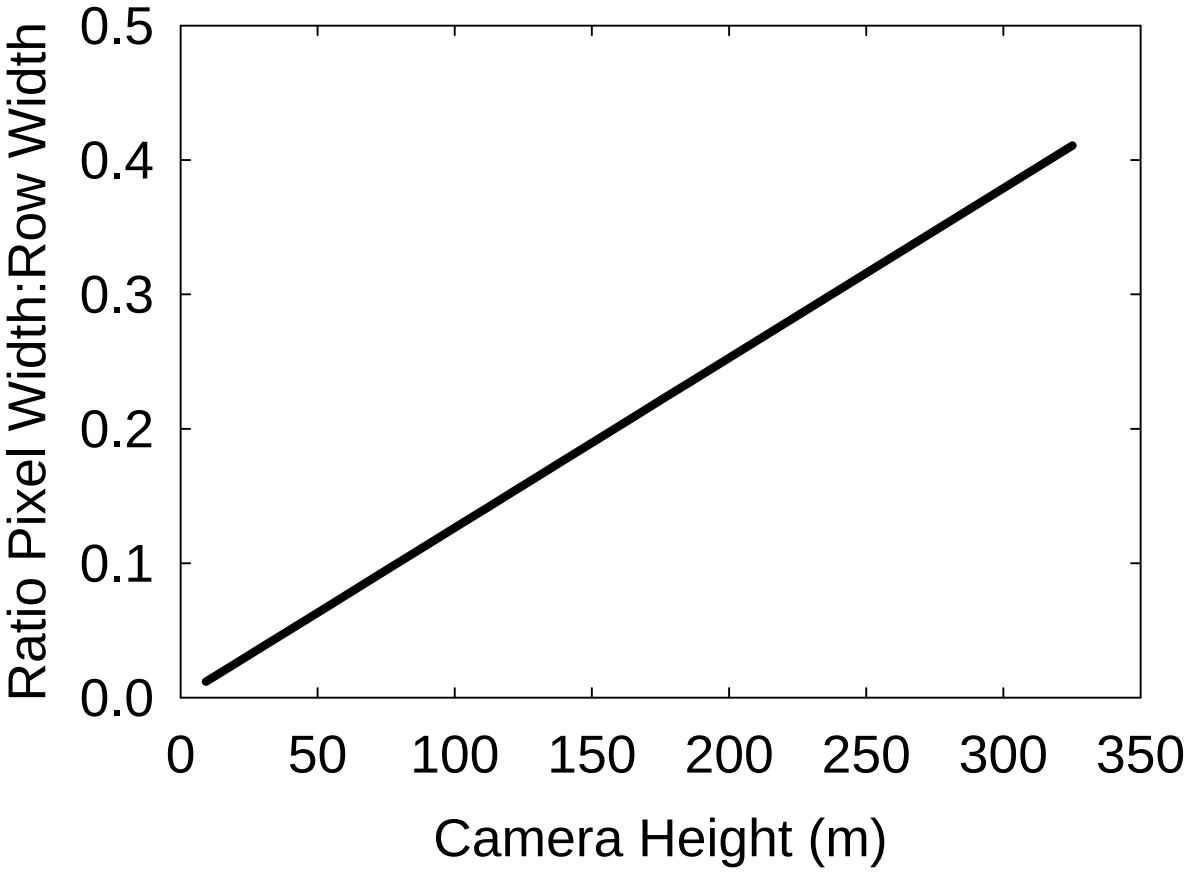

Fig. 4.22. Ratio of pixel width to cotton row width based on camera height.

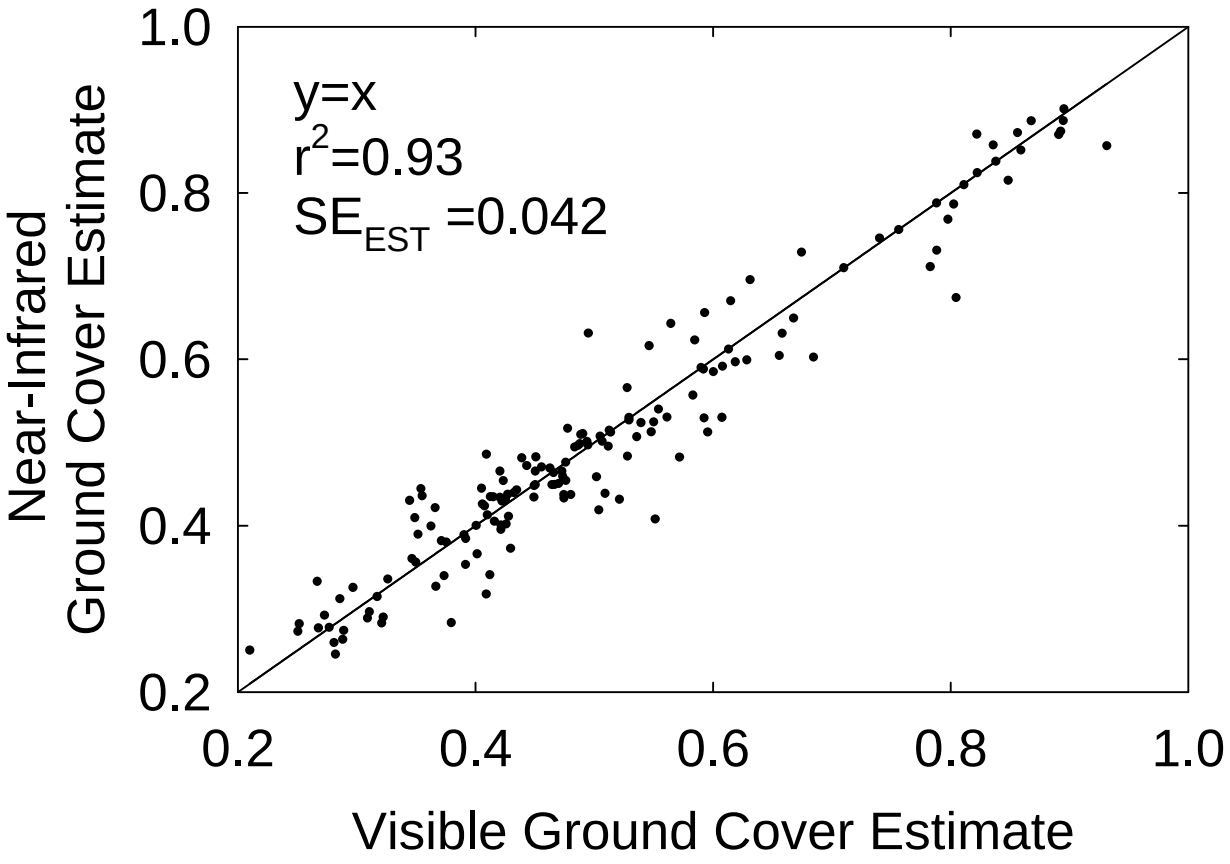

Fig. 4.23. Comparison of visible and near-infrared ground cover estimates during 2004.

Table 4.3. Pearson correlation matrices for 2004-2006.

		Ground Cover	$NDVI_{spec}$	$NDVI_{710}$	Green:Red	$NDVI_{camera}$
2004	Ground Cover	1.00				
	$NDVI_{spec}$	0.83	1.00			
	$NDVI_{710}$	0.85	0.92	1.00		
	Green:Red	0.88	0.85	0.88	1.00	
	$NDVI_{camera}$	0.85	0.83	0.86	0.91	1.00
2005	Ground Cover	1.00				
	$NDVI_{spec}$	0.64	1.00			
	$NDVI_{710}$	0.66	0.85	1.00		
	Green:Red	0.93	0.72	0.80	1.00	
	$NDVI_{camera}$	0.89	0.70	0.79	0.94	1.00
2006	Ground Cover	1.00				
	$NDVI_{spec}$	0.87	1.00			
	$NDVI_{710}$	0.89	0.97	1.00		
	Green:Red	0.92	0.91	0.93	1.00	
	$NDVI_{camera}$	0.91	0.92	0.92	0.96	1.00

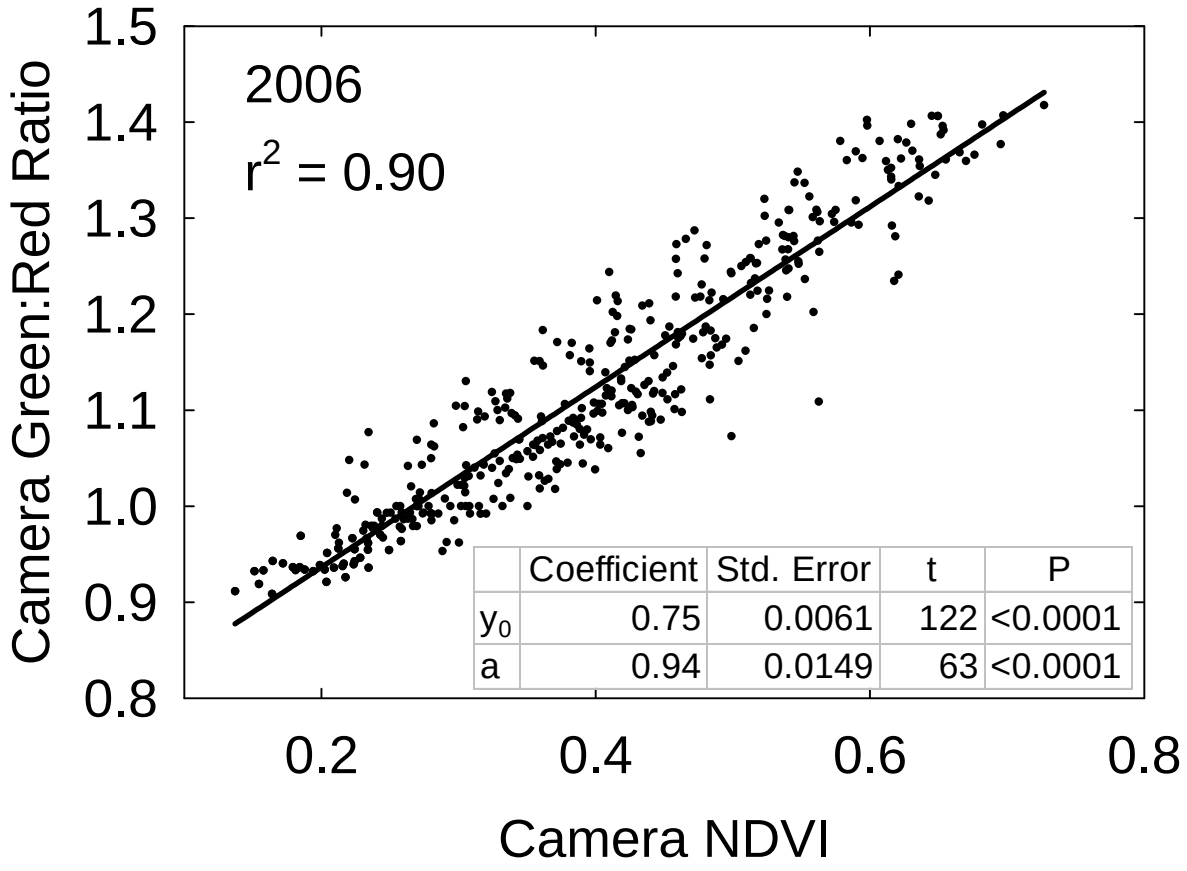

Fig. 4.24. Comparison of visible and NIR camera NDVI with visible camera Green:Red ratio. Green:Red ratio was closely correlated with camera NDVI.

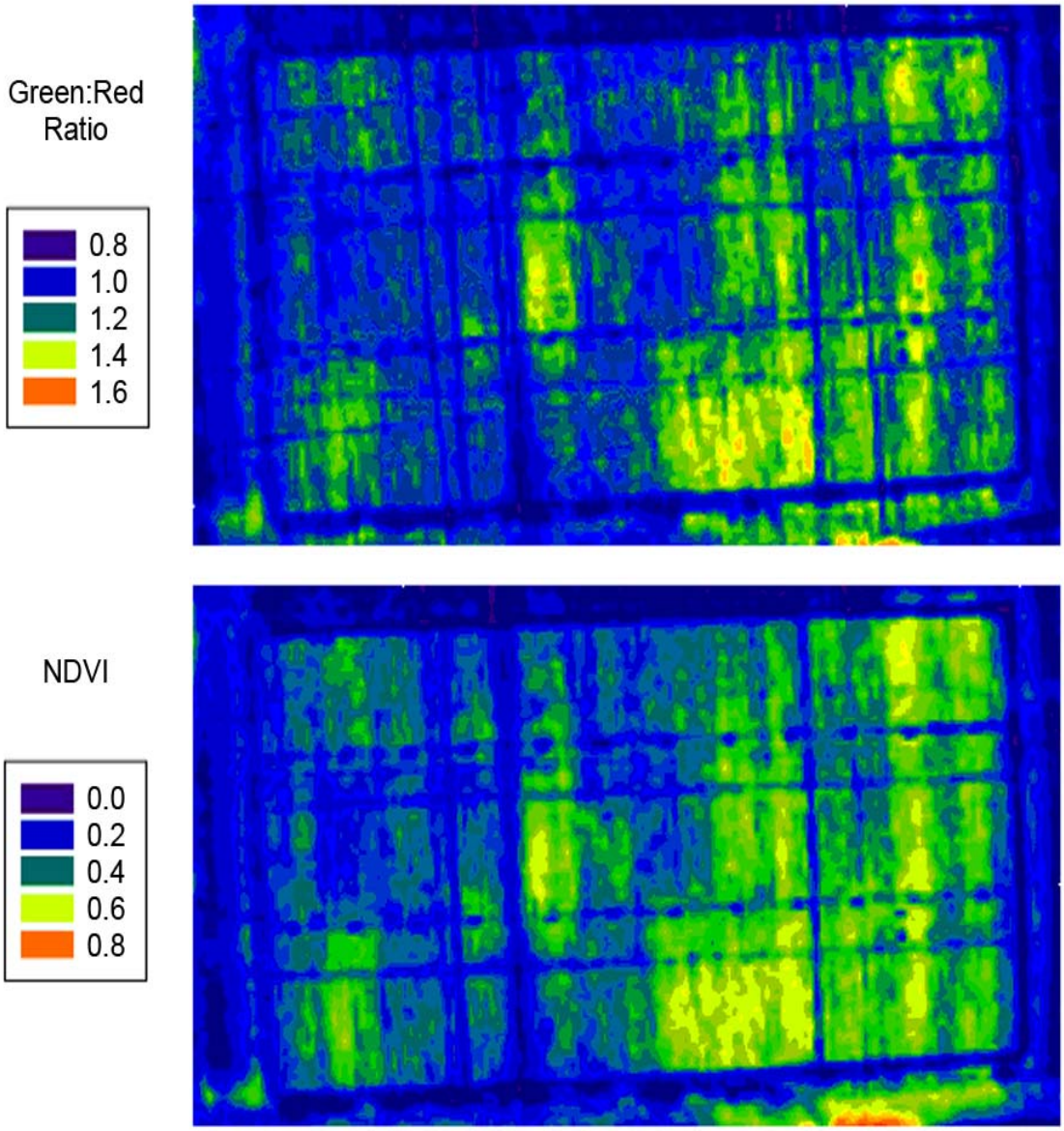

Fig. 4.25. Green:Red ratio and NDVI on July 21, 2006. Both indices showed similar trends throughout the growing season.

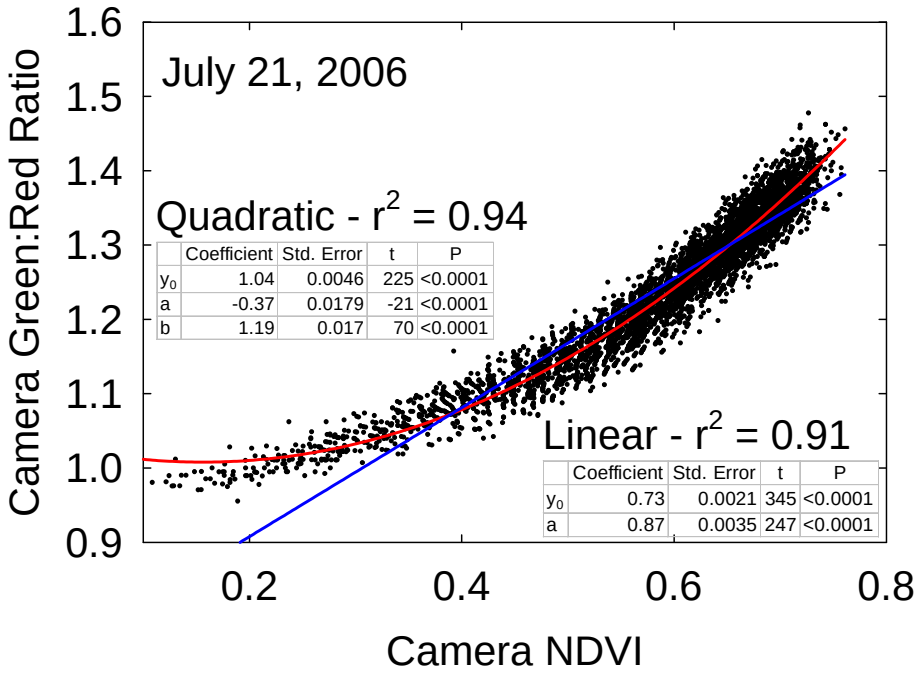

Fig. 4.26. Relationship of camera Green:Red ratio with camera NDVI on July 21, 2006. Both indices were calculated from pixel values over the entire field.

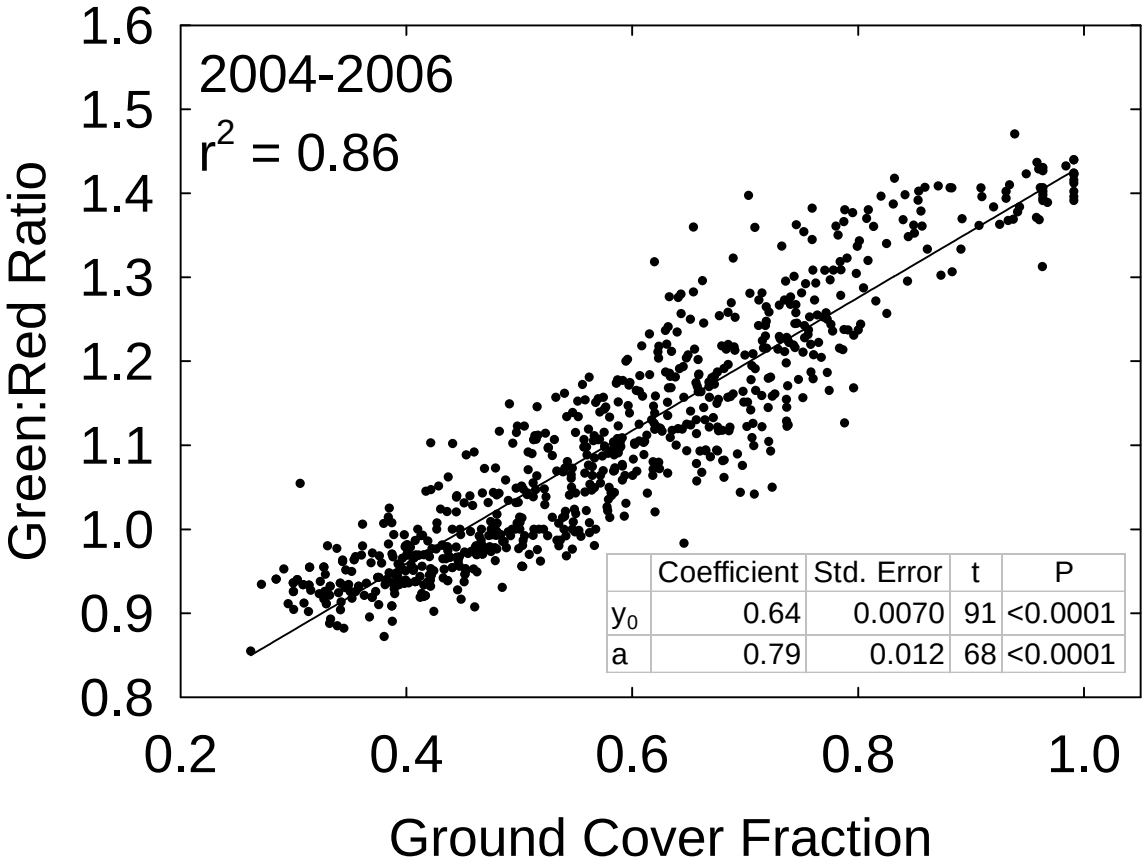

Fig. 4.27. Relationship between Green:Red camera ratio and fractional ground cover (2004-2006).

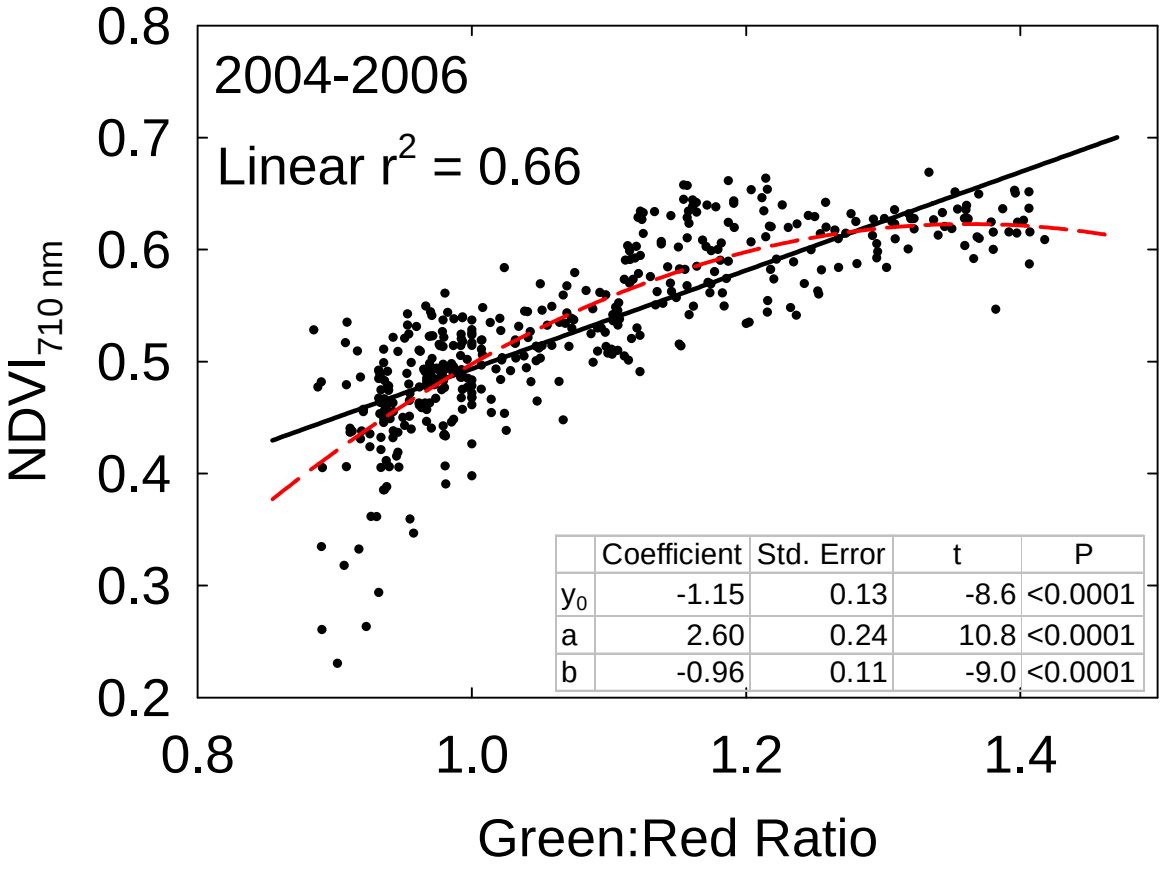

Fig. 4.28. Relationship of $NDVI_{710}$ collected with the spectrometer with the Green:Red ratio collected with the visible camera (2004-2006). The camera measurements continued to trend upward after the spectrometer NDVI stopped its upward movement.

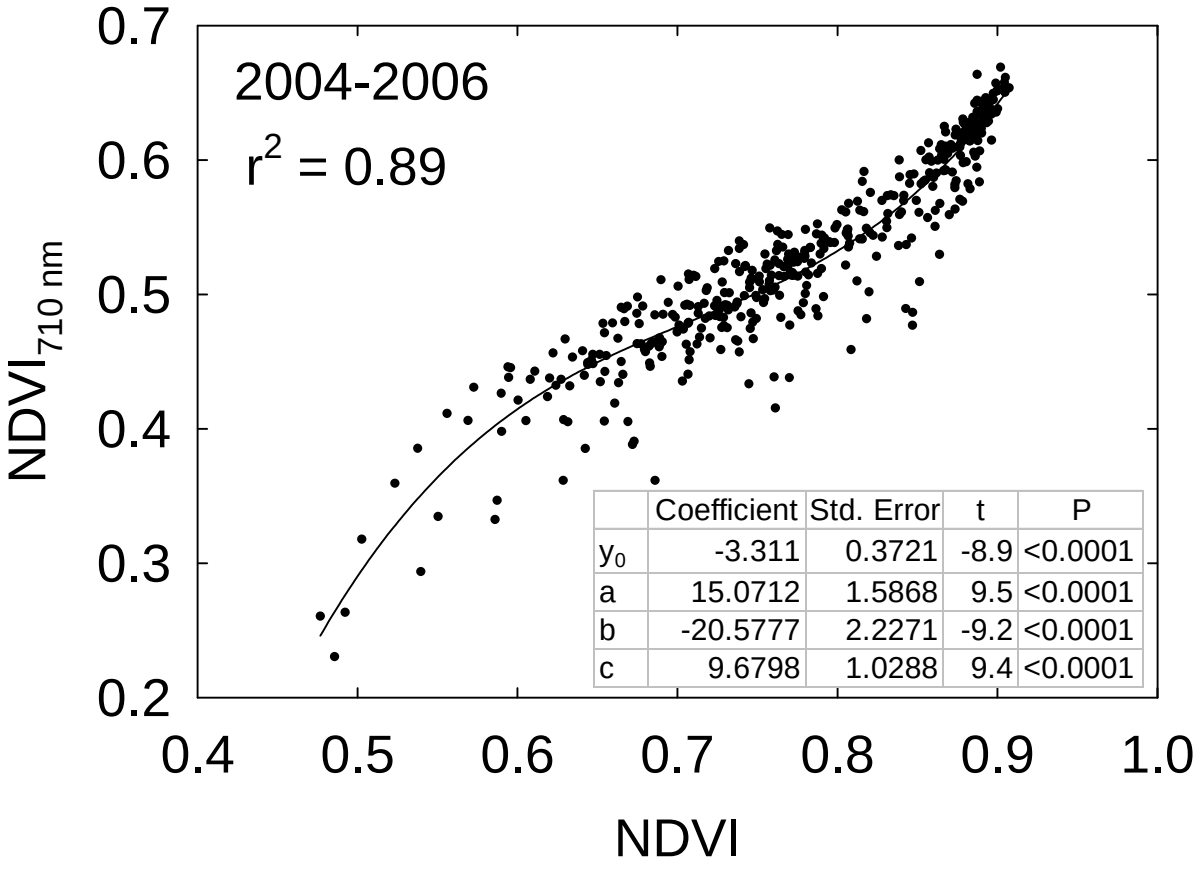

Fig. 4.29. Comparison of spectrometer $NDVI_{710}$ with spectrometer NDVI (2004-2006).

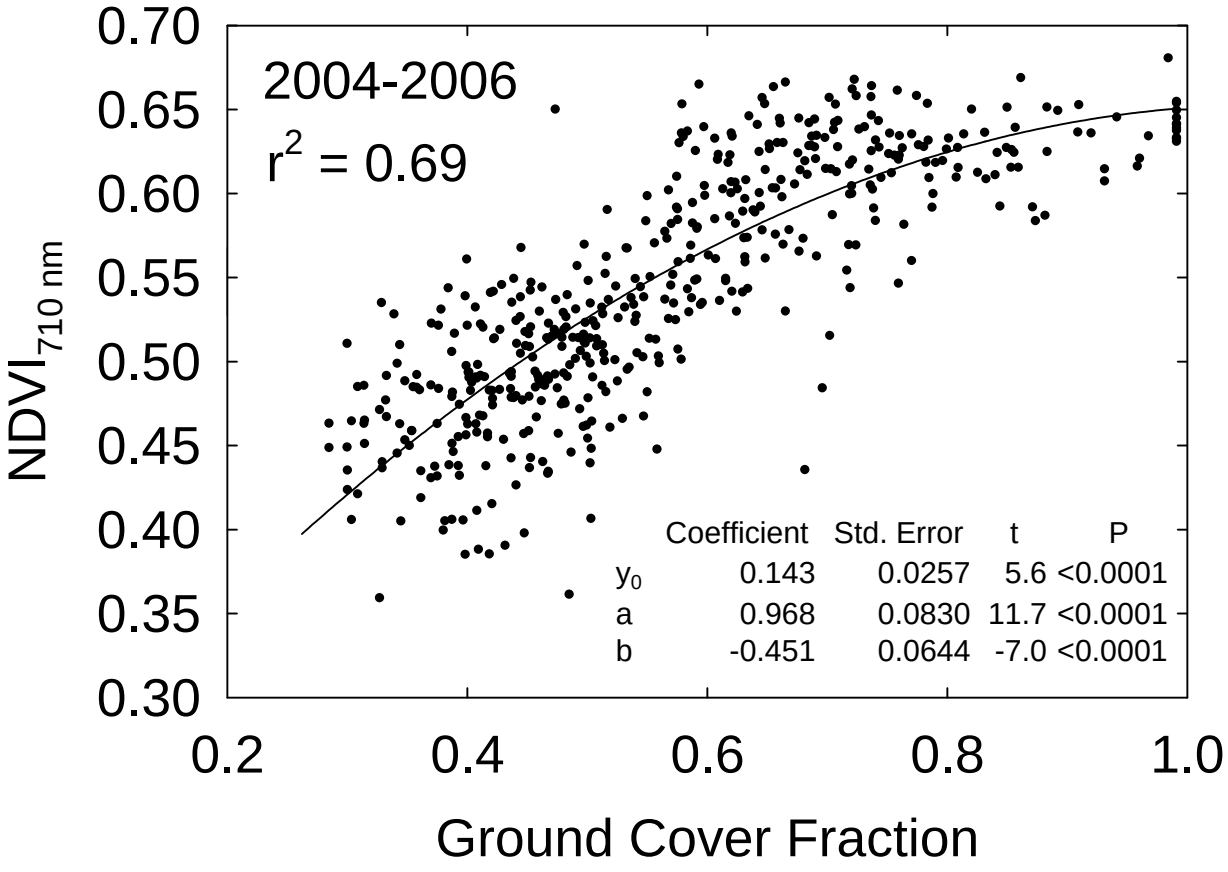

Fig. 4.30. Comparison of spectrometer $NDVI_{710}$ with ground cover fraction (2004-2006).

Table 4.4. Relationship between camera NDVI and spectrometer NDVI by plot over n=8 days.

Conservation Tillage				
Irrigation	Rep	r^2	Slope	Intercept
20-cbar	1	0.93	2.44	-0.85
	2	0.83	2.09	-0.69
	3	0.82	1.58	-0.49
	4	0.96	1.92	-0.63
40-cbar	1	0.91	2.75	-1.05
	2	0.81	2.38	-0.89
	3	0.71	2.12	-0.77
	4	0.75	1.62	-0.48
Aerial	1	0.66	2.29	-0.80
	2	0.86	2.79	-1.07
	3	0.78	1.97	-0.65
	4	0.68	1.25	-0.27
Aerial-3 days	1	0.86	2.15	-0.76
	2	0.60	1.73	-0.58
	3	0.77	1.56	-0.49
	4	0.77	1.75	-0.56
Non-irrigated	1	0.86	3.04	-1.20
	2	0.55	1.67	-0.58
	3	0.52	1.39	-0.36
	4	0.65	0.93	-0.16

Conventional Tillage				
Irrigation	Rep	r^2	Slope	Intercept
20-cbar	1	0.82	2.37	-0.83
	2	0.78	2.31	-0.88
	3	0.83	2.28	-0.84
	4	0.87	2.24	-0.82
40-cbar	1	0.88	2.40	-0.90
	2	0.83	3.16	-1.33
	3	0.90	2.47	-0.94
	4	0.92	2.38	-0.92
Aerial	1	0.89	2.24	-0.80
	2	0.90	2.72	-1.08
	3	0.95	2.34	-0.93
	4	0.88	2.33	-0.93
Aerial-3 days	1	0.81	2.35	-0.85
	2	0.76	2.65	-1.05
	3	0.92	1.89	-0.65
	4	0.80	1.34	-0.38

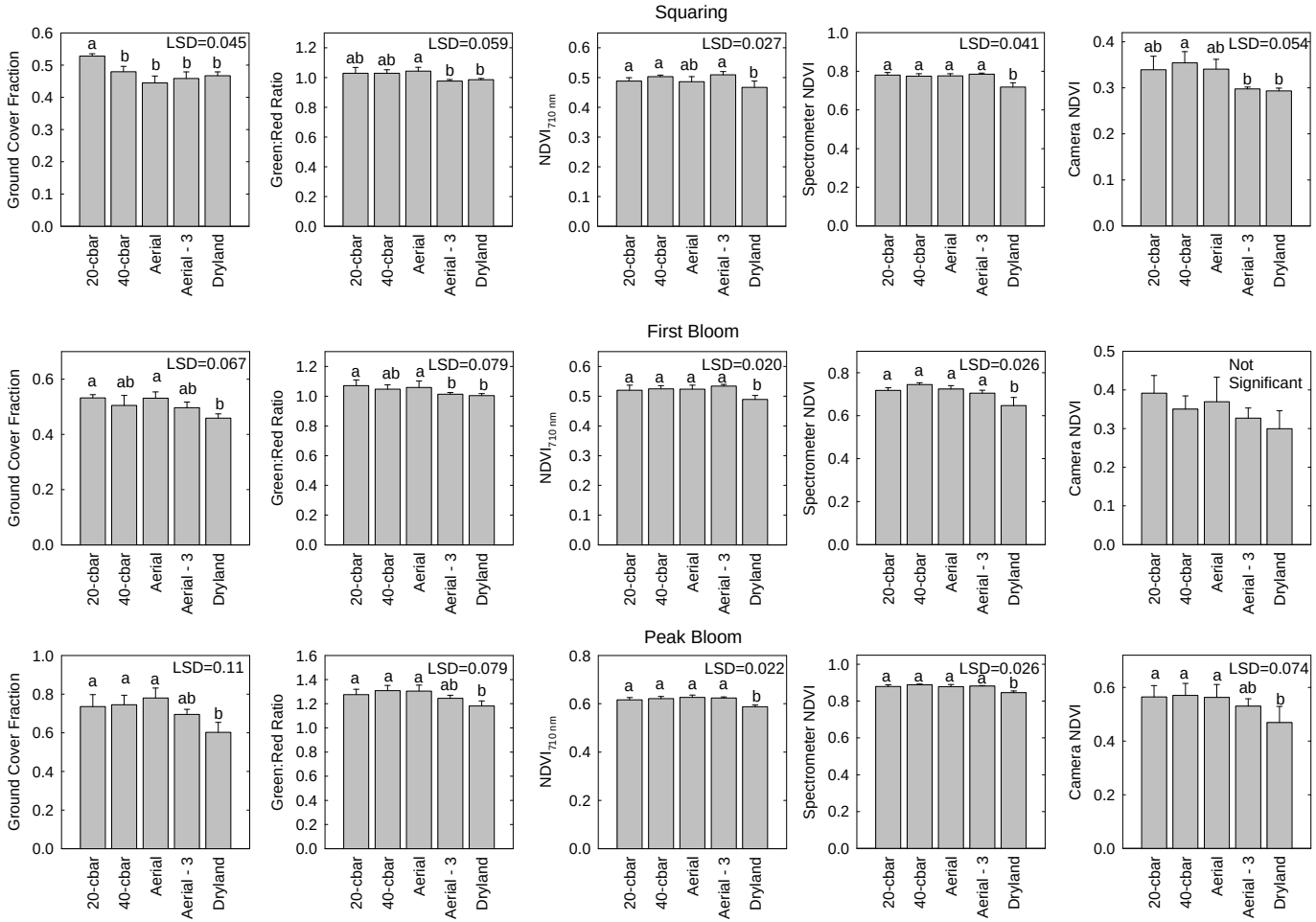

Fig. 4.31. Comparison of treatment means at squaring, early bloom, and near peak bloom, 2006. Error bars represent standard error of mean, and letters represent LSD significant differences at P=0.05. Camera NDVI at first bloom was not significant at the 0.05 level, but was significant at the 0.10 level.

References

Adams, M.L., W.D. Philpot, and W.A. Norvell. 1999. Yellowness index: an application of spectral second derivatives to estimate chlorosis of leaves in stressed vegetation. Int. J. Remote Sens. 20:3663-3675.

Adamsen, F., P. Pinter, E. Barnes, R. LaMorte, G. Wall, S. Leavitt, and B. Kimball. 1999. Measuring wheat senescence with a digital camera. Crop Sci. 39:719-724.

Asrar, G., R.B. Myneni, and B.J. Choudhury. 1992. Spatial heterogeneity in vegetation canopies and remote sensing of absorbed photosynthetically active radiation: A modeling study. Remote Sens. Environ. 41:85-103.

Bannari, A., Morin, D., Bonn, F., and Huete, A.R. 1995. A review of vegetation indices. Remote Sensing Reviews 13:95-120.

Baret, F., and G. Guyot. 1991. Potentials and limits of vegetation indices for LAI and APAR assessment. Remote Sens. Environ. 35:161-173.

Carter, G.A., and B.A. Spiering. 2002. Optical properties of intact leave for estimating chlorophyll concentration. J. Environ. Qual. 31:1424-1432.

Chen, X., and L. Vierling. 2006. Spectral mixture analyses of hyperspectral data acquired using a tethered balloon. Remote Sens. Environ. 103:338-350.

Elvidge, C.D., and Z. Chen. 1995. Comparison of broad-band and narrow-band red and near-infrared vegetation indices. Remote Sens. Environ. 54:38-48.

Famiglietti, J.S., J.A. Devereaux, C.A. Laymon, T. Tsegaye, P.R. Houser, T.J. Jackson, S.T. Graham, M. Rodell, and P.J.v. Oevelen. 1999. Ground-based investigation of soil moisture variability within remote sensing footprints during the Southern Great Plains 1997 (SGP97) hydrology experiment. Water Resources Research 35:1839-1851.

Gitelson, A.A., and M.N. Merzlyak. 1997. Remote estimation of chlorophyll content in higher plant leaves. Int. J. Remote Sens. 18:2691-2697.

Gitelson, A.A., and M.N. Merzlyak. 1998. Remote sensing of chlorophyll concentration in higher plant leaves. Adv. Space Res. 22:689-692.

Hayes, J.C., and Y.J. Han. 1993. Comparison of crop-cover measuring systems. Trans. ASAE 36:1727-1732.

Horler, D.N.H., M. Dockray, and J. Barber. 1983a. The red edge of plant leaf reflectance. Int. J. Remote Sens. 4:273-288.

Horler, D.N.H., M. Dockray, J. Barber, and A.R. Barringer. 1983b. Red edge measurements for remotely sensing plant chlorophyll content. Adv. Space Res. 3:273-277.

Huete, A.R. 1988. A soil-adjusted vegetation index (SAVI). Remote Sens. Environ. 25:295-309.

Jackson, R.D., and A.R. Huete. 1991. Interpreting vegetation indices. Preventive Veterinary Medicine 11:185-200.

Jackson, R.D., P.N. Slater, and P.J. Pinter. 1983. Discrimination of growth and water stress in wheat by various vegetation indices through clear and turbid atmospheres. Remote Sens. Environ. 13:187-208.

Klassen, S.P., G. Ritchie, J. Frantz, D. Pinnock, and B. Bugbee. 2003. Real-time imaging of ground cover: Relationships with radiation capture, canopy photosynthesis, and daily growth rate. In: Digital Imaging and Spectral Techniques: Applications to Precision Agriculture and Crop Physiology. ASA Special Publication no. 66.

Osborne, S.L., J.S. Schepers, D.D. Francis, and M.R. Schlemmer. 2002. Use of spectral radiance to estimate in-season biomass and grain yield in nitrogen- and water-stressed corn. Crop Sci. 42:165-171.

Perry, C.D., S. Pocknee, O. Hansen, C. Kvien, G. Vellidis, and E. Hart. 2002. 2002 ASAE Annual International Meeting / CIGR 15th World Congress, Chicago, IL.

Pinter, P.J., J.L. Hatfield, J.S. Schepers, E.M. Barnes, M.S. Moran, C.S.T. Daughtry, and D.R. Upchurch. 2003. Remote sensing for crop management. Photogrammetric Engineering & Remote Sensing 69:647-664.

Plant, R.E., D.S. Munk, B.R. Roberts, R.L. Vargas, D.W. Rains, R.L. Travis, and R.B. Hutmacher. 2000. Relationships between remotely sensed reflectance data and cotton growth and yield. Trans. ASAE 43:535-546.

Purevdorj, T., R. Tateishi, T. Ishiyama, and Y. Honda. 1998. Relationships between percent vegetation cover and vegetation indices. Int. J. Remote Sens. 19:3519-3535.

Ritchie, G.L., and C.W. Bednarz. 2005. Estimating defoliation of two distinct cotton types using reflectance data. Journal of Cotton Science 9:182-188.

Rouse, J.W., R.H. Haas, J.A. Schell, and D.W. Deering. 1973. Monitoring vegetation systems in the great plains with ERTS, p. 309-317. Third ERTS Symposium, NASA SP-351, Vol. 1. NASA, Washington, DC.

Sui, R., J.B. Wilkerson, W.E. Hart, L.R. Wilhelm, and D.D. Howard. 2005. Multi-spectral sensor for detection of nitrogen status in cotton. Applied Engineering in Agriculture 21:167-172.

Vierling, L., M. Fersdahl, X. Chen, Z. Li, and P. Zimmerman. 2006. The short-wave aerostat-mounted imager (SWAMI): A novel platform for acquiring remotely sensed data from a tethered balloon. Remote Sens. Environ. 103:255-264.

Yang, C., J.M. Bradford, and C.L. Wiegand. 2001. Airborne multispectral imagery for mapping variable growing conditions and yields of cotton, grain sorghum, and corn. Trans. ASAE 44(6):1983-1994.

Yang, C., S.M. Greenberg, J.H. Everitt, T.W. Sappington, and J. J.W. Norman. 2003. Evaluation of cotton defoliation strategies using airborne multispectral imagery. Trans. ASAE 46:869-876.

CHAPTER 5

COTTON IRRIGATION MANAGEMENT USING REMOTE SENSING[1]

[1]Ritchie, G.L. and C.W. Bednarz. To be submitted to *Agronomy Journal*

Abstract

Cotton irrigation scheduling methods tend to be underutilized because they are expensive or time consuming to institute on large acreages. With the introduction of variable rate irrigation systems, remote sensing offers a relatively low-cost method to estimate water status on large acreages and water accordingly. We evaluated overhead imagery as an irrigation scheduling method from 2004 to 2006. Images were collected with visible and near-infrared cameras suspended from a tethered blimp, and remote sensing-based irrigation was compared with irrigation triggered by soil tension measurements using Watermark^{TM} soil moisture sensors. In 2004, the experiment consisted of a control treatment with irrigation triggered by Watermark sensors at a 40-cbar trigger point; a remote sensing treatment where irrigation was triggered at the first identified changes in crop growth; a remote sensing treatment where irrigation was triggered three days after the first identified changes in crop growth; and a non-irrigated treatment. In 2005 and 2006, an additional treatment (irrigation triggered by Watermark sensors at a 20-cbar trigger point) was added. Significant changes in growth between treatments were detected in all three years, particularly for the non-irrigated treatment and the treatment irrigated three days after stress was detected. The non-irrigated treatment yielded significantly lower than the other treatments in 2004 and trended lower in 2006, as well as having higher micronaire levels during all three years. The remote sensing-based irrigation treatments had comparable yield and fiber quality to the Watermark –triggered treatments in all three years. Irrigation treatments triggered by remote sensing data used as much as 60 mm less water per year than the treatments irrigated based on soil moisture triggers.

Introduction

Cotton Growth and Water Stress

The wild ancestors of domestic cotton (*Gossypium hirsutum* L.) were perennial vines, and despite selective breeding for determinate-type growth habits, cotton produces abundant vegetative growth if adequate water and nutrients are available. Excessive vegetative growth diverts the plant's energy away from lint and seed production. Plant growth regulators such as mepiquat chloride are often applied to irrigated cotton to decrease growth, prevent boll rot, and facilitate machine harvest (Jost *et al.*, 2006). However, decreasing irrigation application to a level that allows adequate, but not excessive growth might allow high-yielding cotton with less water usage and lower plant growth regulator requirements.

All plants are affected by soil moisture deficit. In cotton, moisture deficit at varying levels reduces plant height, leaf area index (LAI), fruit production and retention, and ultimately impacts yield (Pettigrew, 2004). Bednarz *et al.* (2002b) stated that cotton grown in South Georgia requires about 460 mm of water for maximum yields. Although South Georgia receives about 600 mm of water during the growing season on average (Anonymous, 2006), periodic dry periods often cause crop water stress, which can be resolved by irrigation (Bednarz *et al.*, 2002b).

Variable Rate Irrigation

In Georgia, an estimated 640,000 acres of cotton are irrigated, mostly with overhead irrigation such as center pivots (Harrison, 2005). However, the increasing water demands and decreased stream flow have made the water supply an important issue, and it is likely that water issues will continue to be dominant factors in future cotton production

(Hutson, 2004). Efficient irrigation techniques that result in high cotton yields will allow cotton producers to maximize their yield for a given water supply.

The introduction of variable rate technology has been shown to increase the application efficiency of several crop amendments (Koch *et al.*, 2004; Yang *et al.*, 2001a) and is being used commercially. However, site-specific technology has only recently been introduced for irrigation (Perry *et al.*, 2002). Irrigation based on site-specific soil moisture measurements would require intensive soil moisture monitoring, increasing price and complexity of irrigation management.

Remote Sensing

Remote sensing has been used as a field-scale production tool for estimating and modeling crop growth (Ko *et al.*, 2006; Plant *et al.*, 2000; Roerink *et al.*, 1996; Yang *et al.*, 2001b). Full-season crop monitoring techniques can help cotton growers produce a quality crop and identify spatial variation in the field. However, for remote sensing to be effective for in-season irrigation management decisions, it must provide a quick, accurate method for identifying crop growth characteristics and detecting stress events (Roerink *et al.*, 1996).

Two types of remote sensing imagery are commonly used for monitoring crop growth and stress. Thermal imagery has been used to detect changes in crop temperature due to water or other stress (Cohen *et al.*, 2005; Pinter *et al.*, 2003), while combinations of visible and shortwave infrared imagery have primarily been used to detect changes in crop growth (Ahlrichs and Bauer, 1982; Boissard *et al.*, 1992; Bouman, 1992; Hinzman *et al.*, 1984; Huete, 1988; Ko *et al.*, 2006; Yang *et al.*, 2004). Of these, reflectance imagery is the least expensive. Shortwave reflectance has also been shown to be

sensitive to leaf water content when measured close to the plant (Aldakheel and Danson, 1997; Danson *et al.*, 1992; Peñuelas *et al.*, 1997; Ripple, 1986), although field-scale measurements using water-sensitive reflectance bands are hampered by absorption by atmospheric moisture (ASD, 1999). Instead, general reflectance indices that estimate crop growth are commonly used to estimate crop vigor, and management focuses on amendments that are the most likely to increase vigor.

Our research objectives for this project were to determine the effects of an irrigation program based on remote sensing data on crop growth and yield characteristics.

Materials and Methods

Plot Setup and Design

The research was conducted at the Stripling Irrigation Research Park in Camilla, Georgia during 2004-2006 in fields planted with Delta & Pineland 555 BG/RR in 0.91 m rows at a seeding rate of 126,000 plants ha^{-1}.

In 2004, the crop was planted on May 5, with a 4x4 Latin square plot design irrigated with a variable-rate center pivot such as the ones described by Perry *et al.* (2002). The treatment plots followed the radial pivot pattern. Buffer regions were designated between treatments to avoid irrigation overlap, and all measurements were performed in the center of each treatment. Plot lengths ranged from approximately 21 m on the inner row of the smallest treatment to 37 m on the outer row of the largest treatment. Watermark™ sensors were buried at depths of 20, 40, and 60 cm in each plot, and the design was a 4 x 4 Latin square with the following treatments:

1. Irrigation based on Watermark triggers of -40 cbars at 20 cm and -50 cbars at 40 and 60 cm (40-cbar trigger);

2. Irrigation based on detection of water deficit using aerial imagery (aerial trigger);
3. Irrigation three days after detection of water deficit using aerial imagery to simulate a remote sensing program that cannot make flyovers when the stress is first detected (aerial-3 days); and
4. Non-irrigated plots with irrigation applied only at the beginning of the season to aid crop establishment (non-irrigated).

1. In 2005 (planted April 20) and 2006 (planted May 2), the plot was a randomized block design with 5 treatments and 4 replicates irrigated with a variable application linear irrigation system. The treatments were the same as for 2004, with the addition of a treatment with irrigation based on Watermark triggers of -20 cbars at all depths (20-cbar trigger).

As with the 2004 study, buffer regions were designated between treatment nozzle packages to avoid irrigation overlap, and all measurements were performed in the center of each treatment. Plot lengths were 21 m. The plots were harvested mechanically, and each plot was weighed and ginned at the University of Georgia Tifton Micro-Gin. In 2004 and 2005, fiber quality analysis was conducted at Cotton Inc. (Cary, NC), with three fiber samples per plot. In 2006, fiber quality analysis was conducted at Starlab, Inc. (Knoxville, TN), with three fiber samples per plot.

Aerial Imagery

Aerial imagery was collected using a 4.5 m long tethered blimp (Southern Balloon Works, Deland, FL) and a two-camera remote system. The blimp has a 4 kg lift rating by the manufacturer. The camera system included two Nikon 4300 digital cameras, one of

which was modified to be near-infrared sensitive, a Digisnap 2100 electronic shutter release device (Harbotronics, Gig Harbor, WA), and a radio control system that allowed simultaneous remote firing of the cameras from the ground. The blimp was flown over the plots at heights that ranged from about 45 m for ground cover measurements to about 180 m for vegetation index measurements. Images were collected 2-3 times per week on average through late bloom, with collection dates determined by environmental factors such as cloud cover and wind (>20 mph). In 2004, six to eight rows from each plot were selected for ground cover and vegetation index measurement because of the variable rate center pivot orientation. In 2005 and 2006, four rows were selected from each plot. In-season remote sensing irrigation decisions were made based on three indicators of changes in crop growth based on water stress. The first indicator was significantly lower ground cover fraction in the remote sensing treatment than the Watermark trigger treatment. The second indicator was a significant decrease in ground cover fraction from one day to the next. This trigger was designed to allow irrigation in the event that all of the treatments, including the soil moisture trigger treatments, showed water stress. Finally, significantly slower growth in the remote sensing treatment compared to the Watermark treatment from one day to the next was used as an indicator. The purpose of this trigger was to identify a decrease in crop growth, even if ground cover fraction of the remote sensing treatment was initially higher than in the Watermark trigger treatment. Significance was determined using a pairwise t-test between the Watermark treatment and the imagery-based treatment with a significance of $P=0.05$. During 2004, early-season physiological wilt due to water stress occurred at soil moisture levels that did not

trigger irrigation at the 40-cb level, so the 2005 and 2006 triggers were based on the difference between the 20-cbar treatment and the aerial image treatment.

Ground Cover Measurements

Plot markers were placed adjacent to each plot for identification purposes after emergence, and images were collected 45-75 m above the cotton plots for ground cover measurements. Ground cover was estimated from the four center rows spanning the length of the plot. Images were opened in Adobe Photoshop CS2, and image angle was corrected using the measure tool and the autorotate function. The rectangular marquee tool was used to select each plot of interest, and the selection included four plant rows and four soil rows. The pixels within the boundaries of each plot were copied and pasted into a new file, which was used for ground cover fraction measurements. Image pixels containing plants were separated from pixels containing soil using the magic wand tool, and the number of plant pixels and total pixels were recorded from the Photoshop histogram values. Ground cover fraction was calculated as the ratio of plant pixels to total pixels. Images were collected 2-3 times per week, as weather permitted.

Camera NDVI and Green:Red Ratio

Normalized difference vegetation index (NDVI) values were calculated from the visible and near-infrared (NIR) images based on camera brightness values and the relationship between camera brightness, camera exposure, and scene reflectance of the two cameras, as determined in Chapter 3. The visible camera was corrected by exposure to the near-infrared camera and camera brightness values were converted to relative reflectance values. NDVI was then calculated using the visible camera red channel and the NIR camera blue channel as $(R_{NIR}-R_{red})/ (R_{NIR}+R_{red})$, where R_{NIR} is the relative reflectance

calculated from the NIR camera and R_{red} is the relative reflectance calculated from the visible red channel. The center four rows of each plot were selected, and the NDVI for each plot was calculated from the mean image brightness for each plot measured from the visible and near-infrared channels. These measurements came from images collected 2-3 times per week. Additionally, ratios of the mean green to mean red brightness values from the visible camera were calculated for each plot, as described by (Adamsen *et al.*, 1999). The purpose of these measurements was to determine whether an index based solely on visible brightness characteristics might be practical for estimation of crop growth.

Spectrometer Measurements

Ground-level reflectance of each plot was measured using an Apogee Vis-NIR spectrometer (Apogee Instruments, Inc., Logan, UT) with an effective spectral range of 400-900 nm and a spectral resolution of 1.4 nm (full width, half maximum height). Each reading consisted of an average of three spectral scans, and two were collected in each plot on each sampling date. A white polytetrafluoroethylene (PTFE) reflectance standard was used as a reference, and reflectance by wavelength was calculated as the ratio of scene reflectance to the reflectance of the standard. NDVI was then calculated as $(R_{800-840}-R_{650-700})/ (R_{800-840}-R_{650+700})$, where $R_{800-840}$ is the reflectance from 800-840 nm and $R_{650-700}$ is reflectance from 650-700 nm. Red edge NDVI ($NDVI_{710}$) was calculated as $(R_{800-840}-R_{707-710})/ (R_{800-840}-R_{707+710})$, where $R_{800-840}$ is the 800-840 nm reflectance, and $R_{707-710}$ is the 707-710 nm reflectance. References were collected at 10-15 minute intervals, or after clouds were passed over. Reflectance measurements were collected only when direct sunlight was available, on average twice a week.

Statistical analyses included a comparison of both in-season growth differences and final yield differences between treatments.

Porometer Measurements

A LI-COR 1600 leaf porometer (LI-COR Biosciences, Lincoln, NE) was used to estimate cotton leaf water status for all treatments based on leaf transpiration and stomatal resistance. For each measurement, a leaf about five nodes below the meristem was clamped to the porometer cuvette, and leaf transpiration and resistance were calculated by the porometer based on measurements of temperature, relative humidity, and the flow rate of air through the cuvette required to maintain a constant humidity (LI-COR, 1989). Porometer measurements were collected near midday to avoid the effects of condensation, and the system was kept clean to avoid moisture effects from debris (McDermitt, 1990).

Results

The study comprised three years with very different rainfall patterns (Fig. 5.1). The 2004 growing season rainfall was significantly lower than the historic seasonal average rainfall for Camilla, despite heavy rainfall due to tropical storm Frances on day 124 (Fig. 5.2). The 2005 growing season was very wet, with heavy rainfall from June until August. As shown in Fig. 5.2, heavy rainfall occurred from 65-80 days after planting, and again from 85-100 days after planting. In 2006, rainfall was about the same as the seasonal average during the growing season, but most of the rainfall during the early and middle of the 2006 growing season came during two periods, 130 mm rainfall from day 17-20 and 250 mm between days 81 and 110.

Although the rainfall differed for the growing seasons, treatments showed similar trends in water application during the growing season. In each growing season, the irrigations based on Watermark readings resulted in the highest cumulative application rates (Fig. 5.3). Irrigation levels for the aerial imagery treatment from 2004-2006 ranged from 20 mm less to 60 mm less over the growing season compared to the highest watering rate for the Watermark triggered irrigation. In 2006, the aerial imagery treatment and the 40-cbar Watermark trigger treatment used the same amount of irrigation water, while in 2004 and 2005 the aerial image treatment used 20 mm less irrigation water on average. The aerial-3 days trigger used less irrigation water during every year of the study than the Watermark trigger treatments (Fig. 5.3) and used less water than the aerial trigger in every year except 2005. The decreased water use compared to the aerial trigger was due to interruption of irrigation by rainfall events.

Watermark Measurements

Watermark measurements for 2004 for all treatments are shown in Fig. 5.4. The value at each depth for each treatment is the average of the Watermark readings in all four replicates. The non-irrigated treatment showed stress based on tension readings of -50 cbar or more at one depth or more from day 62 to day 100. The other treatment that showed extensive water stress based on Watermark readings was the aerial treatment, which had Watermark readings more negative than -50 cbar on three occasions. The aerial -3 days treatment did not show significant stress based on Watermark readings during the season.

In 2005, the wet growing season resulted in very little measured levels of stress based on Watermark readings (Fig. 5.5). The non-irrigated treatment had Watermark averages

approaching -50 cbar from day 63 to day 80, followed by a decrease in the tension at all treatments and depths on day 80, due to the heavy rainfall event shown in Fig. 5.2.

In 2006, two periods of moderate stress occurred, based on Watermark readings (Fig. 5.6). The first occurred prior to day 57, as shown by increasing tension in all treatments, followed by a rainfall event that eliminated this tension at all depths. The second period of soil drying occurred between 70 to 90 days after planting. The treatment most impacted by these drying periods was the non-irrigated treatment. As with 2005, heavy rainfall in the latter part of the season resulted in wetter soils throughout the remainder of the growing season.

Ground Cover

Changes in fractional ground cover between irrigation treatments occurred during all three growing seasons, as shown in Table 5.1. In 2004, significant differences in ground cover were identified on day 64 and continued through the rest of the growing season. However, most of these differences were seen in the non-irrigated treatment and the aerial -3 days treatment compared to the Watermark and aerial trigger treatments. The non-irrigated treatment showed the lowest ground cover fraction on all days after day 64, and the aerial -3 days treatment showed significant decreases in ground cover on days 68 and 69, with a trend toward lower fractional ground cover from day 64 to day 89 of ground cover measurements.

In 2005, significant differences in ground cover fraction between treatments occurred on days 55, 68, 76, 79, and 86, with the Watermark triggers trending highest for all dates except day 55. Ground cover fraction for 2005 for all treatments was higher than for 2004, likely because of the heavy rain and consequent rank growth of the cotton.

In 2006, significant differences between treatments were observed on days 52, 57, 58, 62, 64, 70, 71, 73, 78, and 80. Prior to day 62, the 20-cbar Watermark trigger treatment showed the highest fractional ground cover, but after day 62, this treatment was not significantly higher than the 40-cbar trigger treatment the rest of the season. After day 62, the aerial imagery trigger treatment ground cover fraction values were not significantly lower than those of the 20-cbar treatment except on day 69, when a paired t-test showed a significant difference for a one-tailed test at P=0.05 (t=1.98) between the aerial treatment and the 20-cbar treatment.

Vegetation Indices

Vegetation indices, as shown by the Green:Red ratio example in Table 5.2, showed similar trends to measurements of ground cover in estimating changes in crop growth between treatments. In 2004, significant changes between treatments were identified on days 68, 76, and 89. The camera-based vegetation indices did not identify differences between the 40-cbar and aerial treatments, but the indices were sensitive to the decrease in ground cover between days 58 and 62.

In 2005, day 55 showed high Green:Red values for the non-irrigated treatment compared to the other treatments, but subsequent days showed the non-irrigated treatment values significantly lower than the 20-cbar treatment values on days 68, 76, and 79.

In 2006, significant differences in camera vegetation index values were identified on days 52-80. After day 57, the non-irrigated treatment showed consistently lower vegetation index values than the 20-cbar, 40-cbar, and aerial treatments. The exception was day 69, in which the non-irrigated treatment was not significantly lower than the other treatments.

This may have been due to the recovery growth after the rainfall on days 63 and 65, as shown in Fig. 5.2 and its effect on soil moisture, as shown in Fig. 5.6.

Spectrometer-based vegetation indices (Fig. 5.7) showed similar trends to those observed with ground cover fraction and image-based vegetation indices. In 2004, significant differences in $NDVI_{710}$ were measured on days 69 and 76. In 2005, differences were observed only on day 68, while in 2006, significant differences were observed on days 51, 64, 71, 73, 78, and 80.

The trends for all of the indices in 2006 are shown in Figs. Fig. 5.7 and Fig. 5.8. All methods for estimating crop growth detected differences during the growing season; however, the camera vegetation indices were sensitive to cloud cover, as shown in Fig. 5.8. Cloud cover decreased vegetation index values, but differences between treatments were still significant, as shown on day 73. The other dates included did not have significant clouds during data collection.

Porometer Resistance

Porometer resistance, as shown in Table 5.4, showed similar trends to ground cover and vegetation index measurements of crop stress. In 2004, significant differences were identified on days 65, 69, 82, and 89. However, there were no significant differences between any of the irrigated treatments. In 2005, the non-irrigated treatment did not have significantly higher porometer resistance readings than the other treatments. In 2006, the non-irrigated and aerial-3 days treatments had significantly higher resistance values than the other treatments on day 50, and higher values than the 20-cbar treatment on day 57. The non-irrigated treatment was not significantly higher on the other days.

Lint Yield

The 2004 study was the only year in which significant yield differences between treatments were evident (Fig. 5.9), despite changes in soil moisture and plant growth between treatments in all three years. This can likely be explained by the heavy rainfall in both 2005 and 2006, particularly from July to the end of the growing season. The non-irrigated treatment in both 2005 and 2006 received about 600 mm of rain (Fig. 5.2), while the irrigated treatments in 2004 received a combined total of only about 600 mm rain and irrigation combined, even with the heavy late-season rain from Tropical Storm Frances, which added almost 140 mm to the cumulative total.

Fiber Quality

Fiber quality was impacted by irrigation treatment, as shown in Table 5.5. In 2005, only micronaire showed a treatment effect, with the aerial-3 days treatment cotton having significantly lower micronaire than the 20-cbar treatment. However, in 2004 and 2006, non-irrigated treatment had significantly higher fiber strength and micronaire than the cotton irrigated based on the most conservative Watermark readings. Fiber length also trended toward longer fiber for the non-irrigated treatment, with significant differences found in 2006 between the non-irrigated and 20-cbar treatments.

Discussion

Soil Tension Measurements and Remote Sensing

Watermark readings and vegetation indices both tracked trends in moisture, but created differences in treatment. For instance, during 2004, the aerial trigger treatment showed soil tension values indicative of stress during much of the season (Fig. 5.4), while the aerial -3 days treatment did not show significant stress. However, the aerial -3 days

treatment had lower ground cover fraction averages from day 64 to day 89 than for the 40-cbar and aerial treatments, with a significant difference occurring on day 68. Likewise, the Watermark averages of the aerial trigger in 2006 suggested no water deficit during the early growing season, prior to day 57 (Fig. 5.6). However, significant decreases in ground cover fraction were observed for this treatment compared to the 20-cbar treatment (Table 5.1). These differences are likely due to the heterogeneity of the soil, which can make soil moisture, and hence crop growth, highly variable (Famiglietti *et al.*, 1999). The added scale of remote sensing measurements might improve estimates of plant moisture needs across a field.

Treatment Separation Based on Remote Sensing

Vegetative indices that measure crop growth showed sensitivity to changes in crop growth at low levels of water stress, particularly early in the season. However, with the exception of 2004, remote sensing did not trigger irrigation after about 75 days after planting. The heavy rainfall late in the season in both 2005 and 2006 appears to have provided adequate water for the plants, particularly since measurements of soil moisture content did not show stress. The ability of the indices to indicate late season water deficit stress would require research during additional years when there are periods of late season drought conditions, similar to the conditions of 2004. However, this also suggests that early-season crop growth (prior to 75 days) is very sensitive to water content, and might allow the determination of spatial water conditions that can serve as an irrigation rate template for the rest of the season, decreasing the need for repeated aerial images.

Effects of Remote Sensing Triggered Irrigation on Yield and Fiber Quality

The irrigation treatments based on remote sensing triggers (aerial and aerial – 3 days) had comparable yields with the treatments based on Watermark triggers (Fig. 5.9). These yields were significantly higher than the non-irrigated treatment in 2004 and trended higher in 2006. The yield for all treatments was suppressed in 2005 compared to 2004 and 2006, probably due to the heavy rainfall experienced throughout the season. The non-irrigated treatment was only statistically different from the irrigated treatments in 2004, but the heavy rainfall in 2005 and 2006 and the consequent yield recovery suggest that low or moderate growth reduction in cotton due to decreased soil moisture may not significantly impact yield if adequate water is applied at some point. This agrees with the conclusion by Pettigrew (2004) that the degree of moisture deficit stress is a significant aspect of yield response. This also suggests that cotton can reach levels of water deficit detectable by remote sensing and still produce yields consistent with unstressed cotton. Using remote sensing triggers to detect these changes was shown in this study to both adequately irrigate the crop and save water.

The effects of irrigation treatment on fiber quality may be tied to either changes in maturity rate between treatments or changes in fruiting distribution, both of which can be affected by overhead irrigation. Bednarz *et al.* (2002a) concluded that cotton fiber length, uniformity, and strength were all affected by crop maturity at the time of defoliation, and inadequate irrigation and nutrient application increases crop maturity rate (Reddy *et al.*, 1992).

Pettigrew (2004) reported trends toward higher fiber strength and shorter length in non-irrigated cotton compared to irrigated cotton, but acknowledged that irrigation effects on

length were too inconsistent to be definitively assessed. Pettigrew also noted that micronaire content was related to fiber maturity, and that nonirrigated cotton with higher fiber maturity had higher micronaire content than irrigated cotton.

Conclusion

The results of this study suggest that vegetation indices that measure cotton growth are sensitive to water stress during early fruiting. Therefore, remote sensing may provide an adequate means for setting irrigation rates leading into the period when the cotton plant uses the most water. Timeliness and scheduling flexibility are still challenges with current remote sensing technology, which would make it difficult for full-season irrigation scheduling. Although high-frequency remote sensing throughout the season is not practical at this time, the improvement of low-cost remote sensing platforms may make remote sensing practical for irrigation decisions, particularly when tied to the variable application of other crop amendments. Decreased water application due to irrigation treatment also do not appear to significantly impact yield or cotton quality compared to treatments based on soil moisture measurements.

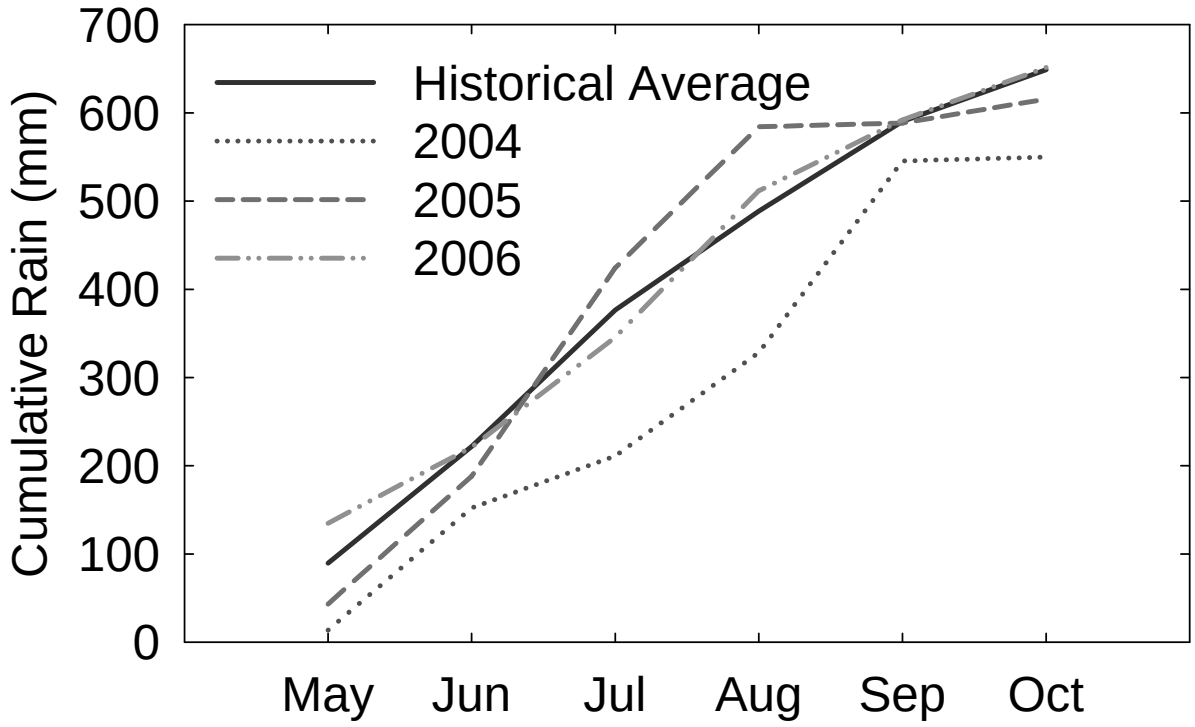

Fig. 5.32. Cumulative rainfall between May and October, 2004-2006, compared with historical rainfall average for Camilla.

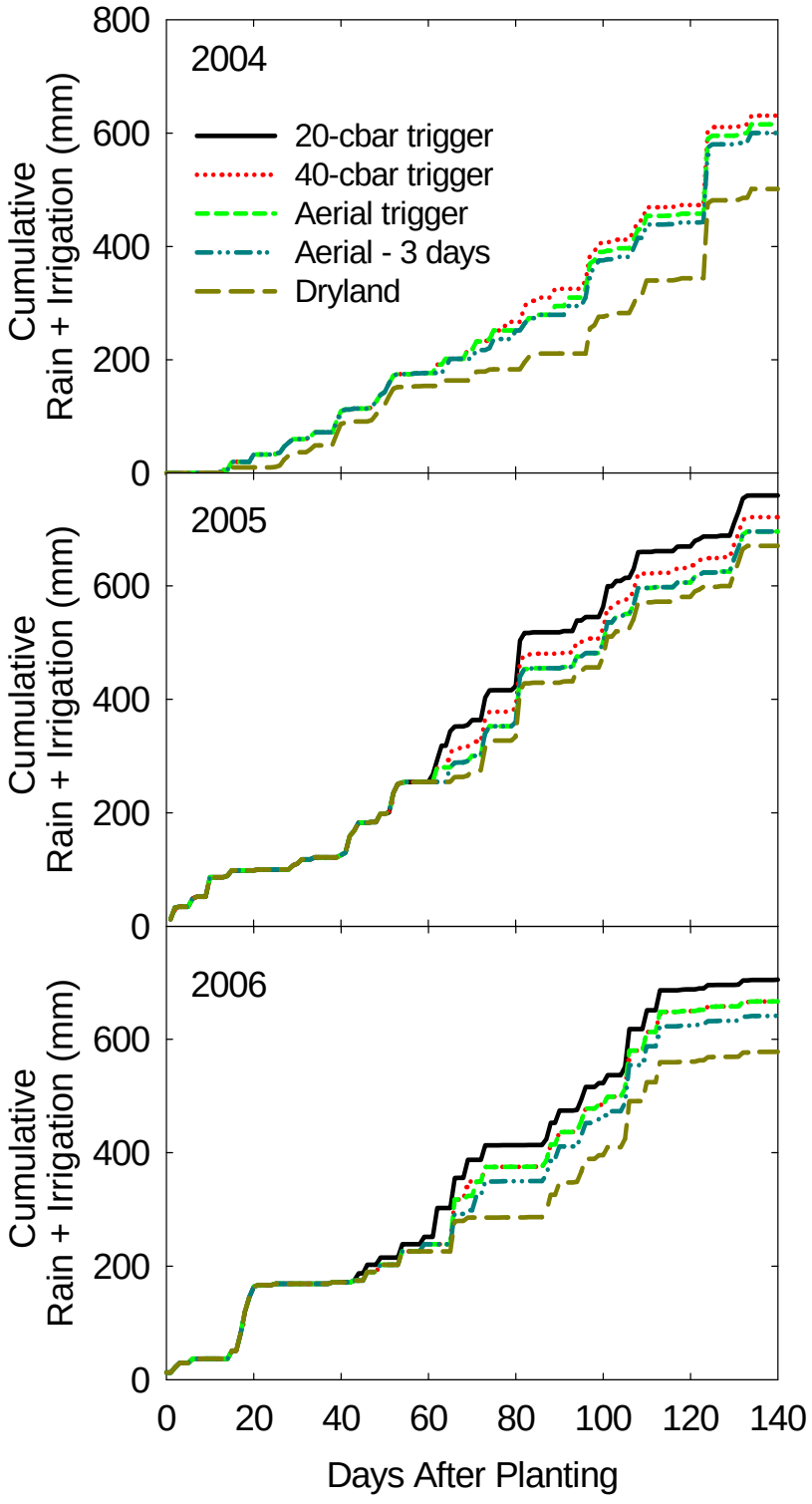

Fig. 5.33. Accumulated rain and irrigation by treatment during the 2004-2006 growing seasons.

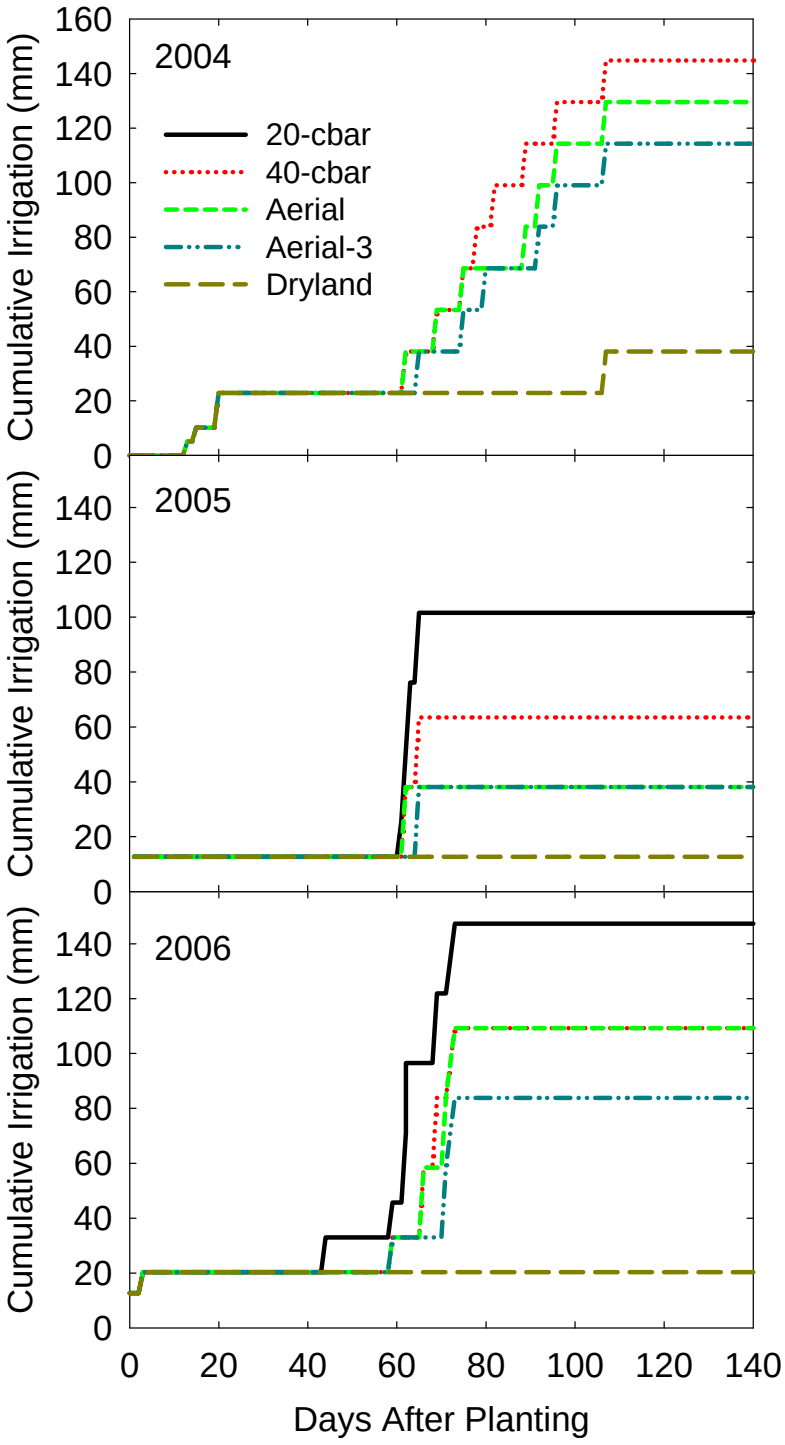

Fig. 5.34. Cumulative irrigation by treatment 2004-2006. The 2004 study did not have 20-cbar trigger treatment.

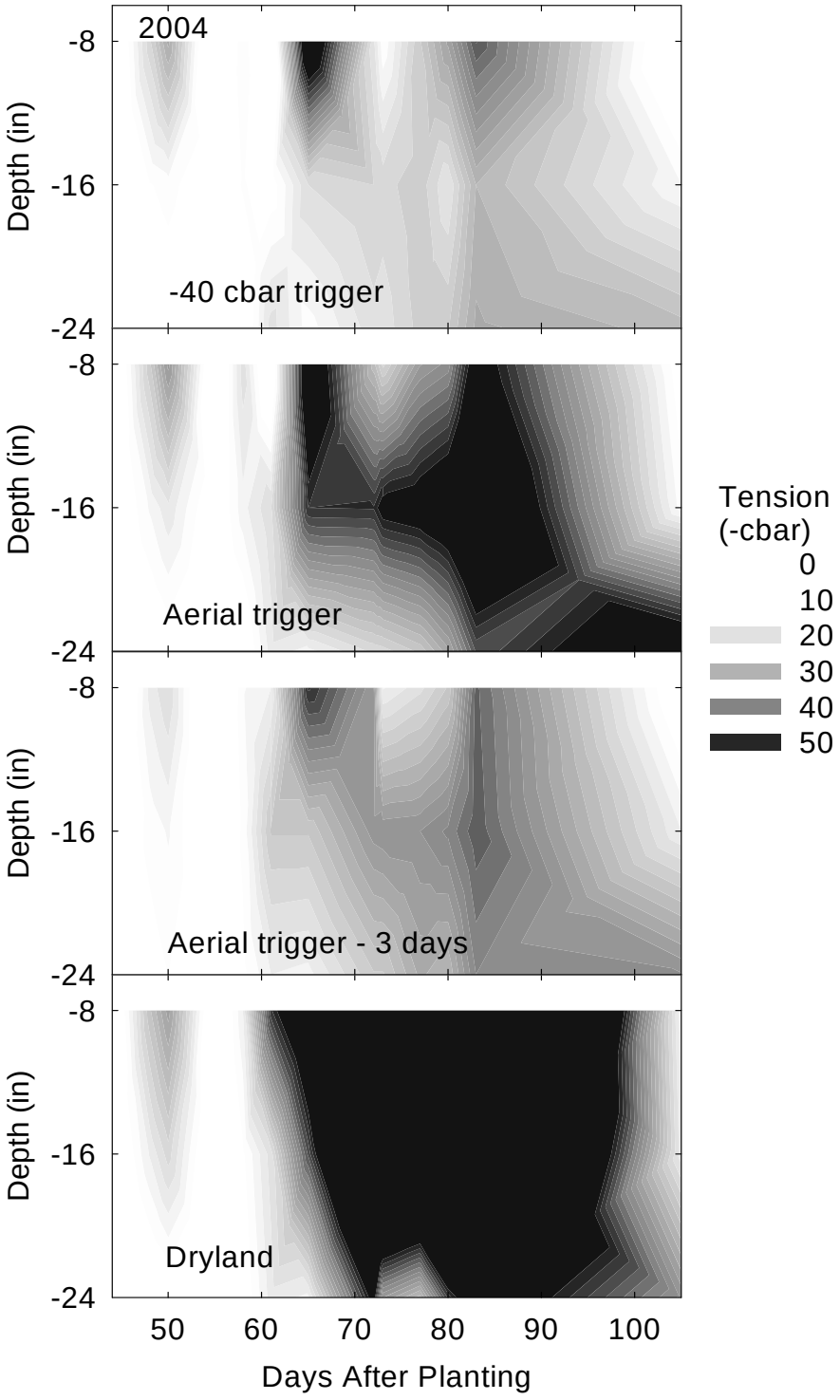

Fig. 5.35. Watermark measurements by depth and treatment, 2004.

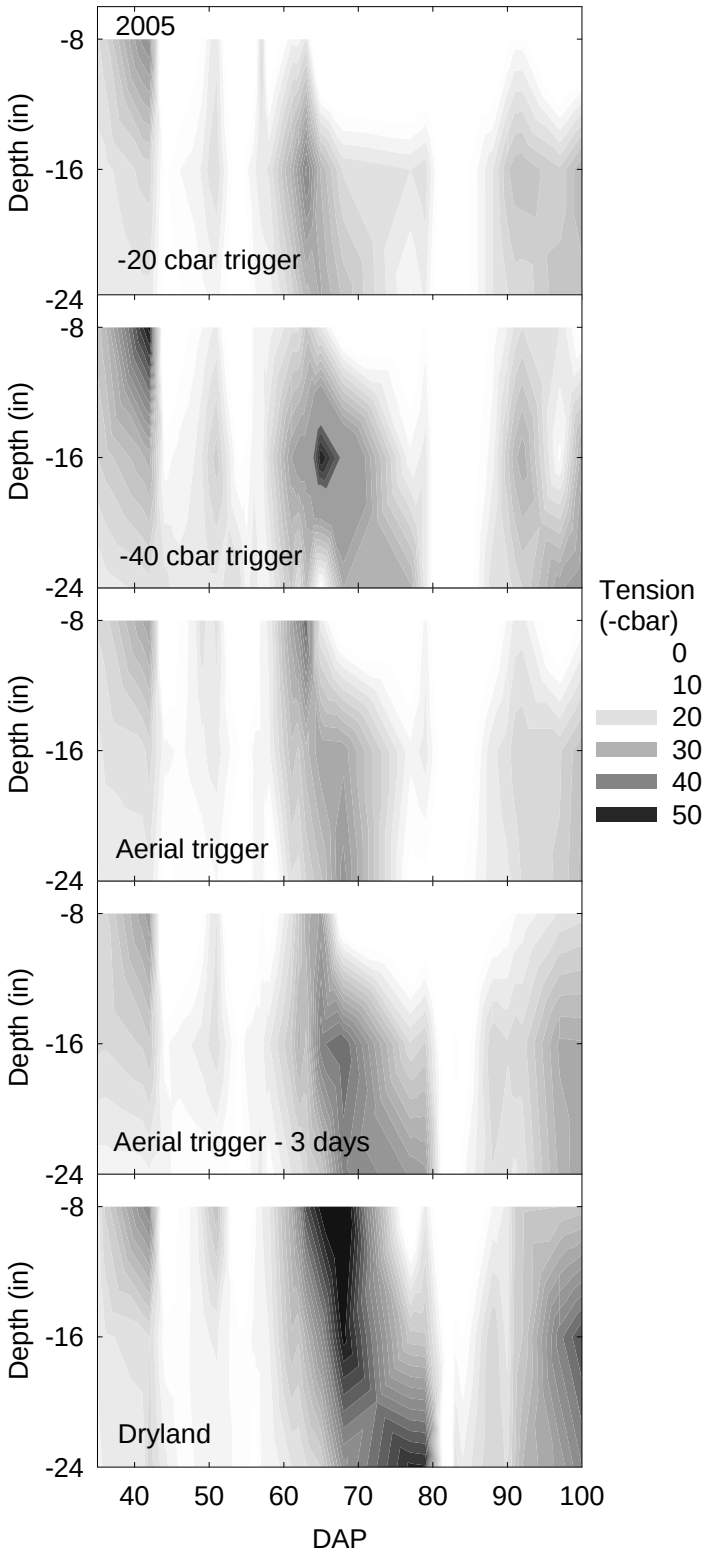

Fig. 5.36. Watermark measurements by depth and treatment, 2005.

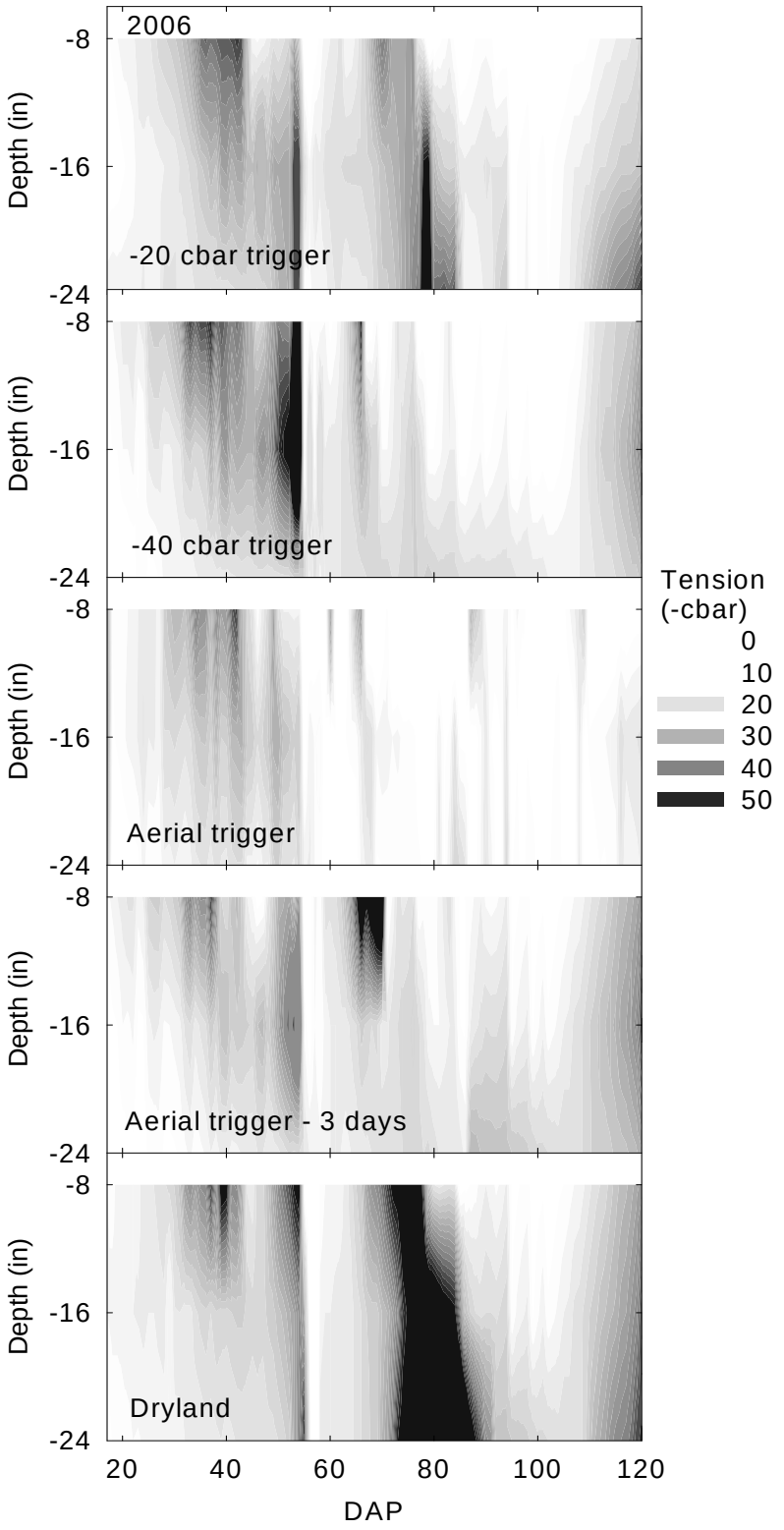

Fig. 5.37. Watermark measurements by depth and treatment, 2006.

Table 5.5. Fractional ground cover by treatment for 2004-2006 growing seasons†.

Days after planting	Irrigation Treatment					
	20-cbar	40-cbar	Aerial	Aerial-3	Non-irrigated	LSD
			Ground Cover Fraction			
2004						
48		0.34±0.016	0.33±0.010	0.33±0.018	0.33±0.017	NS‡
55		0.40±0.027	0.40±0.017	0.40±0.047	0.39±0.019	NS
57		0.39±0.015	0.41±0.023	0.41±0.010	0.37±0.016	NS
58		0.42±0.016	0.42±0.019	0.43±0.016	0.42±0.024	NS
62		0.36±0.014	0.40±0.045	0.39±0.052	0.35±0.030	NS
64		0.46±0.004 a*	0.45±0.020 a	0.41±0.036 ab	0.37±0.014 b	0.055
68		0.53±0.020 a	0.57±0.017 a	0.42±0.027 b	0.35±0.035 b	0.076
69		0.55±0.019 a	0.51±0.022 ab	0.44±0.02 bc	0.41±0.065 c	0.090
76		0.74±0.026 a	0.70±0.040 a	0.67±0.022 a	0.51±0.040 b	0.086
89		0.72±0.009 a	0.73±0.011 a	0.68±0.029 a	0.55±0.045 b	0.071
2005						
55	0.66±0.03 a	0.56±0.03 b	0.58±0.02 ab	0.58±0.02 ab	0.58±0.07 ab	0.086
62	0.60±0.03	0.57±0.03	0.56±0.07	0.58±0.05	0.50±0.04	NS
68	0.68±0.01 a	0.67±0.03 a	0.61±0.02 b	0.60±0.02 b	0.60±0.04 b	0.054
70	0.72±0.04	0.68±0.03	0.65±0.01	0.65±0.02	0.67±0.03	NS
76	0.75±0.01 a	0.75±0.01 a	0.70±0.01 b	0.69±0.02 b	0.69±0.02 b	0.031
79	0.79±0.02 a	0.76±0.02 a	0.74±0.03 ab	0.75±0.01 a	0.69±0.02 b	0.062
86	0.96±0.01 a	0.96±0.01 a	0.95±0.01 a	0.94±0.02 ab	0.92±0.01 b	0.025
91	0.96±0.03	0.96±0.02	0.97±0.02	0.98±0.01	0.96±0.01	NS
2006						
49	0.36±0.03	0.35±0.03	0.38±0.04	0.33±0.03	0.38±0.04	NS
52	0.53±0.01 a	0.48±0.02 b	0.44±0.02 b	0.46±0.02 b	0.47±0.01 b	0.045
57	0.50±0.03 a	0.46±0.03 ab	0.43±0.02 ab	0.41±0.02 b	0.44±0.03 ab	0.083
58	0.53±0.02 a	0.46±0.02 bc	0.49±0.01 ab	0.42±0.02 c	0.43±0.04 c	0.060
62	0.55±0.01 bc	0.58±0.01 ab	0.59±0.01 a	0.57±0.01 ab	0.51±0.02 c	0.038
64	0.53±0.01 a	0.51±0.04 ab	0.53±0.02 a	0.50±0.02 ab	0.46±0.02 b	0.067
69	0.62±0.03	0.61±0.04	0.59±0.06	0.50±0.04	0.58±0.04	NS
70	0.65±0.01 ab	0.62±0.02 ab	0.67±0.03 a	0.59±0.01 b	0.61±0.03 ab	0.063
71	0.69±0.05 ab	0.72±0.04 a	0.69±0.04 ab	0.60±0.02 c	0.62±0.02 bc	0.078
73	0.64±0.03 a	0.63±0.04 a	0.66±0.04 a	0.58±0.06 a	0.46±0.04 b	0.108
78	0.74±0.07 ab	0.77±0.03 a	0.72±0.05 ab	0.64±0.03 bc	0.60±0.02 c	0.113
80	0.74±0.06 a	0.74±0.05 a	0.78±0.05 a	0.69±0.03 ab	0.60±0.05 b	0.113

†Values represent treatment mean for each day after planting ± 1 standard error (n=4).
‡Not significant at P=0.05
*Letters within each row indicate LSD significance at P=0.05 by days after planting.

Table 5.6. Cotton Green:Red ratio by irrigation treatment and date 2004-2006†. Letters indicate LSD significance of each row by date at P=0.05.

	Days after planting	Irrigation Treatment					LSD
		20-cbar	40-cbar	Aerial	Aerial-3	Non-irrigated	
				Green:Red Ratio			
2004	48		0.93±0.006	0.93±0.011	0.92±0.006	0.91±0.011	NS‡
	55		0.96±0.007	0.96±0.009	0.96±0.008	0.96±0.012	NS
	57		0.95±0.013	0.94±0.012	0.95±0.007	0.94±0.010	NS
	58		0.97±0.003	0.98±0.012	0.96±0.011	0.97±0.012	NS
	62		0.95±0.030	0.93±0.009	0.93±0.002	0.95±0.041	NS
	64		0.94±0.013	0.96±0.020	0.93±0.030	0.95±0.033	NS
	68		1.00±0.016 a*	1.01±0.038 a	0.97±0.027 a	0.92±0.027 b	0.0478
	69		1.02±0.019	1.01±0.013	0.95±0.021	0.95±0.045	NS
	76		1.12±0.028 a	1.11±0.027 ab	1.07±0.024 b	0.99±0.018 c	0.0553
	89		1.13±0.007 a	1.13±0.016 a	1.09±0.006 b	0.99±0.016 c	0.0287
2005	55	1.08±0.018	1.11±0.037	1.12±0.021	1.10±0.023	1.14±0.018	NS
	62	1.19±0.060 ab	1.15±0.055 ab	1.12±0.138 a	1.16±0.097 b	1.01±0.071 ab	0.2631
	68	1.16±0.017 a	1.15±0.015 ab	1.13±0.018 a	1.16±0.018 b	1.12±0.002 b	0.0402
	70	1.20±0.018 a	1.18±0.017 ab	1.16±0.022 a	1.17±0.022 b	1.16±0.014 b	0.0484
	76	1.23±0.016 ab	1.21±0.011 ab	1.20±0.032 a	1.20±0.020 bc	1.13±0.024 c	0.0531
	79	1.24±0.005 a	1.25±0.007 ab	1.22±0.013 ab	1.22±0.006 b	1.21±0.012 b	0.0250
	86	1.41±0.010 ab	1.41±0.015 ab	1.37±0.028 a	1.38±0.013 b	1.40±0.034 ab	0.0644
	91	1.41±0.005 a	1.41±0.014 ab	1.41±0.012 ab	1.43±0.010 c	1.39±0.014 bc	0.0311
2006	49	0.96±0.01 a	0.94±0.01	0.94±0.01	0.94±0.02	0.95±0.01	NS
	52	1.03±0.04 ab	1.03±0.02 ab	1.04±0.03 a	0.98±0.01 b	0.98±0.01 ab	0.059
	57	1.00±0.02 a	0.99±0.01 ab	1.00±0.02 a	0.97±0.01 b	0.96±0.01 b	0.034
	58	1.04±0.03 a	1.02±0.02 ab	1.04±0.04 a	0.99±0.01 b	0.98±0.01 b	0.047
	62	1.06±0.03 ab	1.05±0.01 ab	1.07±0.03 a	1.02±0.01 bc	1.01±0.02 c	0.054
	64	1.07±0.04 a	1.05±0.03 ab	1.06±0.04 ab	1.01±0.01 b	1.00±0.01 b	0.058
	69	1.12±0.02 ab	1.13±0.02 ab	1.14±0.06 a	1.06±0.01 b	1.08±0.01 ab	0.072
	70	1.18±0.04 a	1.17±0.05 ab	1.17±0.07 ab	1.07±0.01 c	1.09±0.03 bc	0.084
	71	1.24±0.03 a	1.27±0.04 a	1.24±0.06 a	1.18±0.03 ab	1.13±0.02 b	0.099
	73	1.13±0.03 a	1.14±0.03 a	1.16±0.03 a	1.10±0.01 ab	1.04±0.01 b	0.068
	78	1.27±0.06 a	1.27±0.07 a	1.31±0.05 a	1.23±0.04 ab	1.15±0.04 b	0.117
	80	1.28±0.04 a	1.31±0.04 a	1.31±0.05 a	1.24±0.03 ab	1.18±0.04 b	0.079

†Values represent treatment mean for each day after planting ± 1 standard error (n=4).
‡Not significant at P=0.05
*Letters within each row indicate LSD significance by days after planting at P=0.05.

Table 5.7. Spectrometer $NDVI_{710}$ by treatment and date 2004-2006†.

	Days after planting	Irrigation Treatment					
		20-cbar	40-cbar	Aerial	Aerial-3	Non-irrigated	LSD
				Spectrometer $NDVI_{710}$			
2004	58		0.45±0.016	0.43±0.047	0.47±0.037	0.47±0.028	NS‡
	62		0.37±0.005	0.38±0.038	0.34±0.031	0.37±0.029	NS
	64		0.49±0.012	0.47±0.031	0.48±0.035	0.46±0.029	NS
	69		0.50±0.042 a*	0.51±0.026 a	0.51±0.027 a	0.47±0.049 b	0.027
	76		0.52±0.004 a	0.52±0.017 a	0.52±0.020 a	0.38±0.041 b	0.110
	82		0.64±0.014 a	0.64±0.015 a	0.65±0.023 a	0.59±0.052 a	NS
2005	55	0.57±0.008	0.56±0.034	0.56±0.030	0.57±0.021	0.56±0.040	NS
	58	0.59±0.009	0.60±0.035	0.58±0.030	0.59±0.022	0.59±0.041	NS
	62	0.59±0.012	0.60±0.017	0.59±0.035	0.58±0.019	0.57±0.007	NS
	68	0.63±0.011 a	0.62±0.017 ab	0.61±0.035 ab	0.61±0.019 ab	0.59±0.006 b	0.028
	72	0.64±0.017	0.65±0.013	0.65±0.013	0.64±0.005	0.64±0.006	NS
	93	0.63±0.025	0.63±0.013	0.64±0.027	0.64±0.018	0.63±0.010	NS
2006	49	0.46±0.015	0.46±0.012	0.46±0.019	0.45±0.021	0.47±0.028	NS
	51	0.49±0.011 a	0.50±0.005 a	0.49±0.017 ab	0.51±0.010 a	0.47±0.022 b	0.027
	57	0.50±0.019 a	0.47±0.037 b	0.51±0.017 a	0.51±0.010 a	0.50±0.028 a	0.050
	58	0.48±0.010	0.50±0.012	0.46±0.029	0.50±0.022	0.48±0.005	NS
	64	0.52±0.016 a	0.52±0.011 a	0.52±0.013 a	0.53±0.005 a	0.49±0.014 b	0.020
	71	0.58±0.015	0.57±0.014	0.54±0.008	0.57±0.008	0.55±0.011	NS
	73	0.61±0.010 a	0.63±0.005 a	0.62±0.010 a	0.57±0.027 a	0.49±0.053 b	0.077
	78	0.59±0.015 a	0.61±0.007 a	0.61±0.005 a	0.59±0.010 a	0.54±0.018 b	0.035
	80	0.62±0.010 a	0.62±0.009 a	0.63±0.010 a	0.62±0.004 a	0.59±0.008 b	0.022

†Values represent treatment mean for each day after planting ± 1 standard error (n=4).
‡Not significant at P=0.05
*Letters within each row indicate LSD significance by days after planting at P=0.05.

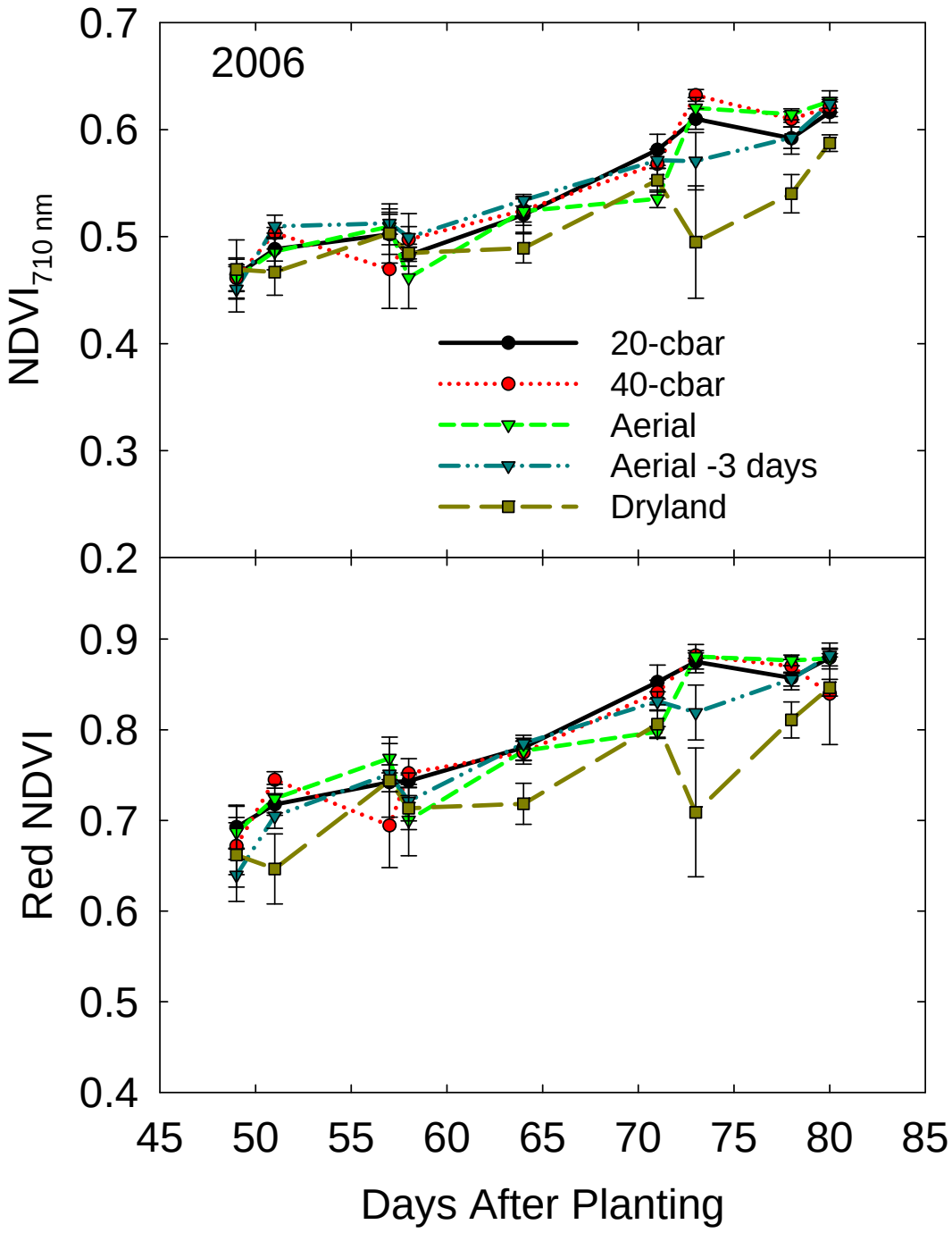

Fig. 5.38. Spectrometer $NDVI_{710\ nm}$ and red NDVI during 2006 growing season. Bars represent the standard error of the mean (SEM; n=4).

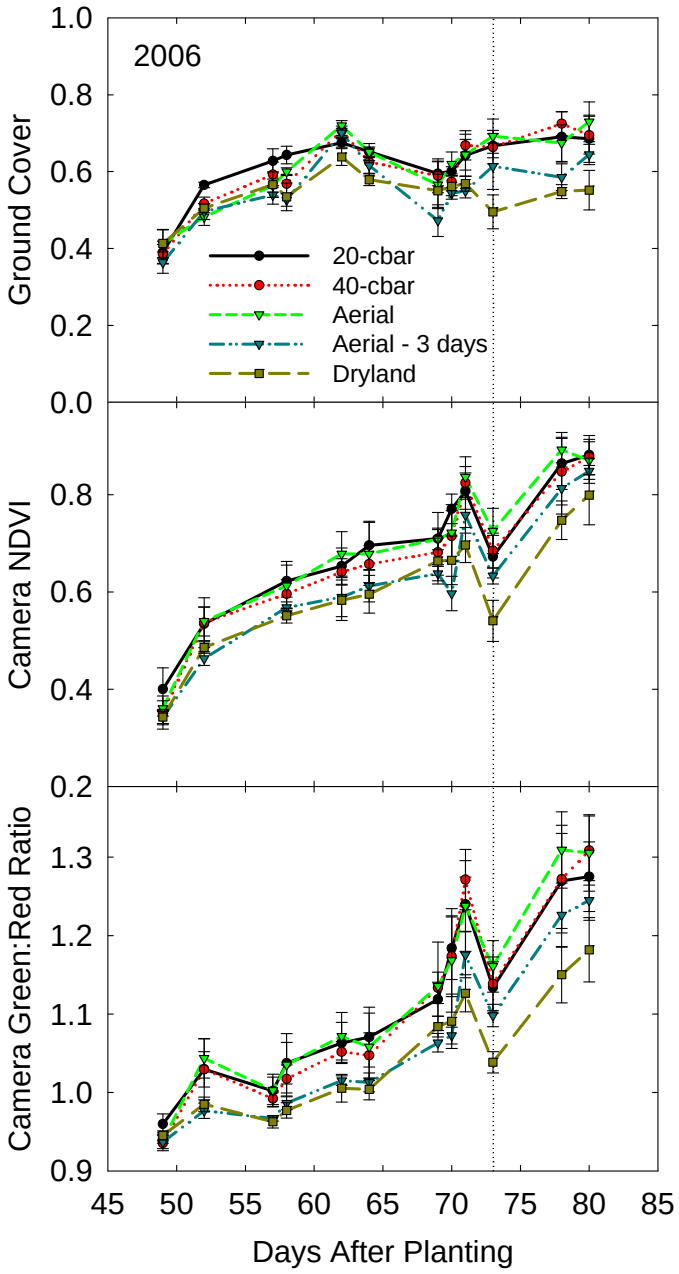

Fig. 5.39. Ground cover fraction, Camera NDVI, and camera Green:Red ratio values during the 2006 growing season. Bars represent SEM (n=4).

Table 5.8. Porometer resistance by treatment and days after planting 2004-2006†.

	Days after planting	Irrigation Treatment					LSD
		20-cbar	40-cbar	Aerial	Aerial-3	Non-irrigated	
				S cm^{-1}			
2004	55		0.36±0.02	0.38±0.03	0.34±0.04	0.42±0.03	NS‡
	58		0.34±0.02	0.45±0.16	0.39±0.02	0.38±0.04	NS
	65		0.44±0.02 b	0.39±0.02 b	0.5±0.02 ab	0.64±0.12 a	0.17
	69		0.38±0.05 b	0.36±0.03 b	0.78±0.36 b	2.21±0.46 a	0.78
	72		0.48±0.06	0.43±0.05	0.46±0.05	0.51±0.05	NS
	76		0.55±0.10	0.64±0.15	0.56±0.12	0.64±0.12	NS
	82		0.4±0.06 b	0.41±0.08 b	0.44±0.04 b	2.29±1.11 a	1.55
	89		0.34±0.01 b	0.4±0.03 b	0.48±0.04 b	0.79±0.14 a	0.19
	93		0.42±0.05	0.41±0.03	0.48±0.07	1.15±0.68	NS
2005	48	0.33±0.03	0.37±0.04	0.34±0.02	0.48±0.18	0.36±0.03	NS
	55	0.24±0.02	0.27±0.01	0.21±0.02	0.27±0.01	0.32±0.07	NS
	62	0.78±0.06 a	0.48±0.1 c	0.66±0.1 ab	0.49±0.02 bc	0.42±0.04 c	0.15
	63	0.4±0.04	0.48±0.15	0.49±0.11	0.5±0.06	0.52±0.12	NS
	68	0.34±0.04	0.38±0.03	0.39±0.06	0.35±0.02	0.33±0.02	NS
	72	0.26±0.02	0.26±0.01	0.3±0.02	0.27±0.01	0.28±0.01	NS
	91	0.21±0.01 b	0.24±0.01 ab	0.26±0.02 a	0.21±0.01 b	0.22±0.02 ab	0.04
2006	45	0.61±0.02 b	0.70±0.08 ab	0.77±0.10 a	0.74±0.09 ab	0.67±0.07 ab	0.15
	48	0.66±0.11	1.07±0.21	1.82±1.31	1.73±0.76	1.35±0.42	NS
	50	0.72±0.08 b	0.73±0.07 b	0.76±0.05 b	3.55±1.39 a	3.87±0.60 a	1.68
	57	0.40±0.03 b	0.45±0.03 ab	0.44±0.02 ab	0.48±0.02 a	0.48±0.03 a	0.08
	64	0.50±0.04	0.73±0.2	0.59±0.12	0.57±0.12	0.52±0.06	NS
	70	0.59±0.05	0.56±0.07	0.54±0.05	0.93±0.32	0.80±0.10	NS
	73	0.63±0.13	0.41±0.03	0.59±0.13	1.15±0.39	1.17±0.90	NS

†Values represent treatment mean for each day after planting ± 1 standard error (n=4).
‡Not significant at P=0.05
*Letters within each row indicate LSD significance by days after planting at P=0.05.

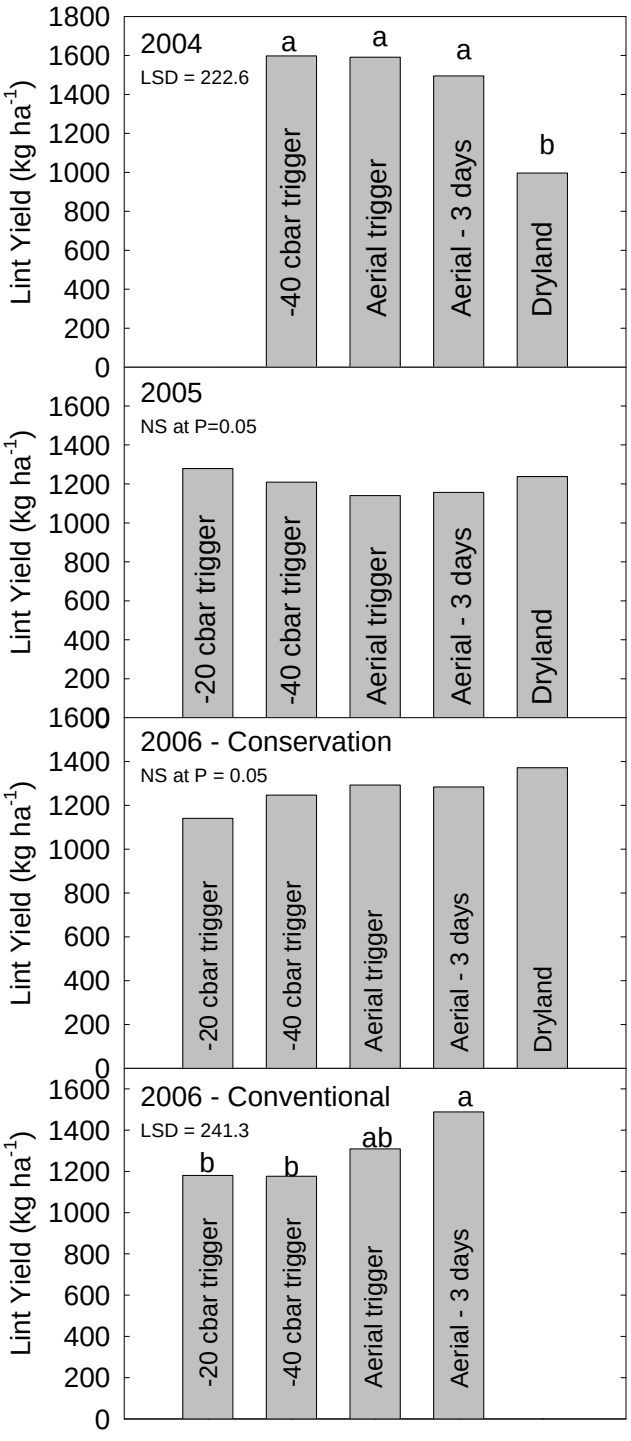

Fig. 5.40. Lint yield 2004-2006.

Table 5.9. Fiber length, uniformity, strength, and micronaire by treatment 2004-2006†.

Irrigation Treatment	Length	Uniformity	Strength	Micronaire
	inches	%	g tex^{-1}	
2004				
40-cbar	1.118±0.006	81.12±0.216	29.86±0.28 b*	4.275±0.103 b
Aerial	1.131±0.008	80.92±0.213	30.38±0.21 b	4.267±0.091 b
Aerial-3	1.120±0.008	81.39±0.381	30.56±0.49 ab	4.325±0.082 b
Non-irrigated	1.137±0.009	81.11±0.176	31.33±0.05 a	4.517±0.057 a
LSD	NS‡	NS	0.82	0.188
2005				
20-cbar	1.107±0.005	80.89±0.18	28.68±0.07	4.483±0.033 a
40-cbar	1.102±0.006	80.88±0.37	28.69±0.68	4.425±0.143 ab
Aerial	1.107±0.005	80.60±0.27	28.88±0.22	4.263±0.113 ab
Aerial-3	1.103±0.003	80.30±0.27	28.41±0.43	4.208±0.088 b
Non-irrigated	1.102±0.003	80.53±0.26	28.04±0.44	4.417±0.081 ab
LSD	NS	NS	NS	0.232
2006				
20-cbar	1.091±0.018 b	80.38±0.28 ab	28.66±0.51 b	4.883±0.068 b
40-cbar	1.093±0.011 ab	80.26±0.22 b	29.48±0.34 ab	4.867±0.103 b
Aerial	1.111±0.003 ab	80.63±0.12 ab	29.13±0.19 ab	4.808±0.107 b
Aerial-3	1.108±0.010 ab	80.56±0.14 ab	29.26±0.33 ab	5.000±0.042 ab
Non-irrigated	1.116±0.010 a	80.84±0.35 a	29.83±0.62 a	5.217±0.048 a
LSD	0.024	0.553	0.906	0.220

†Values represent treatment means ± 1 standard error (n=4).
‡Not significant at P=0.05
*Letters within each column indicate LSD significance by treatment at P=0.05.

References

Adamsen, F., P. Pinter, E. Barnes, R. LaMorte, G. Wall, S. Leavitt, and B. Kimball. 1999. Measuring wheat senescence with a digital camera. Crop Sci. 39:719-724.

Ahlrichs, J.S., and M.E. Bauer. 1982. Relation of agronomic and multispectral reflectance characteristics of spring wheat canopies. LARS Technical Report 121082:26p. Purdue University, Lafayette, IN.

Aldakheel, Y.Y., and F.M. Danson. 1997. Spectral reflectance of dehydrating leaves: measurements and modelling. Int. J. Remote Sens. 18:3683-3690.

Anonymous. 2006. Camilla 3 SE, Georgia (091500): Period of record monthly climate summary. Southeast Regional Climate Center.

ASD. 1999. Analytical Spectral Devices, Inc. technical guide. 3rd ed., Boulder, Colorado.

Bednarz, C.W., W.D. Shurley, and W.S. Anthony. 2002a. Losses in yield, quality, and profitability of cotton from improper harvest timing. Agron. J. 94:1004-1011.

Bednarz, C.W., J.E. Hook, R. Yager, S. Cromer, D. Cook, and I. Griner. 2002b. Cotton crop water use and irrigation scheduling, p. 61-64, *In* A. S. Culpepper, ed. 2002 Georgia Cotton Research-Extension Report.

Boissard, P., J.-G. Pointel, and J. Tranchefort. 1992. Estimation of the ground cover ratio of a wheat canopy using radiometry. Int. J. Remote Sens. 13:1681-1692.

Bouman, B.A.M. 1992. Accuracy of estimating the leaf area index from vegetation indices derived from crop reflectance characteristics, a simulation study. Int. J. Remote Sens. 13:3069-84.

Cohen, Y., V. Alchanatis, M. Meron, Y. Saranga, and J. Tsipris. 2005. Estimation of leaf water potential by thermal imagery and spatial analysis. J. Exp. Bot. 56:1843-1852.

Danson, F.M., M.D. Steven, T.J. Malthus, and J.A. Clark. 1992. High-spectral resolution data for determining leaf water content. Int. J. Remote Sens. 13:461-470.

Famiglietti, J.S., J.A. Devereaux, C.A. Laymon, T. Tsegaye, P.R. Houser, T.J. Jackson, S.T. Graham, M. Rodell, and P.J.v. Oevelen. 1999. Ground-based investigation of soil moisture variability within remote sensing footprints during the Southern Great Plains 1997 (SGP97) hydrology experiment. Water Resources Research 35:1839-1851.

Harrison, K. 2005. Irrigation Survey, 2005. The University of Georgia College of Agricultural and Environmental Sciences Cooperative Extension Service.

Hinzman, L.D., M.E. Bauer, and C.S.T. Daughtry. 1984. Growth and Reflectance Characteristics of Winter Wheat Canopies 111484. Laboratory for Applications of Remote Sensing, Purdue University, West Layfayette, IN.

Huete, A.R. 1988. A soil-adjusted vegetation index (SAVI). Remote Sens. Environ. 25:295-309.

Hutson, S.S., N.L. Barber, J.F. Kenny, K.S. Linsey, D.S. Lumia, and M.A. Maupin. 2004. Estimated use of water in the United States in 2000. U.S. Dept. of the Interior, U.S. Geological Survey ; Denver, CO : For sale by U.S. Geological Survey, Branch of Information Services, Reston, Va.

Jost, P.H., J.R. Whitaker, S.M. Brown, and C.W. Bednarz. 2006. Use of plant growth regulators as a management tool in cotton, *In* U. o. G. C. Extension, (ed.).

Ko, J., S.J. Maas, S. Mauget, G. Piccinni, and D. Wanjura. 2006. Modeling water-stressed cotton growth using within-season remote sensing data. Agron. J. 98:1600-1609.

Koch, B., R. Khosla, W.M. Frasier, D.G. Westfall, and D. Inman. 2004. Economic Feasibility of Variable-Rate Nitrogen Application Utilizing Site-Specific Management Zones. Agron. J. 96:1572-1580.

LI-COR. 1989. LI-1600 steady state porometer instruction manual: p. 3-2.

McDermitt, D.K. 1990. Sources of error in the estimation of stomatal conducance and transpiration from porometer data. HortScience 25:1538-1548.

Peñuelas, J., J. Piñol, R. Ogaya, and I. Filella. 1997. Estimation of plant water concentration by the reflectance water index WI (R900/R970). Int. J. Remote Sens. 18:2869-2875.

Perry, C.D., S. Pocknee, O. Hansen, C. Kvien, G. Vellidis, and E. Hart. 2002. 2002 ASAE Annual International Meeting / CIGR 15th World Congress, Chicago, IL.

Pettigrew, W.T. 2004. Physiological consequences of moisture deficit stress in cotton. Crop Sci. 44:1265-1272.

Pinter, P.J., J.L. Hatfield, J.S. Schepers, E.M. Barnes, M.S. Moran, C.S.T. Daughtry, and D.R. Upchurch. 2003. Remote sensing for crop management. Photogrammetric Engineering & Remote Sensing 69:647-664.

Plant, R.E., D.S. Munk, B.R. Roberts, R.L. Vargas, D.W. Rains, R.L. Travis, and R.B. Hutmacher. 2000. Relationships between remotely sensed reflectance data and cotton growth and yield. Trans. ASAE 43:535-546.

Reddy, V.R., A. Trent, and B. Adcock. 1992. Mepiquate chloride and irrigation versus cotton growth and development. Agron. J. 84:930-939.

Ripple, W.J. 1986. Spectral reflectance relationships to leaf water stress. Photogramm. Eng. Remote Sens. 52:1669-1675.

Roerink, G.J., W.G.M. Bastiaanssen, J. Chambouleyron, and M. Menenti. 1996. Relating Crop Water Consumption to Irrigation Water Supply by Remote Sensing. Water Resources Management 11:445-465.

Yang, C., J.H. Everitt, and J.M. Bradford. 2001a. Comparisons of uniform and variable rate nitrogen and phosphorus fertilizer applications for grain sorghum. Trans. ASAE 44:193-200.

Yang, C., J.M. Bradford, and C.L. Wiegand. 2001b. Airborne multispectral imagery for mapping variable growing conditions and yields of cotton, grain sorghum, and corn. Trans. ASAE 44(6):1983-1994.

Yang, C., J.H. Everitt, and J.M. Bradford. 2004. Airborne hyperspectral imagery and yield monitor data for estimating grain sorghum yield variability. Trans. ASAE 47:915-924.

CHAPTER 6

SUMMARY AND CONCLUSIONS

Ground-based vegetation indices based on red edge and near-infrared reflectance were more sensitive to high and low levels of vegetation than were vegetation indices based on other wavelengths. This was evident both in measurements of leaf area index during cotton defoliation and measuring in-season ground cover fraction. Ground-based vegetation index measurements based on the red edge and near-infrared wavelengths were also highly correlated with leaf area index over a period of days, as well as between years, suggesting that a sensing system based on these wavelengths will allow consistent estimates of defoliation level, as well as in-season measurements of plant growth.

Consumer-grade digital cameras, such as the Nikon COOLPIX 4300, can be modified to provide infrared images, providing an approximation of cotton near-infrared reflectance. Although the spectral range of a consumer digital camera is limited to the visible portion of the spectrum due to a hot mirror integrated into the lens assembly, replacement of the hot mirror with a near-infrared transmitting filter such as the Hoya R710 filter results in a camera that primarily senses near infrared radiation. The visible wavelength sensitivity of the color bands of a digital camera depend upon the color filter array integrated in the photo sensor, but the camera sensitivity of the red, green, and blue channels is closely correlated with red, green, and blue reflectance measured with a spectrometer. The relationship between channel brightness and reflectance is not linear, but the relationship between brightness measurements of a target at different exposure levels within the camera is linear. This linear relationship allows exposure compensation, providing a

correction method between digital brightness values of visible and near-infrared cameras at different exposures. NDVI values based on brightness values and exposure differences between the cameras were shown to provide a consistent estimate of both crop ground cover fraction and ground-based spectrometer vegetation indices.

Comparison of ground cover fraction with camera-based NDVI measurements using visible and near-infrared cameras, visible camera Green:Red ratio, and spectrometer measurements showed that all of the indices estimate cotton vegetative growth consistently at ground cover fractions between 0.30 and 0.75. However, direct comparisons between camera NDVI and camera Green:Red measurements indicate that Green:Red ratio values are less sensitive than NDVI to lower ground cover fractions. Green:Red ratio and camera NDVI measurements had similar correlations to ground cover fraction, with Green:Red ratio tending to have slightly higher correlation values throughout the growing season. However, this variation is very small can probably be explained by small image alignment and exposure issues over a range of several photographs and exposure differences. The similarities between the two indices suggests that Green:Red ratio measurements from a single camera can provide and accurate, low-cost alternative to a two-camera system that collects visible and near-infrared images.

Ground-based spectrometer $NDVI_{710\ nm}$ measurements were more sensitive to both low and high ground cover fractions than $NDVI_{red}$, suggesting that $NDVI_{710\ nm}$ is a more appropriate index for measuring a broad range of ground cover.

Camera and spectrometer vegetation indices and ground cover fraction measurements were sensitive to changes in cotton growth due to water stress. Irrigation treatments based on remote sensing data showed rapid growth recovery upon irrigation, and did not yield significantly different from treatments based on soil moisture measurements alone. In addition, these

treatments used less irrigation water during the growing season than the treatments irrigated based on soil moisture measurements. Irrigation treatments that received less water had higher length, uniformity, strength, and micronaire content.

Cotton irrigation management is important for both production and water conservation. Commercially available variable rate irrigation systems now allow precision irrigation of crops. However, in-season estimates of irrigation timing and rate based on crop growth must be sensitive to a wide range of crop growth, as well as sensitive to changes in crop growth due to water stress. A system that maintains consistent estimates of crop growth from one sampling date to the next is also desirable, particularly if it is simple and inexpensive.

The research presented here suggests that ground-based and aerial remote sensing estimates of ground cover fraction are sensitive to changes in cotton growth due to water stress, and that an irrigation regime based on these changes can provide adequate crop water and reduce irrigation application rates compared to blanket applications of water based on soil moisture measurements in a few locations.

APPENDIX A

Lens Distortion

Lens distortion is common in consumer camera zoom lenses. These lenses are designed to be used over a broad zoom range, and the distortion is in part a tradeoff between the wide angle (zoomed out) and telephoto (zoomed in) characteristics of the lenses. Shih *et al.* {, 1995 #212} attributed this to a compromise between barrel distortion (vertical and horizontal lines in the picture appear to bow outward) at wide angle and pincushion distortion (vertical and horizontal lines in the picture appear to bow inward) at the telephoto zoom. An example of barrel distortion is shown in Fig. A.1.

Lens distortion was estimated at the 8-mm focal length by photographing a reference grid with the camera normal to the grid and correcting the image in Adobe Photoshop CS2 (Adobe Systems, Inc., San Jose, CA) using the lens correction filter until the lines of the grid most closely approximated vertical and horizontal parallel lines.

Lens distortion at the 8-mm focal length was estimated to be about 3.5% for both visible and near-infrared cameras, as shown in Fig. A.2.

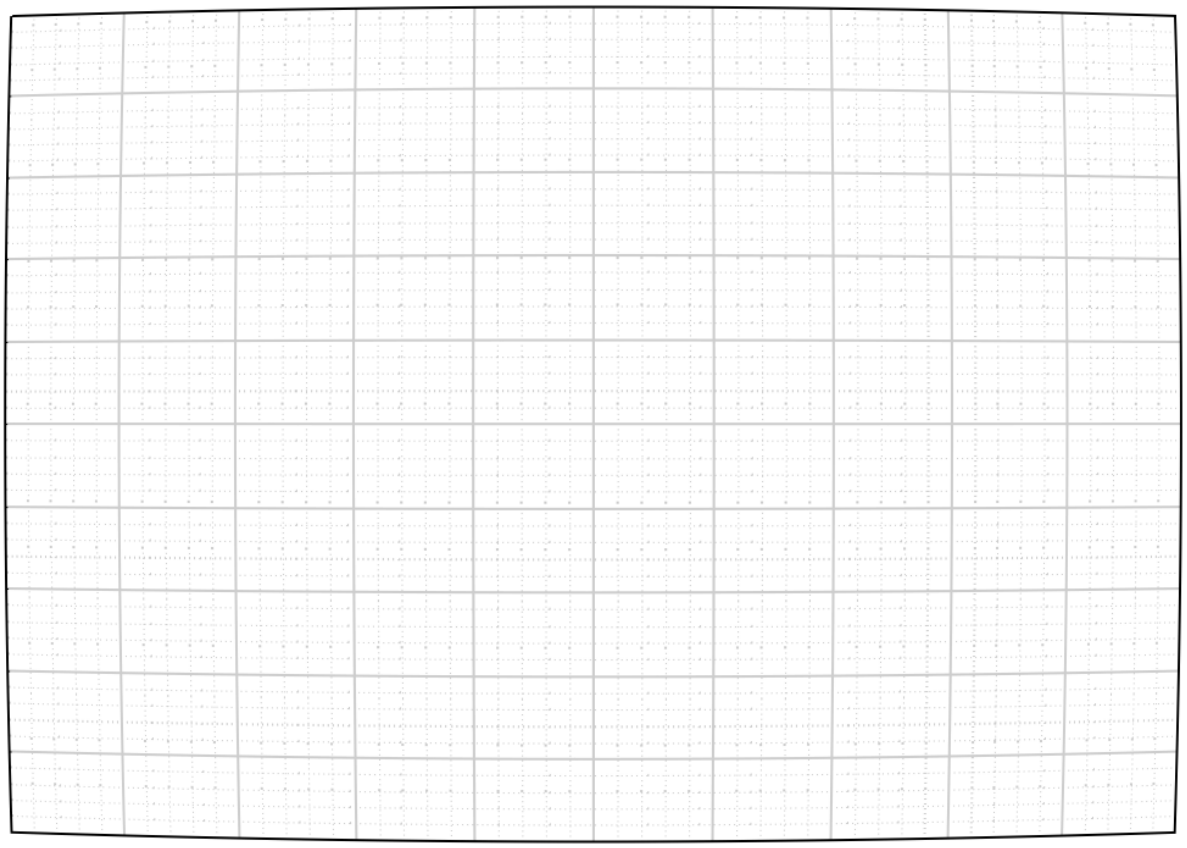

Fig. A.1. An example of 3.5% image barrel distortion. Both the visible and NIR cameras were observed to have about a lens barrel distortion of about 3.5%.

Fig. A.2. Image before (top) and after (bottom) image correction. Image correction was performed using the lens correction filter in Adobe Photoshop with a 3.5% correction filter. The black border around the images emphasizes the correction required to minimize the barrel distortion.

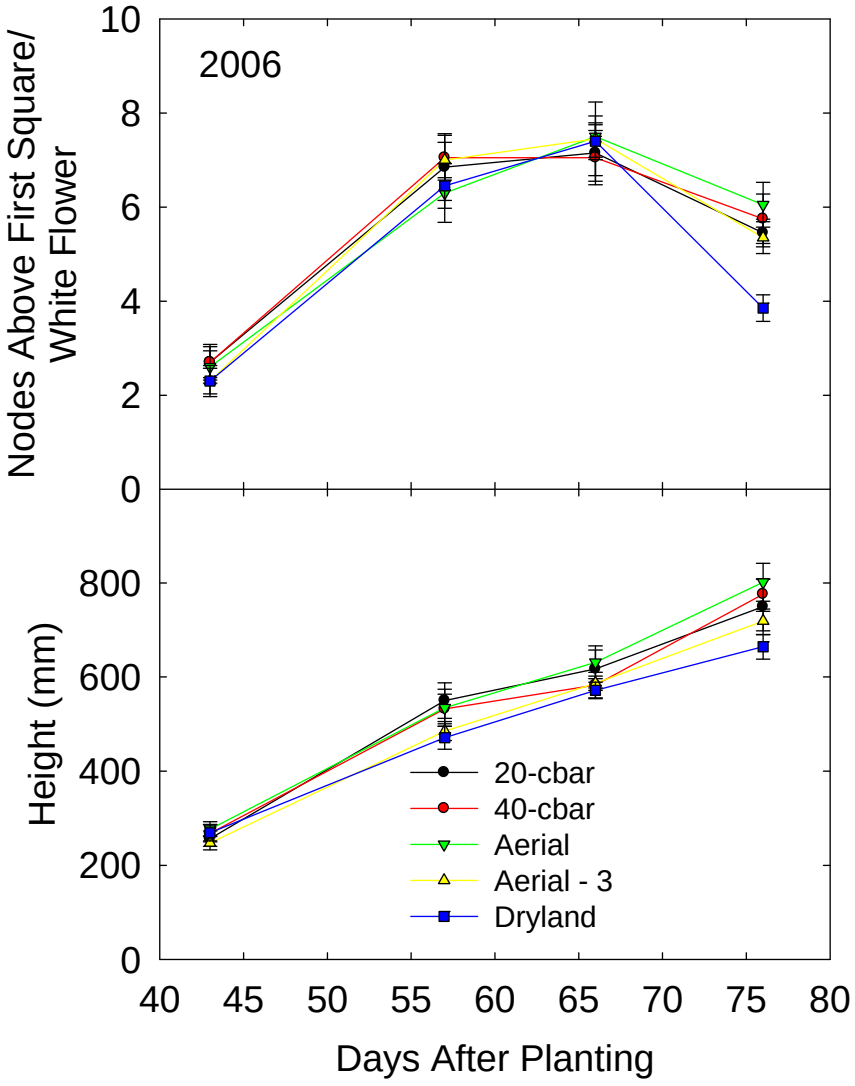

Fig. A.3. Comparison of plant height and nodes above first square/ white flower by treatment in 2006. Error bars represent standard error of the mean (n=4).

Reference

Shih, S., Y. Hung, and W. Lin. 1995. When should we consider lens distortion in camera calibration. Pattern Recognition 28:447-461.